Max-Planck-Institut
für Meteorologie

MAX-PLANCK-GESELLSCHAFT

International Max Planck Research School
on Earth System Modelling

Towards the Assessment of the Climate Effects of Secondary Organic Aerosols

Declan O'Donnell

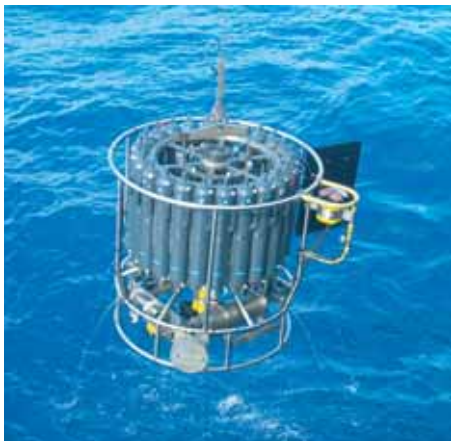

Berichte zur Erdsystemforschung 77
2010

Reports on Earth System Science

Hinweis

Die Berichte zur Erdsystemforschung werden vom Max-Planck-Institut für Meteorologie in Hamburg in unregelmäßiger Abfolge herausgegeben.

Sie enthalten wissenschaftliche und technische Beiträge, inklusive Dissertationen.

Die Beiträge geben nicht notwendigerweise die Auffassung des Instituts wieder.

Die "Berichte zur Erdsystemforschung" führen die vorherigen Reihen "Reports" und "Examensarbeiten" weiter.

Notice

The Reports on Earth System Science are published by the Max Planck Institute for Meteorology in Hamburg. They appear in irregular intervals.

They contain scientific and technical contributions, including Ph. D. theses.

The Reports do not necessarily reflect the opinion of the Institute.

The "Reports on Earth System Science" continue the former "Reports" and "Examensarbeiten" of the Max Planck Institute.

Anschrift / Address

Max-Planck-Institut für Meteorologie
Bundesstrasse 53
20146 Hamburg
Deutschland

Tel.: +49-(0)40-4 11 73-0
Fax: +49-(0)40-4 11 73-298
Web: www.mpimet.mpg.de

Layout:

Bettina Diallo, PR & Grafik

Titelfotos:
vorne:
Christian Klepp - Jochem Marotzke - Christian Klepp
hinten:
Clotilde Dubois - Christian Klepp - Katsumasa Tanaka

Berichte zur Erdsystemforschung 77/2010

Towards the Assessment of the Climate Effects of Secondary Organic Aerosols

Declan O'Donnell

aus Donegal, Irland

Hamburg 2010

Reports on Earth System Science 77/2010

ISSN 1614-1199

Declan O'Donnell
Max-Planck-Institut für Meteorologie
Bundesstrasse 53
20146 Hamburg
Germany

Als Dissertation angenommen
vom Department Geowissenschaften der Universität Hamburg

auf Grund der Gutachten von
Prof. Dr. Hartmut Graßl
und
Dr. Johann Feichter

Hamburg, den 1. Februar 2010
Prof. Dr. Jürgen Oßenbrügge
Leiter des Departments für Geowissenschaften

ISSN 1614-1199

Towards the Assessment of the Climate Effects of Secondary Organic Aerosols

Declan O'Donnell

Hamburg 2010

CONTENTS

ABSTRACT

Atmospheric aerosols influence the Earth's climate by absorbing and scattering solar radiation and by altering the properties of clouds. Measurements have shown that a substantial fraction of the tropospheric aerosol burden consists of organic compounds. Hundreds of different organic species have been identified in aerosols, yet these are typically able to account for only a minority of the total aerosol organic mass. While progress has been made in the understanding of the roles of certain aerosol types in the climate system, that of organic aerosols remains poorly understood and the climate influences resulting from their presence poorly constrained.

Organic aerosols are emitted directly from the surface (primary organic aerosols, POA), and are also formed in the atmosphere by oxidation reactions of gas-phase precursors (secondary organic aerosols, SOA). The significance of the distinction between primary and secondary organic aerosols lies largely in the fact that SOA condense from the gas phase onto the pre-existing aerosol; so that POA and SOA affect the mass, number and size distributions of an aerosol population in quite different ways.

Both anthropogenic and biogenic SOA precursors are known from laboratory studies and from field measurements. Global inventories of anthropogenic precursor emissions have been constructed, as have canopy models that permit estimation of the production of biogenic precursors from a given biome.

Globally, biogenic emissions of aerosol precursors are estimated to be much the larger source (of the order of several hundred Tg per year) and they form a potentially significant natural source of tropospheric aerosol. A mechanism thus exists whereby vegetation can impact climate through its influence upon the atmospheric aerosol loading, and thereby on the radiative budget and on the properties of clouds. In turn, emission of precursor gases from vegetation is climate-dependent; hence a bi-directional dependency between biosphere and atmosphere is established.

For quantitative study of the climatic influence of these aerosols, and of the biosphere-atmosphere interactions outlined above, a global climate/aerosol model is a suitable tool.

This study builds upon one such model, ECHAM5/HAM, to which techniques to model the formation and behaviour of secondary organic aerosols are added, as well as the necessary global emission inventories, with the following goals:

- Estimation of the direct (radiative) and indirect effects of biogenic organic aerosols
- Estimation of the direct and indirect effects of biogenic plus anthropogenic organic aerosols
- Estimation of the influence of changing climate on the formation of organic aerosols from biogenic precursors
- Progress towards understanding the interactions of secondary organic aerosols with other aerosol species and with clouds

If achieved, these objectives will contribute to improving our understanding of earth system processes, in particular the climate response to anthropogenic and biogenic SOA, the coupling via aerosols of the land biosphere and the climate system and the interactions of natural and anthropogenic aerosols.

Chapter 1

1 Organic Aerosols in the Earth System

The effects of aerosols on the climate system are conventionally classified into two separate categories; these are termed the direct and indirect effects. The direct effect refers to the scattering and absorption of radiation by aerosols. The term 'indirect effect' refers to a diverse set of mechanisms whereby aerosols influence the microphysical properties of clouds, altering their extent, radiative properties and lifetimes. Backward scattering of solar radiation by aerosols leads to energy loss to space and thus to a cooling effect, both as observed at the top of the atmosphere (TOA) and at the surface. Absorbing aerosols may exert either a positive or negative TOA forcing; if the underlying surface is dark - more absorptive than the aerosols - then the aerosols increase the albedo as seen from the top of the atmosphere, and therefore lead to a negative radiative forcing. If, on the contrary, the aerosols overlie a bright, highly-reflective surface such as snow, ice, or clouds, then the opposite case holds and the aerosols exert a positive forcing. In both cases, the aerosols act to cool the underlying surface. Organic aerosols both scatter and absorb radiation, and may influence cloud microphysical properties in different ways, depending upon composition.

Organic compounds are almost always found in combination with other species within an aerosol particle, although pure organic aerosols such as bio-aerosols (bacteria, fungi, etc.) do occur. Although aerosol species interact, and each species affects the processing and lifetime of the others in non-linear ways (Stier et al., 2006a), it is conventional in aerosol-climate studies to analyse the effects of different aerosol species separately. By so doing, one may gain insight into how the climate system can be expected to react to a change in the atmospheric loading of any given species that may result, for example, from a change in anthropogenic emissions.

In the following subchapters, a brief overview of the present state of knowledge of the influences of aerosols on the climate system is given; next, observations (focusing on the global scale) are presented that quantitatively estimate such effects. This is followed by a description of the organic contribution to the total tropospheric aerosol. This leads us into the study of secondary organic aerosols (SOA). Current understanding concerning emission of SOA precursors, formation and processing of SOA in the atmosphere is outlined: to this end, findings from observations, laboratory studies, thermodynamic theory and global modelling are used. Finally, addressing some of the questions that this earlier work has left so far unanswered, the objectives of this study are formulated.

1.1 Overview of aerosol direct and indirect effects and climate forcing

Of the various ways in which aerosols interact with the climate system, the simplest to understand is the direct effect, which consists of scattering and absorption of radiation by aerosol particles. Both shortwave and longwave radiation are affected; however, fine particles, meaning those having a diameter of less than 1μm, are most effective at scattering incoming solar (shortwave) radiation back to space. Aerosols may also absorb radiation: particles containing a significant fraction of elemental carbon (also called black carbon) are the most effective absorbers. Absorption of solar radiation by aerosols locally heats the atmosphere, but cools the underlying surface. The total direct effect of an aerosol population depends on its chemical composition, the mixing state of those components, the size distribution of the particles, and, as explained above, the albedo of the underlying surface. Figure 1.1 illustrates such direct aerosol effects under clear-sky conditions in Mediterranean Europe.

Figure 1.1. MODIS image of aerosol haze over northern Italy, extending eastwards to Slovenia

Aerosols are intimately bound together with the properties of clouds and the hydrological cycle. Water vapour at atmospheric concentrations condenses to liquid only in the presence of a condensation nucleus (an aerosol particle). Aerosol indirect effects refer to the outcomes of a number of different microphysical mechanisms whereby aerosols in a supersaturated region of the atmosphere influence the droplet (or ice crystal) number concentration or size distribution in a liquid water (or ice) cloud. A larger number of aerosol particles partitions the available water vapour over a greater number of surfaces and thereby shifts the droplet size distribution downwards to the smaller end of the scale. Smaller particles backscatter radiation more than larger particles; hence the reflectivity of clouds formed on a large number of aerosol particles is greater than that of one formed on a smaller number of aerosols for a given liquid water content (Twomey, 1974). This is termed the cloud albedo effect, first indirect effect or Twomey effect. Several other mechanisms through which aerosols modify the microphysical properties of clouds have been hypothesised. Albrecht (1989) proposed that clouds composed of smaller droplets would have reduced precipitation efficiency and thus a longer lifetime than those composed of larger droplets. This is termed the cloud lifetime effect, second indirect effect or Albrecht effect. On the other hand, local atmospheric heating due to absorptive aerosols could have the effect of evaporating cloud water and thereby decreasing cloud cover (Ackermann et al. 2000), which has become known as the semi-direct effect.

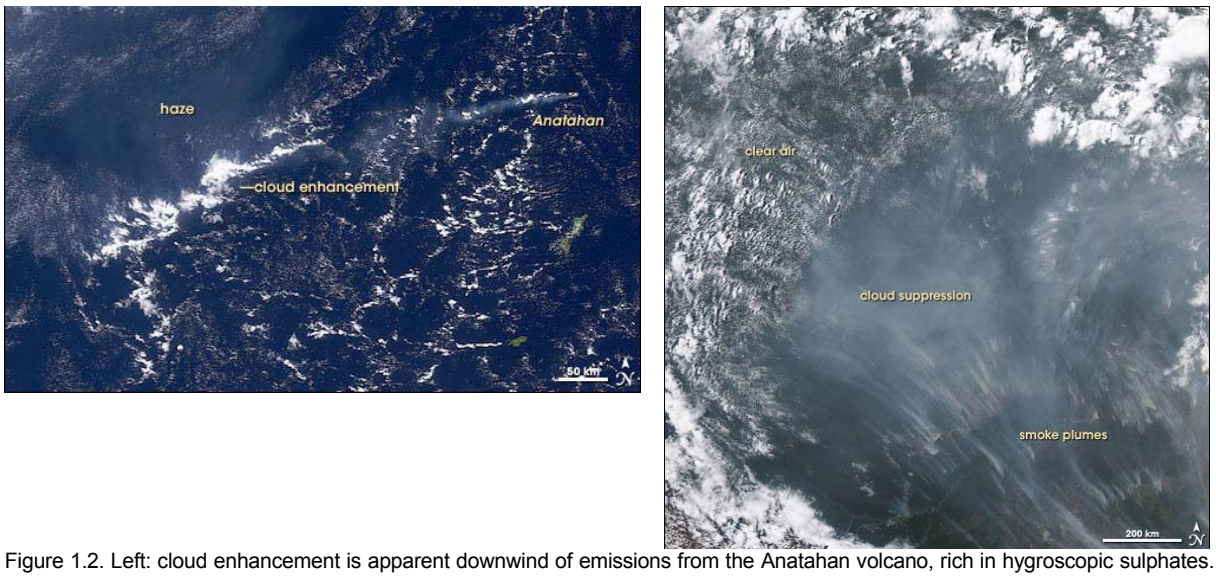

Figure 1.2. Left: cloud enhancement is apparent downwind of emissions from the Anatahan volcano, rich in hygroscopic sulphates. Right: smoke from Amazonian forest fires seem to be associated with a cloud-free portion of an otherwise cloudy sky. MODIS images, source: NASA Earth Observatory.

Other effects may include effects on cloud vertical and horizontal extent (Pincus and Baker, 1994) and contrails.

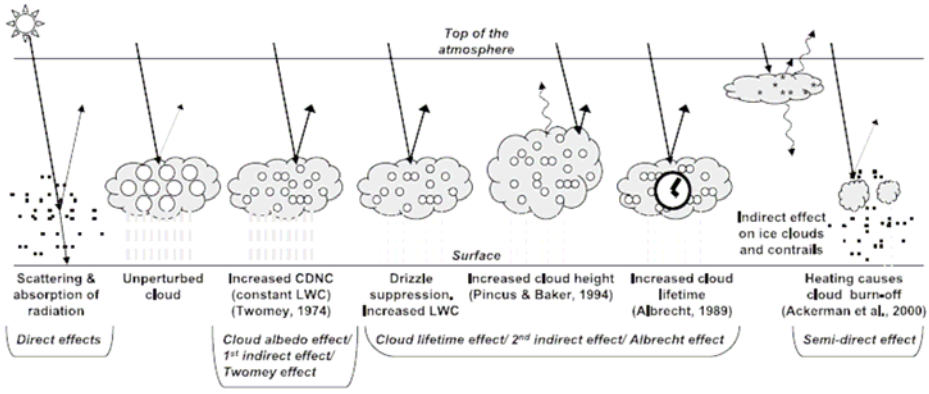

Figure 1.3. Aerosol direct and indirect effects. From Forster *et al.* (2007)

These and other indirect effects were reviewed by Lohmann and Feichter (2005). In addition to the above-described effects, they list additional effects applicable to mixed phase clouds:

- Thermodynamic effect (smaller droplets delay the onset of freezing)
- Glaciation effect (more ice nuclei increase precipitation efficiency)
- Riming effect (smaller droplets decrease the riming efficiency)

Studies of convective cloud systems using cloud resolving models have led to claims for several different physical effects. Results of such studies indicate differing effects for shallow and for deep convective systems (Tao et al., (2007) and the references therein). Furthermore, precipitation changes between simulations starting from different aerosol concentrations exhibit opposite signs for different study cases: for example, in the model studies of Khain and Pokrovsky (2004) and Khain et al. (2005), precipitation

was found to increase with high cloud condensation nuclei (CCN) concentration in an Atlantic deep convective system, but reduced for one continental deep convective study case and again enhanced for another. Detailed explanation of such effects reside in the modelled warm- and cold-rain processes and in the effect that the larger CCN concentration has on the latent heat release within the cloud, which may act to invigorate the convective system and thus enhance precipitation.

In global terms, however, the influence of varying aerosol loading upon convective clouds appears to be limited. Lohmann (2008) applied a double-moment cloud microphysics scheme to convective clouds in the global model ECHAM5, coupled to the HAM aerosol module (the same global models used in this work), with the result that the anthropogenic aerosol forcing, defined as the difference in net radiation at TOA between pre-industrial and present day, was -1.6 Wm^{-2} compared to -1.5 Wm^{-2} when the coupling of aerosols to the convective cloud scheme was not used.

1.2 Global Observations of Aerosol Direct and Indirect Effects and Climate Forcing

At the outset, it should be emphasized that one must distinguish aerosol *direct effects* from aerosol *direct forcing*. The term aerosol *direct effect* refers to the effect, measured as a TOA radiative flux, of all aerosols on the climate system through scattering and absorption of radiation. The term *aerosol direct forcing* refers to the influence of *anthropogenic aerosols only* and is measured as the difference between the aerosol effects at different times, most commonly between preindustrial (normally taken as the year 1750) and the present day or a recent year, for example 2000. Unfortunately, the distinction between direct effect and direct forcing is not always clearly made in the literature. No such distinction is required for indirect effects, since clearly is not meaningful to consider clouds in an aerosol-free atmosphere. As this work is concerned with natural as well as anthropogenic aerosols, both the concepts of aerosol effects and of aerosol forcing are applicable to it.

For global estimates of aerosol direct and indirect effects, satellite retrievals are indispensable. However, one must realise that satellite retrievals are themselves based on an underlying model that derive the aerosol-related property in question, for example the aerosol optical depth (AOD), from radiation measurements by the satellite instruments, and that those instruments differ, for example in wavelengths and in viewing geometry. The retrieval models also differ and are furthermore revised from time to time. Furthermore, earlier retrievals used instruments, for example the Advanced Very High Resolution Radar (AVHRR) and Total Ozone Mapping Spectrometer (TOMS) that were designed for entirely different purposes. Thus different satellites estimates can differ substantially from one another in their estimates of the same quantity.

For these reasons, high-quality ground-based measurements are also needed; in addition, they can provide simultaneous aerosol chemical speciation and information about local aerosol variability and trends. The AErosol Robotic Network (AERONET) (Holben et al., 1998) provides globally-distributed observations of aerosol optical depth and other aerosol-related quantities. The locations of AERONET sites are indicated by red squares in the image below.

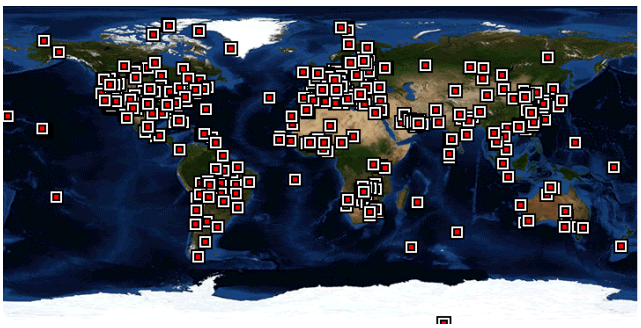

Figure 1.4. AERONET measurement sites

LIDAR measurements can provide vertically resolved measurements from ground-based networks (e.g. EARLINET) (Matthias et al. 2004), ship or aircraft in field studies, and, since 2006, from the CALIPSO satellite.

Satellite retrievals of the direct radiative effect (DRE) from multiple studies (Forster et al. 2007) give a mean estimate of -5.4 Wm^{-2} *over ocean* with a standard deviation of 0.9 Wm^{-2}. Satellite retrievals are limited to a range of approximately 60°N to 60°S because of issues related to low solar irradiance and the high reflectance of snow and ice. Over land, estimates of DRE from satellite retrievals are much more poorly constrained due to the greater difficulty of accurately characterising reflection from the land surface, which is highly anisotropic and wavelength dependent (Yu et al. 2006).

Remote sensing techniques that estimate the anthropogenic fraction of the total aerosol (e.g. Kaufman et al. 2005) have been developed. This enables estimation of both the anthropogenic aerosol direct radiative forcing (RF) as well as the aerosol direct radiative effect from satellite retrievals. Kaufman et al. (2005) estimated an anthropogenic direct aerosol RF of -1.4 Wm^{-2} over oceans. Other studies have blended satellite retrievals with modelling, such as Christopher et al. (2006), who arrived at a forcing estimate of -1.4 ± 0.9 Wm^{-2}. Quaas et al. (2008) used CERES and MODIS data to estimate a direct aerosol radiative forcing of -0.9 ± 0.4 Wm^{-2}.

It is not possible to obtain a true indirect aerosol forcing estimate in terms of the difference between present and preindustrial times, since no data exist that can yield reliable global information on the properties of preindustrial clouds. However, observational evidence exists for the cloud albedo affect and for the cloud lifetime effect. Coakley et al. (1987), showed evidence that, under stable meteorological conditions, satellites could detect the effect of ship exhaust on clouds, increasing the cloud albedo. During the INDOEX field campaign, which studied conditions influenced by the aerosol outflow from the Indian subcontinent, Heymsfield and McFarquhar (2001) measured large concentrations of small droplets under the high aerosol loading compared with the pristine clouds south of the inter-tropical convergence zone (ITCZ). In polluted regions, droplet concentrations were 300% higher, droplet effective diameters 35% smaller and drizzle observed only 25% as often compared to pristine regions. Feingold et al. (2003) showed that cloud drop size is negatively correlated with subcloud aerosol amount for clouds of similar liquid water path (LWP). Quaas et al. (2008) derived a statistical relationship between cloud properties and column aerosol concentration, and combined these with a data set of satellite-derived anthropogenic aerosol fraction to estimate an anthropogenic forcing of -0.2 ± 0.1 Wm^{-2} due to the cloud albedo effect.

1.3 Organic aerosol in the global aerosol system

Organic matter makes up a large fraction (~20-50%) of the total submicron aerosol mass at continental mid-latitudes, with this fraction rising as high as 90% over tropical forests (Kanakidou et al. 2005). Organic aerosols are observed not only close to the surface, but also in the free troposphere (Huebert et

al. 2004; Heald et al. 2005) and the upper troposphere (Murphy et al. 1998; Froyd et al. 2009). Observations have identified hundreds of separate organic species, of both natural and anthropogenic origin, and both hydrophilic and hydrophobic. A number of studies have indicated that organic aerosol plays an important role in both direct and indirect aerosol effects (Liousse et al. 1996; Jacobson, 2001; Chung and Seinfeld 2002; Roeckner et al. 2006). One should state that most such studies addresses *carbonaceous* aerosol, meaning both organic compounds as well as elemental (or black) carbon. The difference is significant in particular because of the highly light-absorbing nature of black carbon.

Sources of organic aerosols include combustion of all kinds of organic materials: this comprises fossil fuel use, large-scale biomass burning (which may be either naturally or anthropogenically ignited), biofuel burning, which is of particular importance in low-income regions, and aerosol formation from atmospheric chemical processing of organic precursor gases. Organic aerosols are also emitted from the ocean, through bursting of sea-spray bubbles containing organic material of phytoplanktonic origin (O'Dowd et al. 2004); however a credible quantified source function that would enable one to estimate the input to the atmosphere is still lacking. Primary biogenic particles, such as plant debris, humic substances and microbial particles (bacteria, fungi, pollen, etc.) also constitute organic aerosols. However, no information that would permit a global estimate of the contribution of such material to the total aerosol mass is available. Secondary organic aerosols are formed from both anthropogenic and biogenic precursors, which is discussed in more detail in chapter 1.5.

Organic aerosols are removed from the atmosphere by wet deposition, dry deposition and sedimentation.

Organic aerosols are predominantly light-scattering at optical wavelengths, but certain species do absorb ultra-violet and some absorb weakly in the optical regions of the spectrum (Myrhe and Nielsen, 2004), though measurement information on the optical properties of observed atmospheric organic aerosol species is sparse. Predominance of scattering over absorption leads to the expectation that the direct effect of the aerosols under consideration is a negative TOA forcing; weak absorption further implies that such aerosols do not have a significant semi-direct effect. Global model studies that have explicitly estimated the radiative forcing of organic aerosols conclude that the overall effect of organic aerosols is indeed a cooling effect (Forster et al., 2007).

Several field campaigns have pointed out an underestimation of the observed organic aerosol by models. Since most published campaign data predate the inclusion of SOA simulations in global models, the question naturally arises if models that include SOA can better match observations.

Secondary organic aerosols are formed from gas-phase oxidation of anthropogenic and biogenic precursors and the subsequent condensation of the reaction products into the aerosol phase. As this definition contains both a gas-phase chemical transformation clause and a phase change clause, it follow that substances emitted as gases that subsequently condense into the aerosol phase are not classified as SOA, nor are those emitted as particles that undergo aerosol-phase chemical transformation.

Identified biogenic precursors are overwhelmingly plant emissions, in particular isoprene, monoterpenes and sesquiterpenes. Isoprene was considered *not* to be a SOA precursor under atmospheric conditions, until recently, when a seminal paper by Claeys and colleagues (Claeys et al., 2004), in which methyl tetrols, highly oxygenated compounds having a signature isoprene backbone, were identified in Amazonian aerosol. This is a particularly significant finding, because of the huge amount of isoprene that is emitted into the atmosphere (Guenther et al., 2006; Arneth et al., 2007).

Many anthropogenic SOA precursors have been so far been identified, of which the most significant (in terms of global annual emissions) are aromatic species, for example toluene and xylene. A more

comprehensive list is given in Table 1.1. Such precursor emissions include fossil fuel production and use, and industrial solvents.

Atmospheric oxidants relevant to SOA production are the hydroxyl radical (OH), ozone (O_3) and the nitrate radical (NO_3). Which oxidant-precursor reactions are most significant for SOA production is discussed in chapter 1.5. Atmospheric OH and O_3 are photochemically formed, and NO_3 photochemically destroyed. Accordingly one expects diurnal and seasonal variability in SOA production.

SOA first came to light as aerosol species of importance in air quality studies in areas of heavy photochemical pollution, especially Los Angeles (e.g. Grosjean, 1984 and the references therein). Separating the primary and secondary components of observed organic aerosols is not straightforward, but for urban environments, measurements indicate that SOA can typically constitute 20% of the total organic mass, though this can rise considerably in polluted episodes (Rodrigo et al. 2009 and the references therein). Went (1960) first pointed out the relation of biogenic emissions to aerosol haze, though his estimate that biogenic hazes "…probably absorb about 20 per cent of all the Sun's radiation reaching the earth" is rather surprising. The biogenic contribution was estimated by Kanakidou et al. (2005) as regionally varying between 10%-70% of the total organic aerosol, but this was based on studies that did not include isoprene as a SOA precursor.

Certain organic aerosols are semi-volatile, with gas-aerosol phase partitioning that is strongly temperature-dependent, favouring the aerosol phase at low temperatures. This is an important factor in determining the vertical distribution of the aerosol, as the low temperatures of the mid- and upper troposphere favour condensation of semi-volatile gases. The vertical distribution is in turn important in determining the radiative effect and cloud impacts of the aerosols.

Another important characteristic of secondary organic aerosols is that emissions of precursors of all biogenic SOA and some anthropogenic SOA are unrelated to combustion processes and therefore not related to black carbon emissions.

Both volatility and relationship with black carbon have implications for measurements; this will be discussed further in chapter 1.4.

Lastly, the biogenic origin of certain SOA precursors gives rise to a coupling between the biosphere and aerosols, clouds and climate. The emission of biogenic SOA precursor gases is strongly dependent on temperature and in some cases dependent on photosynthetically active radiation. Kulmala et al. (2004b) proposed, based on these dependencies, that there exists a feedback mechanism linking vegetation, aerosols and climate (a proposal sometimes referred to as the "biogenic thermostat" hypothesis). The hypothesis is that if global temperatures increase, so will biogenic emissions of SOA precursors. This would enhance organic aerosol production, which would, in turn, lead to a cooling influence and so establish a negative feedback that counteracts a warming climate.

In the following subchapters, methods of measurement of organic aerosols will first be discussed, with particular consideration of the methods' suitability for measurement of SOA in different parts of the troposphere. Thereafter, the chemistry involved in SOA formation will be outlined at a basic level; followed by a discussion of the thermodynamics of SOA (insofar as gas-aerosol phase partitioning and hygroscopic growth are concerned). Previous global model studies will then be considered. Proceeding from these descriptions, the specific goals of this research will be formulated. Subsequent chapters describe the tools and methods used to investigate these scientific questions and the results obtained.

1.4 Observations of organic aerosols

Measurements of organic aerosols in general, and of semi-volatile species in particular, present numerous difficulties. Techniques presently used to analyse the organic fraction of aerosol may be divided into as in-situ (often referred to as 'on-line') or laboratory ('off-line') methods; and into *direct* methods that analyse the chemical composition of the organic mass and *indirect* methods that analyse only the total carbonaceous mass and infer the partition into organic carbon (OC) and black carbon (BC) (usually called elemental carbon (EC) in such studies).

On-line techniques include use of the Aerosol Mass Spectrometer (AMS) (Jayne et al., 2000) and Particle Into Liquid Sampler (PILS) (Weber et al., 2001). AMS measurements have been widely deployed in recent years.

Off-line techniques suffer from drawbacks when it comes to secondary organics and semi-volatile species. Volatility is highly temperature-dependent: volatilisation of sampled material will lead to under-estimation of the organic content of the sampled aerosol (negative artefact); conversely, condensation of ambient organic vapours onto the sample will give a positive artefact (Jacobson et al., 2000). This means that in-situ characterisation is necessary for aerosol samples taken in extreme conditions, for example in the tropical upper troposphere, where temperatures are typically 75K or more below those at the surface. Likewise, chemical evolution of the aerosol means that the analysed sample differs from the collected sample. Extraction of both polar and non-polar compounds from the same sample also presents further challenges (Saxena and Hildemann, 1996).

Indirect measurement methods analyse the total carbonaceous content of an aerosol sample. The apportionment of the total carbonaceous mass into OC/EC depends on the measurement method. Comparisons among two of the most widely-used methods, the thermal optical reflectance (TOR) and thermal manganese oxidation (TMO) methods, showed that although the two methods agree well on the total carbon mass, the derived EC and OC mass values can be quite different (Seinfeld and Pandis 2006). Furthermore, these methods measure the mass of organic carbon, not the mass of organic aerosol: the mass of oxygen and other elements that make up the organic molecules in the sample is not taken into account. Various multiplicative factors (typically 1.4, but ranging from 1.2 to 1.8) are used to convert the mass of organic carbon into mass of organic aerosol.

Accordingly, care is needed when one attempts to use measurements of organic aerosol mass and knowledge of the technique used to obtain it is indispensable. Because of the strong temperature dependency of semi-volatile SOA, it cannot be overemphasised that for purposes of model to measurement comparison, temperature conditions must be near-constant between sampling and analysis. This excludes all analyses of mid- or upper-tropospheric aerosol performed with offline techniques based on high-altitude filter samples subsequently analysed at ground level laboratories.

Surface-level measurements of organic carbon are routinely made at surface station networks, for example the EMEP network of European stations, and the IMPROVE network in the United States. Within the last 15 years, a number of large-scale field campaigns have analysed aerosol composition in different regions of the globe. The ACE-1 campaign in November-December 1995 (Bates et al., 1998) targeted remote marine aerosols; campaigns that studied anthropogenic pollution include the July 1996 TARFOX campaign off the north-eastern United States (Russell et al., 1999), the Indian Ocean Experiment (INDOEX) of 1998-1999 (Ramanathan et al., 2001) and the 2001 ACE-Asia study (Huebert et al., 2003). More recently clean conditions in West Africa at the onset of the African monsoon season were studied in the July-August 2006 AMMA campaign, (Capes et al., 2009).

The results obtained from such point measurements can be used – to a limited extent – to evaluate model results. Limitations arise both from the inherent disconnect in comparing measurements made at

a single point in space and time with results of a GCM that is designed to calculate only spatially and temporally averaged values, as well as from the methodological difficulties in characterising OC outlined above. The limitation of intensive field campaigns in this regard is particularly severe: such measurements represent a very particular air mass history that cannot be resolved by a global climate models whose resolution in the horizontal is of the order of hundreds of kilometres. For this reason, more extensive networks such as EMEP and IMPROVE are better suited to model evaluation, as they provide wide-area and longer-term observations. However, such networks are necessarily land surface-based, so that field campaigns in maritime regions, in remote terrestrial regions and in the free and upper troposphere are the only means of characterising the aerosols in those areas. Unfortunately, from the point of view of this study, few of such published studies have been equipped with the on-line measurement means, operating at ambient temperatures, that are prerequisite to obtaining estimates of secondary organic aerosol properties.

1.5 Secondary Organic Aerosols: precursors and chemical formation

SOA has both biogenic and anthropogenic precursors. Identified biogenic precursors include isoprene, several monoterpenes and sesquiterpenes. Many anthropogenic precursors have been found; a partial list is given in Table 1.1. Several such precursors are recent discoveries. These precursor gases react with one or more of the atmosphere's oxidants OH, O_3 and NO_3, and some of these reactions yield, at the end of a complex chain of chemical reactions, condensable species that may be absorbed into aerosols. Of these, probably the most intensively studied is the reaction of the monoterpene α-pinene with ozone. A *highly simplified* chemistry scheme that describes production of a few of the observed first-generation condensable species from the oxidation of *α*- and *β*-pinene is shown in figure 1.5 (Jenkin, 2004). Reaction products drawn within squares have been empirically identified in SOA produced by these reactions.

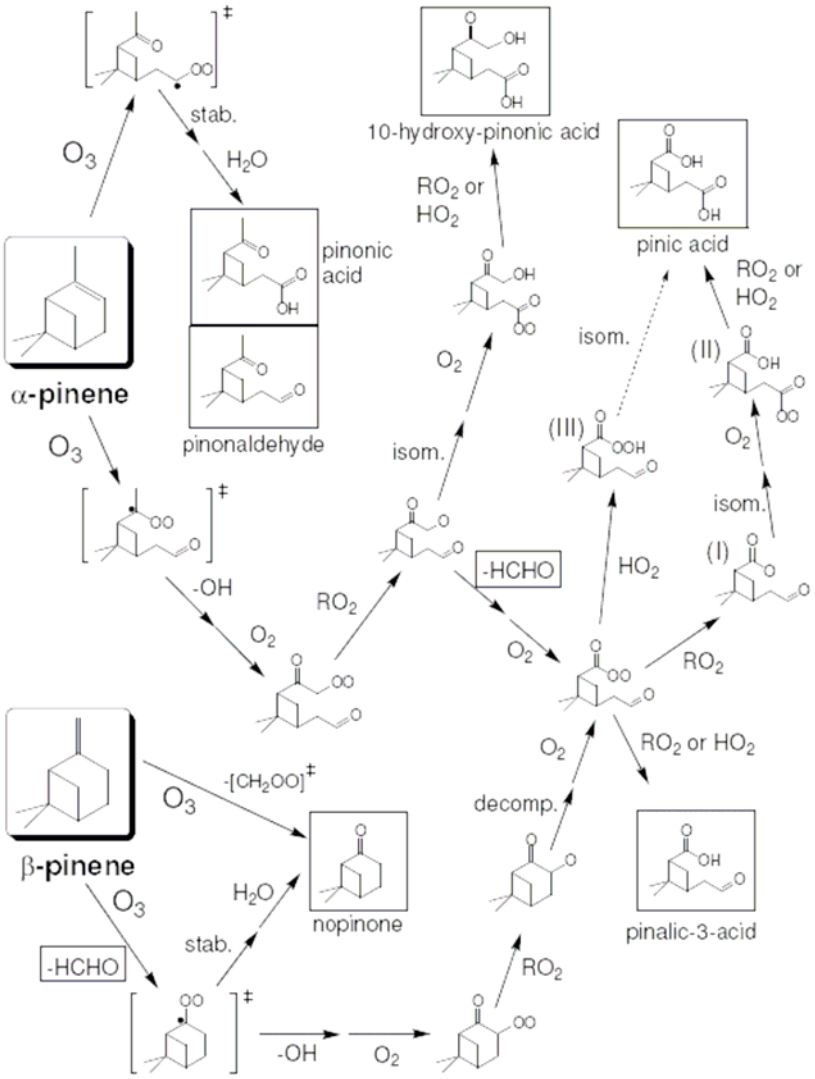

Figure 1.5. Simplified SOA production from α- and β-pinene. From Jenkin (2004)

Subsequent oxidation reactions occur over several generations and in both gas and aerosol phases. Gas-phase oxidation reactions can both reduce volatility by adding polar functional groups or reduce volatility by cleaving the carbon chain, splitting compounds into lower molecular weight, more volatile products (Hallquist et al. 2009). Oxidation reactions in the aerosol phase are sometimes referred to as "aerosol aging". Chemical mechanisms are in general similar to those of the gas phase (Kroll and Seinfeld 2008), but with the addition of oligomerisation reactions that form high molecular weight, low-volatility molecules. Empirical knowledge of subsequent-generation oxidation is still very sparse, and no quantitative method that can account for the aging exists at this time.

It has also been found that several environmental factors affect the reaction pathways and therefore the final SOA yield of a given reaction. In particular, the presence of nitrogen oxides (NO_x), relative humidity and the presence of a seed aerosol (and the acidity of that seed) are known to influence many such reactions. In particular, NO_x alters the organic radical chemistry, converting NO into NO_2 by taking oxygen from organic peroxy radicals (RO_2), which are converted to oxy radicals (RO). These yield more

volatile, fragmented (split carbon chain) products compared to the reaction pathway of peroxy radicals in the absence of NO_x, which is dominated by reaction with HO_2 and produces a higher yield of more oxygenated, polar compounds

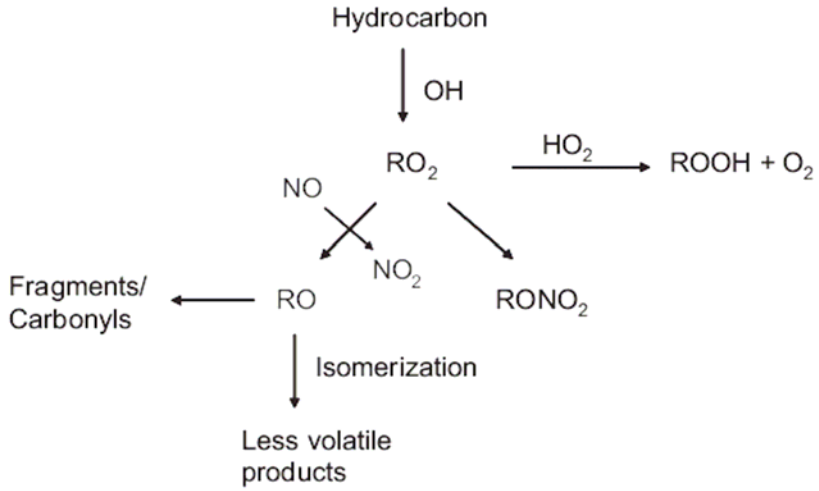

Figure 1.6. Schematic of the role of NO_x in SOA formation. From Ng et al. (2007)

The NO_x effect is significant since many industrial activities are sources of both NO_x and anthropogenic SOA precursors.

Several SOA yields are observed to increase in the presence of acidic seed aerosol, which may be because of acid-catalysed organic oligomerisation reactions (Jang et al. 2002; Iinuma et al. 2004; Gao et al. 2004b). Another factor may be that reaction rates of many particle-phase reactions are increased considerably in acidic environments (Kroll and Seinfeld 2008). Formation of organosulphates has also been observed (Liggio and Li, 2006; Surratt et al. 2007). These results show that there are other mechanisms than chemically inert absorptive uptake at work in SOA formation. However, all the suggested mechanisms still lack quantified description.

The complexity of the chemistry involved in SOA production, and its critical dependency on very short-lived radicals - the α-pinene-ozone reaction example given above is typical in this regard – precludes explicit chemical modelling of SOA production on a global scale. A much simpler alternative is the so-called two-product model of SOA formation. This model is founded on the work of Odum et al. (1996), who showed that for a reaction yielding many semi-volatile species, the aerosol yield *Y*, defined as

$$Y = \frac{\Delta M}{\Delta HC} \tag{1.1}$$

where ΔM is the change in aerosol mass and ΔHC is the mass of precursor hydrocarbon consumed, can be modelled by assuming that the reaction produces only two condensable species. Denoting these species as P_1 and P_2, the aerosol mass yield for a given reaction can be characterised in terms of four empirical parameters, one to describe the stoichiometric mass yield of each product from the precursor-oxidant reaction, and another to describe the volatility of each product. The gas-phase reaction of a precursor *PRE* and oxidant *OX* and subsequent gas-aerosol partitioning of the two hypothetical products is described by

$$PRE + OX \rightarrow \alpha_1 P_1 + \alpha_2 P_2 \quad (1.2)$$

where α_1 and α_2 are mass-based stoichiometric coefficients (note that any purely gas phase products of the reaction are neglected), and

$$A_i = K_{p,i} M_0 G_i \quad (1.3)$$

where A_i (i = 1,2) denotes the mass of product P_i that resides in the aerosol phase and G_i in the gas phase, $K_{p,i}$ is a partitioning coefficient for the organic fraction, and M_0 is the total SOA-absorbing mass in the aerosol phase. SOA production from this reaction is then is then fully characterised by the parameters α_1, α_2, $K_{p,1}$ and $K_{p,2}$. Two products are used since the observed yield curves of a semivolatile product cannot be fitted assuming a single product, and the fit is not improved by supposing three or more products.

Since then, many other smog chamber studies have been carried out and the SOA yield from various precursors characterised in terms of the two-product model. A selection is listed below.

Precursor	Type of reaction	References
Toluene	Photoxidation	Kleindienst et al. (1999, 2004)
		Forstner et al. (1997a)
		Ng et al. (2007a)
Xylene	Photooxidation	Odum et al. (1997a, 1997b)
		Forstner et al. (1997a)
		Kleindienst et al. (1999)
		Ng et al. (2007a)
Benzene	Photooxidation	Ng et al. (2007a)
Other aromatics	Photooxidation	Odum et al. (1997a, 1997b)
α-pinene	O_3	Hoffman et al. (1997)
		Presto et al. (2005)
		Saathoff et al. (2008)
	OH	Griffin et al. (1999)
Isoprene	various	Carlton et al. (2009)
Sesquiterpenes	Photoxidation	Griffin et al. (1999)
		Lee et al. (2006)
Alkenes	O_3	Kalberer et al.(2000)
	Photooxidation	Forstner et al. (1997b)
n-Alkanes	OH	Lim and Ziemann (2005)

Table 1.1. Selected studies of SOA precursor species.

The real atmosphere is of course a more complex environment than the artificially controlled conditions of the smog chamber. However, field observations show that compounds identified in chamber-produced SOA are also observed in the atmosphere (e.g. Spanke et al. 2001; Tunved et al. 2006). Smog chamber studies are frequently aimed at elucidating the chemistry of a single reaction. To this end conditions are often idealised, for example by the use of OH scavengers in studies connected with ozonolysis, which also absorb OH radicals generated by the ozonolysis reaction under study and thereby may affect the SOA yield in an unnatural way if, as often is the case, OH also produces SOA from the studied precursor. Furthermore, precursor and oxidant concentrations used in chamber studies are usually much higher than those observed in the atmosphere because of the difficulty in obtaining accurate measurements at the lower concentrations typical of atmospheric conditions. Perhaps more importantly, chamber studies are forcibly of limited duration (~12 hours). This means that products of subsequent

oxidation reactions are not represented in the results of such studies. Indeed, mass spectrometry studies indicate that laboratory-generated SOA is substantially less oxidised than ambient oxygenated organic aerosol (Kroll and Seinfeld 2008). Nonetheless, smog chamber studies remain the only source of quantitative information about SOA yield from a given precursor and oxidant.

1.6 Thermodynamics of SOA

1.6.1 Gas-Particle partitioning of SOA

The theoretical foundation for the partitioning of SOA between the gas and aerosol phases was laid down in 1994 by Pankow (Pankow 1994a; 1994b). Pankow's theory supposes a number of semi-volatile organic species together with some particle phase mass M_0 that can absorb such organics. M_0 may include non-volatile as well as semi-volatile material. Pankow described the partitioning of each semi-volatile species using a *partitioning coefficient* K_p (having units of, for example, $m^3\ \mu g^{-1}$). For the i^{th} such species, the aerosol mass concentration A_i and the gas phase concentration G_i are related by (1.3):

$$A_i = K_{p,i} M_0 G_i \tag{1.3}$$

so that, provided that there exists some absorbing mass M_0, some of the semi-volatile mass is found in the particle phase, even when the vapour pressure of that species in the gas phase is less than the saturation vapour pressure.

Pankow's theory is a foundation of the 2-product model of SOA formation, as discussed in the previous subchapter. However, it has some shortcomings:

Ambiguity of M_0: when considering internally mixed aerosol particles, that contain not only organic substances, but also inorganics and water, it is not obvious what should be included in M_0. Since some semi-volatile organic species are to some degree water-soluble and others nearly insoluble, it is unclear whether one should include water mass in M_0, or even if a unique definition of M_0 can be found that applies to a diverse group of organic compounds.

Limited to total gas-particle phase partitioning: Pankow's theory only describes the relationship between total gas and total particle phase mass concentrations. For the purposes of the present work, a description of the partition between gas phase and size-resolved aerosol classes is required. Later in this work, the theory will be extended to also predict how the particle phase mass is distributed among different aerosol sizes.

1.6.2 Hygroscopicity of SOA and of mixtures containing SOA

Laboratory studies (for example Gysel et al., 2004; Baltensperger et al., 2005; Duplissy et al., 2008; Meyer et al., 2009) show that SOA takes up water. No known SOA species is close to the hygroscopicity (at high relative humidity) of the inorganic salts such as ammonium bisulphate or sodium chloride that are commonly found in tropospheric aerosols. Hygroscopic growth factors for SOA at 90% RH are typically of the order of 1.05-1.15, compared to a factor of 1.7 for ammonium bisulphate. Within the limits of detectability, many SOA species take up water at any RH. They do not exhibit the deliquescence and efflorescence that are typical of inorganic salts.

Theoretical prediction of the water uptake of aerosol requires knowledge of the water activity of the solution that comprises the aerosol phase. A number of theoretical models have been developed that enable the prediction of the activity of multicomponent solutions containing electrolytic inorganic species

as well as non-dissociating organics, such as the species interaction model of Clegg et al. (2001), the extended Zdanovskii-Stokes-Robinson (ZSR) model of Clegg and Seinfeld (2004) and various approaches based upon group contribution methods (Topping et al. 2005; Erdakos et al. 2006). More recently, a semi-empirical approach based on the so-called κ-Köhler theory (Petters and Kreidenweis, 2007) has been introduced that describes the hygroscopic growth of aerosols in terms of a single free parameter κ per species. The simplicity that this single-parameter approach affords makes it the method of choice for calculation of water uptake by mixed organic/inorganic aerosols in a global modelling study.

1.7 The possible role of SOA in the nucleation of new aerosol particles

While several of the smog chamber studies cited in table 1.1 used no seed aerosol and no other aerosol source, and therefore can only have observed aerosols formed through nucleation of organic compounds, nucleation of pure organic substances in the atmosphere has never been observed, indicating that in nature, the saturation vapour pressure of condensable organics is never reached. In the real atmosphere, because of the measurement detectability limit of typically 3 nm particle diameter, the process of particle formation from gas-phase precursors has to be inferred from the composition of detectable particles. Observations of nucleation events in both clean boreal and polluted environments have shown that freshly nucleated particles in the smallest detectable size range contain a significant organic fraction (e.g. Smith et al., 2008). Furthermore, the occurrence of such events is observed to be correlated with the concentration of sulphuric acid vapour (Sihto et al., 2006). One theory of nucleation (considering only neutral and not ion-induced nucleation) posits that during nucleation events there exists a population of molecular clusters (called 'background clusters'), of sizes less than the detectability limit, which may be activated into detectable particles through condensation of vapours (sulphuric acid or organics, or both) (Kulmala et al., 2004b, 2006a). A key question is whether organics play a role in the initial formation of such clusters (in which case they influence the number of particles as well as the aerosol mass) or only condense upon clusters formed by exclusively inorganic species (in which case aerosol numbers are determined by inorganics alone). This question remains open at this time.

1.8 Influence of SOA on clouds and of clouds on SOA

By condensing on the pre-existing aerosol population, SOA increases the size of the particles in that population. Thereby SOA can influence the number of particles that can activate as cloud condensation nuclei (CCN). Therefore one would expect SOA to have some influence at least on warm stratiform clouds. Certain organic substances are also surfactants that lower the surface tension of the droplet solution, thereby lowering the activation barrier (Decesari et al. 2003). However, Duplissy et al. (2008) showed that the CCN activity of SOA species generated in the smog chamber can be reliably predicted using the surface tension of pure water.

Clouds are of course, major sinks of aerosol through in-cloud scavenging of soluble particles and below-cloud scavenging of both soluble and insoluble particles by precipitation. For SOA, one should also recognise that clouds can remove not only particles, but also condensable gas-phase species.

Oligomerisation reactions that produce high molecular weight, low-volatility compounds are known to take place in the particle phase. This has been observed in SOA derived from all classes of precursor included in this study (Gao et al., 2004 a,b; Iinuma et al., 2004; Baltensperger et al., 2005; Surratt et al., 2006; Kalberer et al, 2004; Sato et al., 2007). This is expected to increase SOA production, but no quantitative estimation technique is yet available.

Aqueous phase reactions have also been shown to lead to the production of high molecular weight compounds, as well as to the formation of organic acids such as malic, malonic, oxalic and succinic

acids, which are essentially non-volatile (Hallquist et al., 2009, and the references therein). However, this process also lacks any quantified description.

Likewise, important gaps remain in our knowledge of interactions of SOA with ice clouds. Prenni et al. (2009) found that SOA derived from ozonolysis of many types of alkenes (including certain terpenes and sesquiterpenes) are not efficient ice nuclei. However, Mohler et al. (2008) found that coating of dust particles with SOA generated from the ozonolysis of α-pinene reduced the ice-nucleating ability of the dust. Studies of low-temperature effects of SOA remain few, and once again no quantitative information is available on how SOA may influence ice clouds.

1.9 Modelling Studies

Relatively few global modelling studies that explicitly include SOA have been published to date. Some studies, such as those participiating in the AEROCOM initiative (Schulz et al., 2006), treat SOA implicitly by assuming that SOA is formed immediately and in fixed proportion to a precursor species (monoterpenes in the AEROCOM case) at the surface level (Dentener et al., 2006). Volatility is not treated in such models. With this approach these is no distinction between SOA and primary organic aerosols (POA), and accordingly both are lumped together.

Explicit treatment of SOA in models has to date been performed mainly for purposes of atmospheric chemistry studies rather than to examine the climate influence of such aerosols. The earliest such global model study is that of Chung and Seinfeld (2002). Only biogenic precursors (excluding isoprene, since this study predates the discovery that isoprene can be a significant source of SOA) were included in that study. A global annual mean SOA burden of 0.19 Tg from a production of 11.2 Tg/yr was estimated. Tsigaridis and Kanakidou (2003) included aromatic anthropogenic precursors (except benzene, also not known at that time to be a significant SOA precursor) in a sensitivity study that attempted to constrain the SOA production and atmospheric burden, estimating the production bounds to be 2.5 – 44.5 Tg/yr. Henze and Seinfeld (2006) first included SOA from isoprene in a global study, with the result that SOA production was increased by 17% and the SOA burden approximately doubled compared with the same model without isoprene. Hoyle et al. (2007), although using isoprene emissions lower than other models, estimated SOA production of 55-69 Tg/yr and a SOA burden of 0.52 – 0.70 Tg in the global annual mean. All these studies refer to present-day climate and emissions of SOA precursors. None made any attempt to describe the consequences for the climate system of the presence of SOA.

Other studies have attempted to describe the evolution of SOA over time. Tsigaridis et al. (2006) examined the evolution of the aerosol loading from preindustrial to present. Tsigaridis and Kanakidou (2006) estimated the change in aerosol composition from projected changes in future emissions, while Lathière et al. (2006) coupled a dynamic vegetation model to project future vegetation cover (and thence biogenic precursor emissions). Heald et al. (2008) applied a more sophisticated model that includes projected land use changes to the same end. All studies project a large future increase in SOA production and burden, largely due to a projected substantial increase in biogenic precursor emissions, which are known to rise with increasing temperature. However, none of these studies addresses the dependency of biogenic emissions on ambient CO_2 concentration.

To date, only one study has estimated radiative forcing of SOA (Hoyle et al., 2009). Recall that we define forcing as anthropogenic input to the climate system: accordingly, this study analysed the radiative effect of present day compared to preindustrial anthropogenic SOA precursor emissions, using an offline radiative transfer model, and found a direct forcing of -0.06 - -0.09 Wm^{-2}. Given that estimates of emissions of biogenic SOA precursors exceed those of anthropogenic precursors by an order of magnitude, this by itself indicates that the effect of biogenic SOA may be substantial.

No modelling study has so far attempted to quantify the biogenic contribution to the total aerosol direct effect. Neither has any modelling study attempted to estimate the indirect effects of SOA.

Furthermore, so far no study with explicit SOA treatment has been published based on a model that prognostically resolves the size distribution and mixing state of the aerosol. The advantages that such a model offers over bulk models in which these properties are prescribed are outlined by Stier (2005). Of these, it is worth repeating two here: that aerosol indirect effects are highly sensitive to the size distribution and that the radiative effect is affected by the mixing state. Thus for a study of SOA in the global climate system, a model that combines explicit SOA treatment with prognostic size distribution and mixing state as well as online radiative calculations offers great advantages.

1.10 Objectives of this work

In summary, considering that:

- Measurements and model studies indicate that the atmospheric SOA loading may be comparable to that of primary organics
- Models that do not take SOA into account frequently underestimate organic mass compared to observations
- SOA are found in pristine as well as polluted environments
- SOA may have very different horizontal and vertical distributions than POA or black carbon
- SOA may act as the key to a potentially significant biosphere-climate feedback

a study of the global influences of SOA is well warranted. This study will undertake a model-based approach that addresses the questions:

- What is the contribution of SOA to the aerosol direct effect? In particular, what is the contribution of the biosphere to this effect?
- What is the contribution of SOA to the aerosol indirect effect?
- Can the inclusion of SOA in a model resolve the discrepancy between observed and modelled organic aerosol concentrations?
- Does the inclusion of SOA in a model improve the agreement between model and globally observed aerosol properties (optical depth, size distribution,…) ?
- Are published projections of large future increases in SOA loading viable in the light of the dependence of biogenic emissions on CO_2?
- Does modelling of biogenic SAOA support the “biogenic thermostat” hypothesis?
- How do the biogenic and anthropogenic aerosols interact?

In the following chapters, these questions will be addressed in the following way: first, the model that will be used as the primary tool of this investigation will be described and evaluated. The properties of the tropospheric aerosol simulated by this model, with and without SOA, will be presented, together with estimates of the direct and indirect effects of SOA.

Thereafter, the dependency of the biogenic fraction on climate will be studied, and the “biogenic thermostat” hypothesis examined by model studies of different climate states.

Finally, the role of SOA in an atmosphere firstly free of, and then with, anthropogenic perturbation will be studied. Insights into how the role of biogenic aerosols in the atmosphere has been changed by the presence of anthropogenic aerosols will be presented.

A summary of findings and suggestions for future research directions will conclude this work.

Chapter 2

2 Estimating the effects of secondary organic aerosols upon the present climate

ABSTRACT

In recent years, several field measurement campaigns have highlighted the importance of the organic fraction of aerosol mass, and with such spatial diversity that one may assert that these aerosols are ubiquitous in the troposphere, with particular importance in continental areas. Investigation of the chemical composition of organic aerosol remains a work in progress, but it is now clear that a significant portion of the total organic mass is composed of secondary organic material, that is, aerosol that is not emitted to the atmosphere in particulate form, but formed *in situ* from gaseous volatile organic carbon (VOC) precursors. A number of such precursors, of both biogenic and anthropogenic origin, have been identified. Experimental, inventory building and modelling studies have followed. Laboratory studies have yielded information on the chemical pathways that lead to secondary organic aerosol (SOA) formation, and provided the means to estimate the aerosol yields from a given precursor-oxidation reaction. Other empirical studies have focused on the biogenic precursors, and have found that such emissions depend upon plant species, temperature, and, in certain cases, photosynthetically active radiation. Global inventories of anthropogenic VOC emissions, and of biogenic VOC emitter species distribution and their emission potential have been constructed. Building upon the results of empirical and inventory-building efforts, global models have been developed that provide estimates of global SOA precursor VOC emissions, SOA formation and atmospheric burdens of these species. Yet any overall estimate of the direct and indirect effects of these aerosols is still lacking. This paper makes a first step in that direction, presenting global estimates of these quantities, and tries to identify areas of research in this area that require prioritisation in the large-scale effort to better constrain our knowledge of the aerosol-climate system.

2.1 Introduction

Organic aerosols constitute an important part of the tropospheric aerosol loading. In regions affected by anthropogenic pollution, organic species have been observed to be the second most abundant component by mass after sulphate, and frequently the most important contributor to aerosol light scattering (Hegg et al., 1997; Novakov et al., 1997; Ramanathan et al., 2001).In tropical forested area, it forms the dominant part of the aerosol mass (Andreae and Crutzen, 1997; Artaxo et al., 1988, 2002), even in the absence of large-scale biomass burning. Organic aerosols are found in the remote marine environments (Middlebrook et al. 1998), in the free troposphere (Huebert et al., 2004; Heald et al., 2005) and in the upper troposphere (Murphy et al., 1998; Froyd et al., 2009).

Organic aerosol may be formed by direct emission into the atmosphere in the particle phase (primary organic aerosols, POA) or by condensation into the particle phase of organic species created by the oxidation of a gas-phase precursor (secondary organic aerosol, SOA). Both biogenic and anthropogenic precursors are known. Estimates of global emissions of precursors of biogenic (Guenther et al. 1995, 2006) and of anthropogenic (van Aardenne et al., 2005) precursors indicate that biogenic emissions (of the order of hundreds of Tg) are an order of magnitude greater than those of known anthropogenic precursors.

In 1997, Andreae and Crutzen (Andreae and Crutzen, 1997) suggested, based only on then-known biogenic precursors, that SOA production could be of the order of 30-270 Tg/yr, comparable to contemporary estimates of sulphate aerosol production. Furthermore, some measurements show a concentration of organic aerosol that is well above that predicted by the current generation of global aerosol-climate models (Heald et al., 2005; Volkamer et al., 2006). Most such models include only POA or include SOA in a very simple, implicit treatment, for example the AEROCOM approach (Dentener et al. 2006), in which SOA is considered to be formed in fixed proportion to prescribed monoterpene emissions in each grid box, and to have identical properties to (and therefore possible to lump together with) POA.

Explicit treatment of SOA in models has to date been performed mainly using atmospheric chemistry models and few have attempted to quantify the climate influence of such aerosols in isolation. Chung and Seinfeld (2002), considering only biogenic precursors, estimated a global annual mean SOA burden of 0.19 Tg from a production of 11.2 Tg/yr. Tsigaridis and Kanakidou (2003) included anthropogenic aromatic precursors (not including benzene, also not known at that time to be a significant SOA precursor) in a sensitivity study that attempted to constrain the SOA production and atmospheric burden, estimating the production bounds to be 2.5 – 44.5 Tg/yr. These studies exclude isoprene, since they predate the discovery that isoprene can be a significant source of SOA. Henze and Seinfeld (2006) first included SOA from isoprene in a global study, with the result that SOA production almost doubled and the SOA burden more than doubled (to 16.4 Tg/yr and 0.39 Tg respectively) compared with the same model without SOA from isoprene. Hoyle et al. (2007), although using isoprene emissions lower than other models, estimated SOA production of 55-69 Tg/yr and a SOA burden of 0.52 – 0.70 Tg in the global annual mean. All these studies refer to present-day climate and emissions of SOA precursors. None made any attempt to describe the consequences for the climate system of the presence of SOA. Hoyle et al. (2009), using an offline radiative transfer model, and assuming an external aerosol mixture, estimated the radiative forcing of anthropogenic SOA to be -0.06 - -0.09 Wm^{-2}.

In this chapter, we will study how the aerosol direct effect and indirect effects are affected by secondary organic aerosols using the aerosol-climate model ECHAM5/HAM, which has been extended to handle SOA. This allows us to deploy a model with online radiation and cloud microphysics that are coupled to an aerosol population which is resolved in both aerosol size distribution and mixing state. Both particle size distribution and mixing state are important for the calculation of radiative properties, and at least the size distribution is important for aerosol indirect effects (Stier et al., 2005).

2.2 Model Description

The model upon which in this study is based is ECHAM5/HAM, described and evaluated in Stier et al. (2005), with extensions described in Stier et al. (2007), and with cloud microphysics described in Lohmann et al. (2007). Here, only a brief synopsis of the main model features is given: for details, the reader is referred to the works cited above.

ECHAM5/HAM is a modal model that describes the aerosol population as a superposition of seven pseudo-lognormal modes. For each mode, aerosol mass and number concentration are prognostic variables. Four of these modes are termed ‘soluble’, which means, in the context of this model, that the mode may take up water. Soluble modes are regarded as internally mixed, and cover the size ranges 1-10 nm (nucleation mode), 10-100 nm (Aitken mode), 100nm - 1μm (accumulation mode) and > 1 μm (coarse mode) particle diameter. Insoluble modes do not take up water, are regarded as externally mixed and cover Aitken, accumulation and coarse modes. The modelled aerosol species are sulphate, black carbon, organic carbon, sea salt and mineral dust. In the original model version, ‘organic carbon’ refers to POA plus SOA formed by assuming a fixed 15% SOA yield from the monoterpene emissions estimates of Guenther et al. (1995), with immediate non-volatile SOA production in the emitting gridbox. This approach is no longer used. Modelled processes include emission, aerosol microphysics (water

uptake, condensation of SO_4 from the gas phase, new particle nucleation, and coagulation), sink processes (wet deposition, dry deposition and sedimentation) and cloud droplet activation. Cloud droplet number concentration (CDNC) and ice crystal number concentration (ICNC) are calculated as functions of the aerosol size distribution and possibly composition, depending on the activation scheme chosen. The model includes a simple sulphate chemistry scheme, for which prescribed monthly mean oxidant concentrations with a superimposed diurnal cycle are used.

2.2.1 Emission of SOA Precursors

Precursor species included in the model are isoprene and monoterpenes, which are emitted by vegetation, and toluene, xylene and benzene, which are anthropogenic.

Emission of biogenic species is calculated online in the model using MEGAN (Guenther et al. 2006; Guenther, 2007) for isoprene and the earlier work of (Guenther et al. 1995) for monoterpenes. No distinction is made between different monoterpene species: α-pinene is used as a surrogate for all monoterpenes. Isoprene emission is calculated using the parameterised canopy environment emission activity (PCEEA) approach of the MEGAN model. Leaf age and soil moisture are not taken into account in this implementation. Leaf area index (LAI) is prescribed, varying monthly. Emissions of monoterpenes then depend on temperature and LAI only and those of isoprene on temperature, LAI and photosynthetically active radiation. Note that in the formulations provided by these parameterisations, 'temperature' means leaf temperature. This is not available in ECHAM5/HAM; instead the lowest model level temperature is used.

Emission of anthropogenic species is according to the EDGAR (fast-track 2000 issue, hereafter FT2000, (van Aardenne et al., 2005)). The FT2000 issue does not provide explicit speciation of the emitted volatile organic compounds (VOC), in contrast to the 1990 issue. We assume that the species mix is identical in both. The fraction of total VOC that each included species makes up is calculated from the 1990 dataset and applied in turn to the FT2000 dataset to obtain the year 2000 estimate. The 1990 dataset includes emissions of trimethylbenzene and a group labeled 'other aromatics'. Trimethylbenzene is a known SOA precursor and is lumped together with xylene. 50% of the 'other aromatics' are also included in this class. No information is available on the diurnal or seasonal variation of anthropogenic VOC on a global basis, so emissions are treated as constant in time. The annual flux of each anthropogenic precursor is shown below.

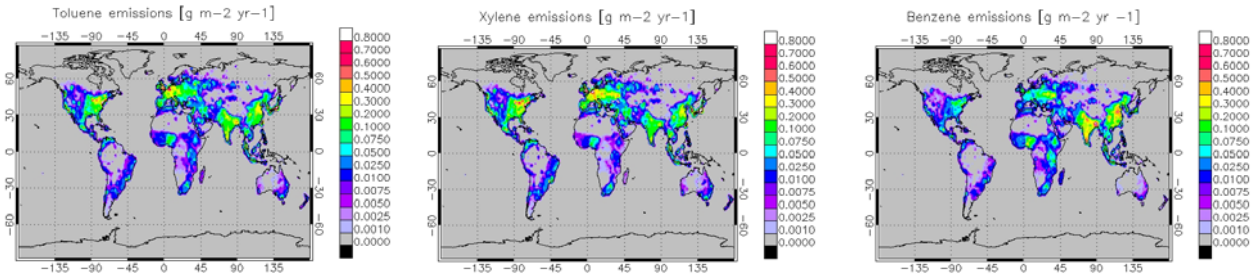

Figure 2.1. Anthropogenic SOA precursor emissions.

Toluene and xylene emissions are closely connected to fossil fuel production and use, and emission of these species is greatest in north-western Europe, the north-eastern United States and in East Asia. Benzene is a known carcinogen and is tightly regulated in the United States and Europe; it has greatest emission in south and east Asia.

Precursors only exist in the gas phase in the model.

2.2.2 Formation of SOA

In this model version, due to the heavy computational cost of the many tracers introduced into the aerosol scheme, chemistry is kept to a bare minimum. For biogenic precursor species, oxidation reactions with OH, O_3 and NO_3 are taken into account, but only the major pathway (OH in the case of isoprene and O_3 in the case of monoterpenes) are considered to produce SOA. For aromatics, only oxidation by OH is considered, with the exception of the reaction of xylene with NO_3 (which is not considered to produce SOA).

A drawback of this approach is that the known dependency of SOA yield on ambient NO_x (Presto et al. 2005; Kroll et al. 2006; Ng et al. 2007b) is lacking in the model. The entire atmosphere is treated as low-NO_x, a point to which we shall return in the discussion of the model results.

The two-product model of SOA formation is used. This model is founded on the work of Odum and colleagues (Odum et al. 1996), who showed that for a reaction yielding many semi-volatile species, the aerosol yield *Y*, defined as

$$Y = \frac{\Delta M}{\Delta HC} \tag{2.1}$$

where ΔM is the change in aerosol mass and ΔHC is the mass of precursor hydrocarbon consumed, can be modelled by assuming that the reaction produces only two condensable species. Denoting these species as P_1 and P_2, the aerosol mass yield for a given reaction can be characterised in terms of four empirical parameters, one to describe the stoichiometric mass yield of each product from the precursor-oxidant reaction and another to describe the volatility of each product. The gas-phase reaction of a precursor *PRE* and oxidant *OX* and subsequent gas-aerosol partitioning of the two hypothetical products is described by

$$PRE + OX \rightarrow \alpha_1 P_1 + \alpha_2 P_2 \tag{2.2}$$

where α_1 and α_2 are mass-based stoichiometric coefficients and

$$A_i = K_{p,i} M_0 G_i \tag{2.3}$$

where A_i (i = 1,2) denotes the mass of product P_i that resides in the aerosol phase and G_i in the gas phase, $K_{p,i}$ is a *partitioning coefficient* for the organic mass, and M_0 is the total SOA-absorbing mass in the aerosol phase.

Ng et al. (2007a) found that in the case of low NO_x, SOA formed from xylene, toluene and benzene is effectively non-volatile. This allows us to represent the SOA yield from these precursors in terms of a single product species that, after formation, condenses immediately to the aerosol phase.

The concentrations of oxidant species are assumed to be governed by much faster reactions than these, that is, a quasi-steady state assumption applies, and the oxidant concentrations are prescribed (as in Stier et al. (2005)), except that NO_3 is added using the multi-model mean computed for year 2000 by the RETRO re-analysis project (http://retro.enes.org/index.shtml). The constancy of the oxidant fields over each model timestep makes the system simple enough to solve analytically. The scheme and its solution are presented formally in Appendix I. Two-product parameters and reaction rates are given in Table 2.1.

Gas	Oxidant	α_1	α_2	$K_{p,1}$	$K_{p,2}$	Source	Rate[4]	Source
MT	O_3	Note 1	Note 2	2.3	0.028	Saathoff et al. (2008)	$6.3x10^{-16}$exp(-580/T)	IUPAC
MT	OH	-	-	-	-	-	$1.2x10^{-11}$exp (440/T)	IUPAC
MT	NO_3	-	-	-	-	-	$1.2x10^{-12}$exp(490/T)	IUPAC
IS	O_3	-	-	-	-	-	$1.03x10^{-14}$exp(-1995/T)	IUPAC
IS	OH	0.232	0.0288	0.00862	1.62	Henze and Seinfeld (2006)	$2.7x10^{-11}$exp(390/T)	IUPAC
IS	NO_3	-	-	-	-	-	$3.15x10^{-12}$exp(-450/T)	IUPAC
TOL	OH	0.36	0	Note 3	Note 3	Ng et al. (2007a)	$1.81x10^{-12}$exp(338/T)	MCM[5]
XYL	OH	0.30	0	Note 3	Note 3	Ng et al (2007a)	$2.31x10^{-11}$	MCM[5]
XYL	NO_3	-	-	-	-	-	$2.6x10^{-16}$	MCM[5]
BENZ	OH	0.37	0	Note 3	Note 3	Ng et al (2007a)	$2.33x10^{-12}$exp(-193/T)	MCM[5]

Note 1: Temperature dependent, given as 0.715-0.002*T* by Saathoff et al. (2008)
Note 2: Temperature dependent, given as 1200*exp*(-*T*/35) by Saathoff et al. (2008)
Note 3: Treated as non-volatile
Note 4: *T* is temperature in Kelvin
Note 5: Master Chemical Mechanism, University of Leeds, United Kingdom. http://mcm.leeds.ac.uk/MCM/

Table 2.1. Reaction rates and SOA formation parameters.

2.2.3 SOA gas-aerosol partitioning

Equation (2.3) describes only the partitioning between the gas phase mass and the total aerosol phase SOA mass. In our model, this is not sufficient since we must determine the mass that partitions to each of the size-resolved modes. Firstly, we must consider what is meant by the term M_0 in (2.3). The underlying theory developed by Pankow (Pankow, 1994a, 1994b) is based on absorption and not *ad*sorption. This means that SOA must be able to partition into the bulk of the material considered as absorber, not just attach to surface sites. For this reason, we exclude black carbon, mineral dust and crystalline salts as SOA absorbers. Note, however, that in ECHAM5/HAM, 'sulphate' encompasses more than just salts; in particular it includes sulphuric acid. In the light of the effect of seed particle acidity on SOA discussed in chapter 1.5, this suggests that sulphate may play a role in determining the gas-aerosol partitioning of SOA; however, all such identified mechanisms are chemical and not purely thermodynamic mechanisms, which means that they cannot be quantified through the Pankow theoretical framework. Nonetheless, previous studies (Tsigaridis and Kanakidou, 2003; Hoyle et al. 2007) have examined the effect of counting sulphate mass as SOA absorbing. That approach is not repeated here because of the non-physical nature of such calculation.

Perhaps a more intractable question concerns SOA and aerosol water. Many SOA species are to some degree water-soluble and SOA is (usually weakly) hygroscopic. So one may pose the question: does water take up SOA or does SOA take up water? The answer can of course be 'both'. However, since, in most regions, water uptake is mainly determined by the aerosol inorganic fraction, for the purposes of this study, the answer will be taken to be that SOA takes up water but water does not take up SOA. This leaves organic carbon as the only absorber of SOA. We assume SOA uptake on primary organics and that each aerosol phase SOA species can take up all SOA species from the gas phase. Hence, the non-volatile absorbing mass m_{nv} of Pankow's theory consists of POA and non-volatile SOA only.

Pankow (1994a) derived an expression for the partitioning coefficient $K_{p,i}$ in terms of temperature and aerosol solution properties, here presented in the slightly modified form of Seinfeld and Pankow (2003), and in terms of SI units:

$$K_{p,i} = \frac{RT}{MW_{OM}\zeta_i p_i^0} \tag{2.4}$$

where MW_{OM} is the mean molecular weight of the organic aerosol, R the universal gas constant, T the temperature, ζ_i the activity coefficient of compound i and p_i^0 its saturation vapour pressure. We take the activity coefficient of each compound to be unity. The Clausius-Clapeyron equation for the temperature dependence of p_i^0 applied to (2.4) then allows us to calculate $K_{p,i}$ at any temperature from that at a reference temperature T_{ref}, where the partitioning coefficient is $(K_{p,i})_{ref}$:

$$K_{p,i} = \left(K_{p,i}\right)_{ref} \frac{T}{T_{ref}} \exp\left[\frac{\Delta H_i}{R}\left(\frac{1}{T} - \frac{1}{T_{ref}}\right)\right] \tag{2.5}$$

where ΔH_i is the enthalpy of vaporisation of compound *i*. ΔH_i is taken as 42 kJ/mol (Henze and Seinfeld 2006) for isoprene-derived SOA. For monoterpene-derived SOA, the two products are assigned ΔH_i values of 59 kJ/mol and 24 kJ/mol (Saathoff et al. 2008).

The aerosol absorbing mass M_0 has been qualitatively discussed above. Knowing this parameter is a prerequisite for calculation of the gas-aerosol phase partitioning. Here it is described how this is quantitatively handled. In this model, SOA partitioning is calculated independently of SOA formation. SOA is transported and can evaporate or condense as ambient conditions vary. The total (aerosol plus gas) SOA mass for each species is transported, and subsequently the gas and aerosol phase masses in each size class are diagnosed. This results in considerable CPU saving compared to transporting mass of gas and of each applicable aerosol size class for each species. Where S_i is the total mass of semi-volatile SOA species *i,* and A_i and G_i its aerosol and gas phase masses respectively, then of course

$$S_i = A_i + G_i \tag{2.6}$$

Substituting from (2.3) and rearranging gives

$$G_i = \frac{S_i}{1 + K_{p,i} M_0}, \text{ and} \tag{2.7}$$

$$A_i = \frac{K_{p,i} M_0 S_i}{1 + K_{p,i} M_0} \tag{2.8}$$

Thus the SOA absorbing mass M_0 must be known before the partitioning can be calculated, although it is itself a function of the SOA aerosol mass, as discussed in the first paragraph of this subchapter. Recalling that in this model, M_0 consists of a non-volatile part M_{NV} (which consists of POA and non-volatile SOA), plus all condensed SOA,

$$M_0 = M_{NV} + \sum_i A_i \tag{2.9}$$

Substituting from (2.8), we have finally

$$M_0 = M_{NV} + M_0 \sum_{i=1}^{n} \frac{K_{p,i} S_i}{1 + K_{p,i} M_0} \tag{2.10}$$

Thus, since the total non-volatile and semi-volatile masses M_{NV} and S_i are known, we can compute M_0 and thence the gas and aerosol phase masses of the semi-volatile species. So far, we have presented nothing new with respect to SOA partitioning and (2.10) and the foregoing equations have been stated in many previous works (e.g. Seinfeld and Pankow (2003), Tsigaridis and Kanakidou (2003), Hoyle et al. (2007)) However, none has established whether (2.10) has a unique solution. Is it possible that a system consisting of many semi-volatile species has multiple gas-aerosol equilibria with different aerosol compositions? Note that by multiplying both sides of (2.10) successively by $(1+K_{p,i}M_0)$ for each *i,* it can be expressed as a polynomial of degree n+1, having accordingly n+1 solutions. So at least mathematically, (2.10) does not, *a priori*, exclude such multiple equilibria. In Appendix II it is shown that there is only one physical (real, nonnegative) solution and equilibrium is indeed unique. Furthermore, since there is no general solution to a polynomial of degree 5 or higher, (2.10) must be numerically solved for $n \geq 4$ (i.e. 2 or more precursors).

We now come to the question of how SOA partitions between aerosols of different size classes. Repeating the derivation of Pankow (1994a, 1994b) supposing that there exists a partitioning coefficient $K_{p,i,j}$ for species i in each mode j results in a similar expression to (2.4)

$$K_{p,i,j} = \frac{RT}{MW_{OM,j} \zeta_{i,j} p_i^0} \tag{2.11}$$

where $MW_{OM,j}$ is the mean molecular weight of the organic species in mode j, and $\zeta_{i,j}$ the activity coefficient for species i the mode. The ratio of mode to bulk partitioning coefficient is then

$$\frac{K_{p,i,j}}{K_{p,i}} = \frac{MW_{OM} \zeta_i}{MW_{OM,j} \zeta_{i,j}} \tag{2.12}$$

Since the activity coefficients are taken to be unity for all modes, only the ratio of the mean molecular weights remains, for which unity is a reasonable assumption. Then the bulk partitioning coefficient can be used for all modes.

It is shown in Appendix III that the neglect of the activity coefficient ζ_i is consistent with a SOA partitioning between different size classes according to the fraction of *non-volatile* absorbing aerosol mass in each mode. That is, if M_{NV} and A_i are the total non-volatile absorbing mass and the total aerosol phase mass of the i^{th} SOA species, and M_{NVj} and A_{ij} the respective quantities in mode j, then

$$\frac{A_{ij}}{A_i} = \frac{M_{NVj}}{M_{NV}} \tag{2.13}$$

Since mass is proportional to the cube of the radius (all particles are assumed spherical in ECHAM5/HAM), this means that at equilibrium, SOA partitions strongly in favour of the larger modes. In reality, of course, the size distribution of an aerosol population is not static, as has been implicitly assumed in the derivation of (2.10). However, vapour-liquid equilibration times are very short (Seinfeld and Pandis 2006) compared to the model timestep, which allows us to make this assumption. (2.11) has particular consequences for impact of SOA on cloud condensation nuclei (CCN), for these are larger particles: so SOA will preferentially condense on particles that are already of CCN size.

A consequence of the choice of an absorption model and the exclusion of mineral dust as absorber is that, in the model, SOA cannot condense on the accumulation and coarse insoluble modes, which, in ECHAM5/HAM contain only mineral dust. However, thermodynamic data (such as enthalpy of adsorption) that would permit one to calculate adsorptive partitioning do not exist.

2.2.4 Measuring model SOA production

In this model, gas phase oxidation of the precursor species yields gas phase condensable species. For biogenics, such species may condense and re-evaporate at each subsequent timestep until their removal from the atmosphere. In other words, since chemistry of SOA production is pure gas phase chemistry, the idea of 'SOA production' actually means 'net condensation flux'. This is not a problem for anthropogenic species, since they are considered non-volatile and 100% of the oxidation products condense and remain in the aerosol phase. For semi-volatile species, it is not obvious how to measure this quantity, since the aerosol mass changes in response to ambient conditions. For the same reason the notion of SOA *yield* as defined in (2.1) is not applicable to the semi-volatile species either.

We can, nonetheless, measure these quantities for semi-volatile species in another way. While the total net condensation flux is not directly available from the equilibrium partitioning scheme, we do know the total sink flux. On the assumption of source-sink aerosol mass balance over a model integration period, (in which one may have some confidence, if not proof, if the total semi-volatile budget is balanced for the species in question), then the production term may be assumed to be the same as the sum of the sink terms. The *model SOA yield* can then de defined as the ratio of the ratio of the production (or sink) flux to the total precursor emission flux, averaged over an integration period. Formally, for a model integration between times T_1 and T_2, the model SOA yield Y_M is

$$Y_M = \frac{\int_{T_1}^{T_2} F^{\downarrow}(t)dt}{\int_{T_1}^{T_2} E^{\uparrow}(t)dt} \tag{2.14}$$

where $F^{\downarrow}(t)$ is the sum of the deposition fluxes derived from a given precursor as a function of time t and $E^{\uparrow}(t)$ the emission flux of that precursor. This is fully equivalent to the usual chamber study definition of SOA yield (2.1) when the chamber yield is measured after consumption of the total precursor mass.

Similarly, the *model lifetime* τ_M of semi-volatile species in the aerosol phase can be defined as the ratio of the mean aerosol burden $B(t)$ to the integrated production (sink) flux:

$$\tau_M = \frac{\frac{1}{T_2 - T_1}\int_{T_1}^{T_2} B(t)dt}{\int_{T_1}^{T_2} F^{\downarrow}(t)dt} \tag{2.15}$$

Clearly, (2.14) and (2.15) are applicable only as global total metrics. Similarly, for semi-volatiles, SOA production only has meaning as a global total, not as a per-gridpoint quantity.

2.2.5 Aerosol water uptake

The original ECHAM5/HAM water uptake scheme is that of Jacobson et al. (1996), which models water uptake by electrolytic species. In order to take into account uptake of water by organics, the semi-empirical scheme of Petters and Kreidenweis (2007) has been chosen on the basis of its computational efficiency (it requires computation of only a single free parameter κ). For sulphate, sea salt and organic species, the appropriate mean growth factor (GF) derived κ value found in Petters and Kreidenweis (2007) is used.

The overall internally mixed aerosol κ is the volume-weighted sum (over the soluble fraction, i.e. in the soluble modes only, and excluding any black carbon and dust) of the individual compound κ values, as per equation (7) in Petters and Kreidenweis (2007). The growth factor can be calculated using equation (11) in that paper, *viz.*

$$RH \exp\left[-\frac{A}{D_d\, gf}\right] = \frac{gf^3 - 1}{gf^3 - (1-\kappa)} \tag{2.16}$$

where *gf* is the growth factor, *RH* the relative humidity (in the *cloud-free* fraction of the gridbox) on the fractional scale, D_d is the particle dry diameter and *A* is the Kelvin term

$$A = \frac{4\sigma_{s/a} M_w}{RT\rho_w} \tag{2.17}$$

where $\sigma_{s/a}$ is the surface tension of water (0.072 Jm^{-2}) (note that any surface tension effect of the solutes are encapsulated in the κ parameter), M_w is the molecular weight of water and ρ_w its density. In this implementation, to minimise computational costs, (2.17) is solved offline for *gf* as a function of *T*, *RH*, D_d and κ and the results stored in a lookup table. Once D_d and κ have been calculated for each mode, we can then simply look up the growth factor (interpolation to the lookup table values is linear in *T*, *RH* and κ, and linear in the logarithm of D_d).

2.2.6 *Nucleation*

Organics do not participate in the nucleation process in the model. While there is ample observational evidence of organic material in freshly-nucleated particles, (for example, Smith et al. (2008) observed organic content of up to 84% by mass in freshly-nucleated particles), we must note that such organic content could arise either purely by condensation of organic vapours on a pre-existing particle, or by participation by organics in the creation of the particle from the gas phases, as suggested by Bonn and Moortgat (2003) and Bonn et al. (2008) for sesquiterpene oxidation products. The distinction is important, for in the former case, organics influence only aerosol mass, and in the latter case aerosol number as well as mass. This point is further discussed in chapter 2.6.3.

Growth of nucleation mode particles by condensation of SOA vapours has been implicitly discussed in the section on partitioning (chapter 2.2.3). There the idea of SOA uptake by inorganic species, namely sulphate and water, was discussed. (In ECHAM5/HAM, the nucleation mode contains only sulphate and water). Allowing SO_4 to contribute to the SOA absorbing mass M_0 is thus a crude (and non-physical) way

to represent growth of freshly-nucleated particles by SOA condensation. Such an approach also affects fresh and aged, smaller and larger, and acidic and neutral particles in the same manner. The nucleation mode is likely to contain the highest fraction of unneutralised sulphuric acid. A physical representation of this process requires some more sophisticated chemistry and is thus beyond the scope of this study

2.2.7 Sink processes for SOA

SOA is subject to wet deposition, dry deposition and sedimentation (Stier et al. 2005) as for all other model aerosol species. In addition, wet and dry removal of the condensable gas phase species is considered. However, ECHAM5/HAM includes below-cloud scavenging only for aerosols, not gases.

2.2.8 SOA and cloud processes

In the simulations described herein, cloud droplet activation is calculated according to the scheme of Lin and Leaitch (1996), in which only the aerosol size, not its composition, is taken into account. Thus SOA affects cloud droplet number only through its effect on particle size, not hygroscopicity or by affecting the surface tension of droplets. Clouds affect SOA through the above-described wet sink processes.

No aqueous-phase SOA chemistry is included.

2.3 Model Results: Introduction of SOA

The experiments described herein are simulations of the year 2000, obtained by nudging the model to the ECMWF ERA-40 reanalysis data (Uppala et al.,2000) for that year (following three months' spinup time). The model dynamics are calculated in spectral space with triangular truncation at term 63 (T63), while physics are calculated on a 1.8°*x*1.8° Gaussian grid. The simulations use 31 vertical levels, from the surface to 10 hPa.

The model diagnostics are output 6 simulated hours. A diagnostic variable may be a mean over the period or an instantaneous value at the output timestep, as appropriate (precipitation rate is an example of the former, surface pressure an example of the latter).

2.3.1 Biogenic Emissions

Seasonal averages of the spatial distributions of isoprene and monoterpene emission for the northern hemisphere winter and summer are shown in figure 2.2. Observe that different scales are used for isoprene and for monoterpenes. Global annual totals are calculated as 446 Tg/yr isoprene and 89 Tg/yr monoterpenes. This compares with a figure of 17 Tg/yr for the sum of the anthropogenic precursors (6 Tg/yr toluene, 6 Tg/yr xylene and 5 Tg/yr benzene).

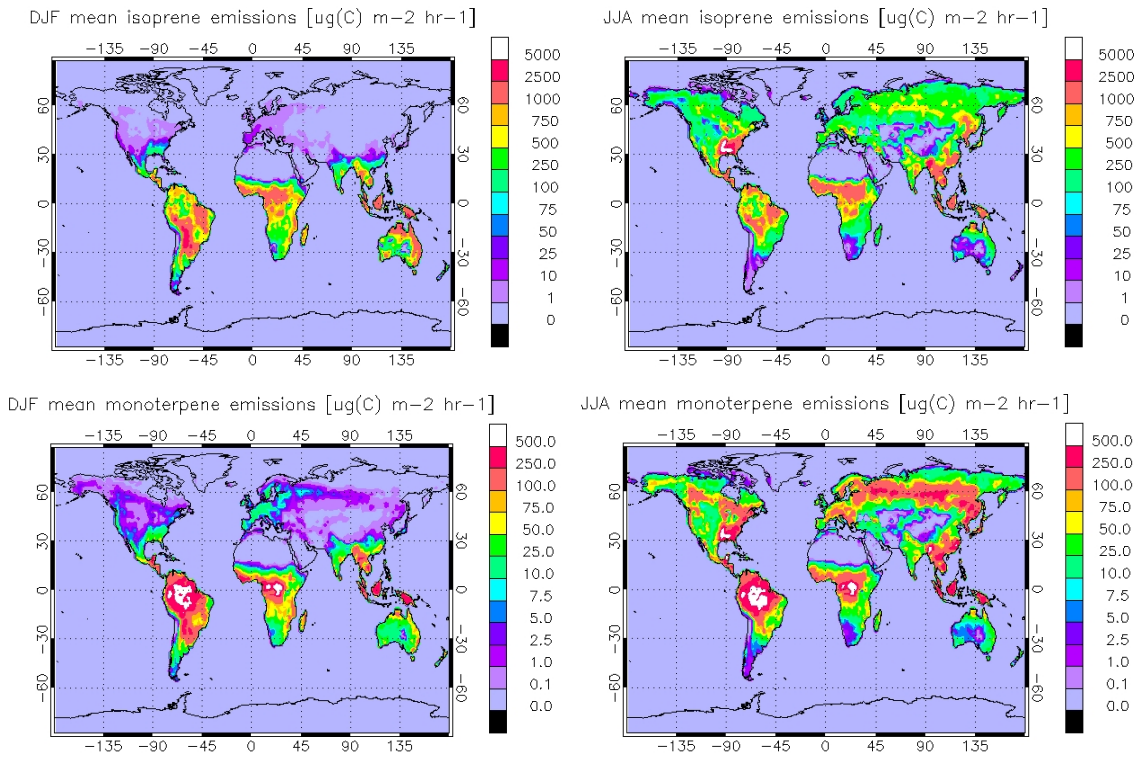

Figure 2.2. Seasonal variations of biogenic emissions

The year-round high temperatures and insolation of the tropics, together with the large LAI of tropical broadleaf trees, means that these are the dominant source regions. Over three quarters of the total model biogenic VOC emission (77% and 79% isoprene and monoterpenes respectively) takes place in tropical latitudes.

Anthropogenic precursors are prescribed model inputs as described in chapter 2.2.1 and are not further treated here.

2.3.2 Sinks of SOA precursors

While dry deposition is applied to all precursor gases, and wet deposition to the weakly soluble biogenic precursors, the great majority of all precursor gases in the model are chemically removed from the atmosphere. The precursor mass budget is presented in Table 2.3, with wet deposition excluded (it is five orders of magnitude weaker than the dry deposition term).

2.3.3 Precursor burden and lifetime

There is a clear contrast between the anthropogenic and biogenic precursors in that the highly reactive biogenic precursors are essentially confined to the regions of their production, whereas the more slowly reacting (at least in wintertime) anthropogenic precursors spread across the northern hemisphere.

Despite the lack of any seasonality in the anthropogenic emissions, a clear seasonal cycle can be seen in the precursor burdens. In the northern hemisphere high latitudes, the precursor concentrations build up under the weak wintertime photochemical sink and fall again in spring as sunlight returns to the polar regions. This gives rise to enhanced anthropogenic SOA production under the Arctic spring, which

suggests an anthropogenic SOA contribution to the formation of Arctic haze. However, it must be emphasised that at no time does this model produce an aerosol optical depth sufficient to be qualified as 'haze' at these latitudes. Furthermore, one should bear in mind the model assumption that anthropogenic precursors remain in the gas phase at all times. Given that all these species exist primarily as liquids even at room temperature, at polar winter conditions this assumption may well be flawed.

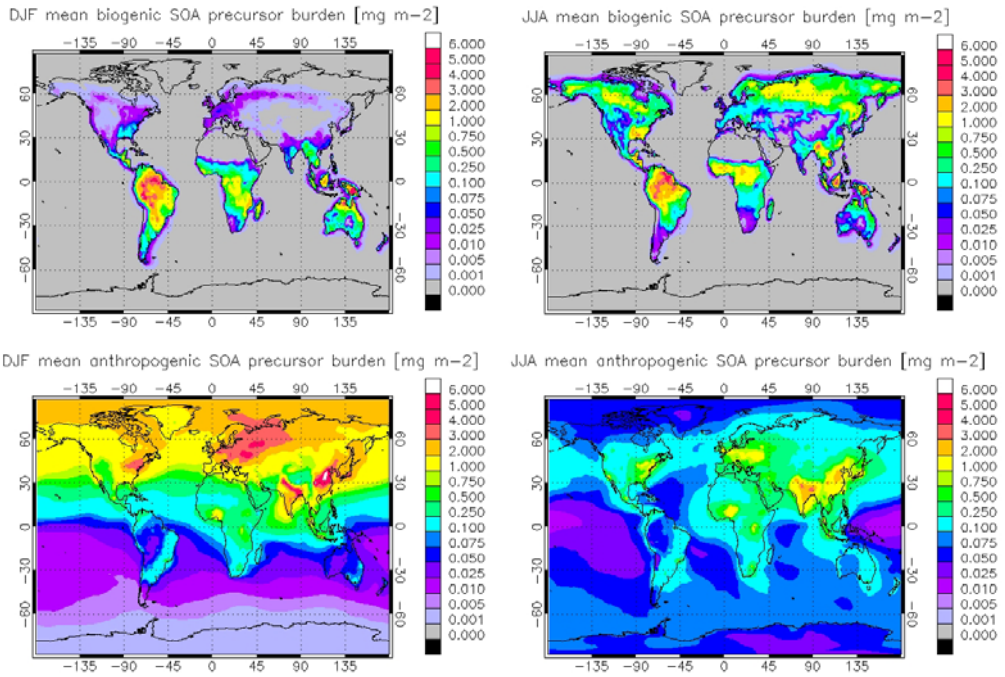

Figure 2.3. Wintertime (left) and summertime (right) mean burden of biogenic (above) and anthropogenic (below) SOA precursors

Precursor	Emission [Tg/yr]	Chem. Sink [Tg/yr]	Dry Dep. [Tg/yr]	Balance[1] [%]	Burden[2] [Tg]	Lifetime [days]
Isoprene	446	445	1.4	0.02	0.042	0.034
Monoterpenes	89	87.5	1.3	0.00	0.018	0.074
Toluene	5.7	5.5	0.22	0.75	0.037	2.4
Xylene	6.3	6.1	0.17	0.30	0.014	0.83
Benzene	4.9	4.7	0.26	2.0	0.13	9.4

[1] (source – sink)/source, absolute value
[2] annual mean

Table 2.2. SOA precursor budget.

2.3.4 SOA Production

Anthropogenic precursor emissions having no diurnal or seasonal variation in the model, the seasonal variability in anthropogenic SOA production is, as one would intuitively expect, rather limited, with monthly global total production varying from 0.42 to 0.50 Tg/month. The global maximum production takes place in Northern Hemisphere (NH) spring, due to the precursor reservoir built up at high latitudes during the winter. Springtime production within the NH high latitudes (60°- 90°N) is approximately double the summertime production despite the increased insolation. However, the contribution of these latitudes to the global total is small (about 3% in spring), and Europe, the United States, Japan, China and India are the main source regions.

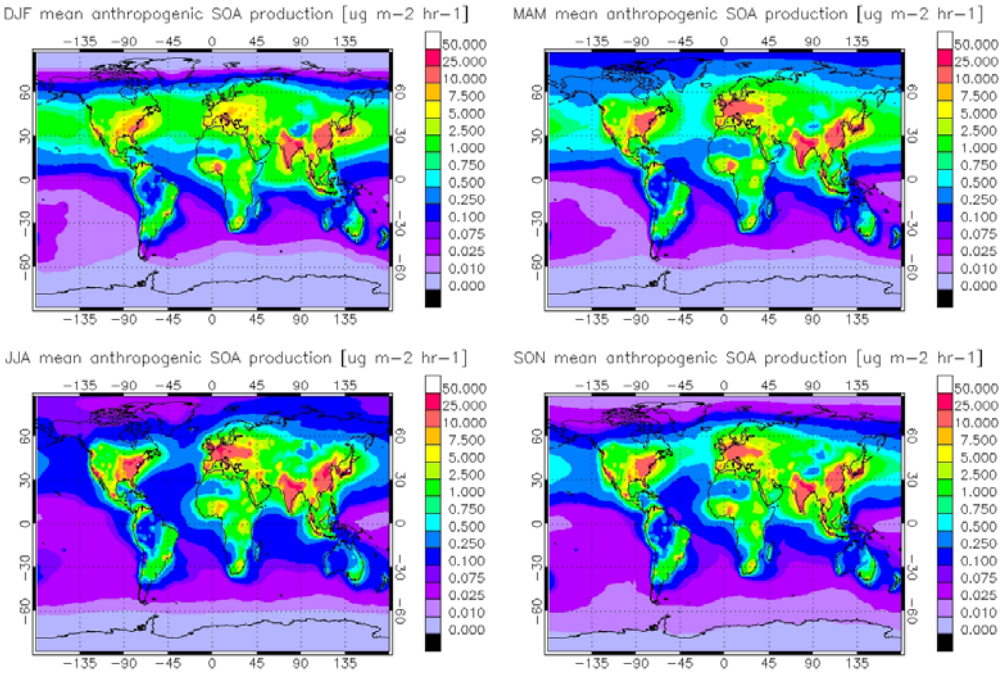

Fig 2.4 Seasonal mean anthropogenic SOA production (vertically integrated)

Production of biogenic species, since these are semi-volatile, is only possible to estimate as a global total according to the methodology of chapter 2.2.4.

2.3.5 SOA sinks and atmospheric burden

Once produced, the behaviour of semi-volatile and non-volatile species in the atmosphere is quite different. Non-volatile species remain permanently in the aerosol phase, and thus have only same sinks (wet deposition, dry deposition and sedimentation) as primary aerosol species. For semi-volatile species, in contrast, we must also consider removal of the species from the gas phase.

For the non-volatile species, the sink fluxes are in much the same ratios as for primary OC, with wet deposition removing over 90% of the aerosol mass from the atmosphere. One may note that despite the affinity of SOA for larger aerosol particles in the model, sedimentation remains a very weak sink for organic mass. This is especially so for the biogenic species, most likely because they are semi-volatile and evaporate in warm near-surface conditions.

For semi-volatile SOA formed form isoprene and monoterpenes, the largest sinks are directly from the gas phase.

The methodology proposed in chapter 2.2.4 for SOA production and lifetime leads to estimates of 17 Tg/yr and 4.0 Tg/yr aerosol from isoprene and monoterpenes respectively. Together with the estimated 5.6 Tg/yr from anthropogenic precursors, this gives a total of approximately 27 Tg/yr, compared with the total model POA sources of 47 Tg/yr. It is notable that the model isoprene-derived SOA burden exceeds that of SOA from monoterpenes and anthropogenic precursors by an order of magnitude, a ratio considerably greater than that between the estimated respective aerosol production fluxes, and that its estimated lifetime is also much larger. This is due to the particular vertical distribution of model isoprene SOA, which is discussed in chapter 2.3.7.

The SOA budget is presented in table 2.3.

SOA Precursor	Prod[1] [Tg/yr]	Wet Dep.(g) [Tg/yr]	Wet Dep.(a) [Tg/yr]	Dry Dep.(g) [Tg/yr]	Dry Dep.(a) [Tg/yr]	Sed [Tg/yr]	Balance[2] [%]	Burden[3] [Tg]	Lifetime[3] [days]
Isoprene	17	64	16	24	0.70	0.027	3.0	0.71	15.5
Monoterpenes	4.0	6.0	3.7	2.8	0.32	0.013	2.0	0.064	5.8
Anthropogenics	5.6	0	5.3	0	0.26	0.032	0.75	0.074	4.8

[1] production of SOA from isoprene and monoterpenes is estimated as Wet Dep(a) + Dry Dep(a) + Sed
[2] (production-all sinks)/production, absolute value
[3] annual mean

Table 2.3. Budget of modelled SOA per precursor species

2.3.6 Geographical and seasonal distribution of SOA

The geographical distributions of the annual mean and seasonal mean anthropogenic SOA burdens are shown in figure 2.5.

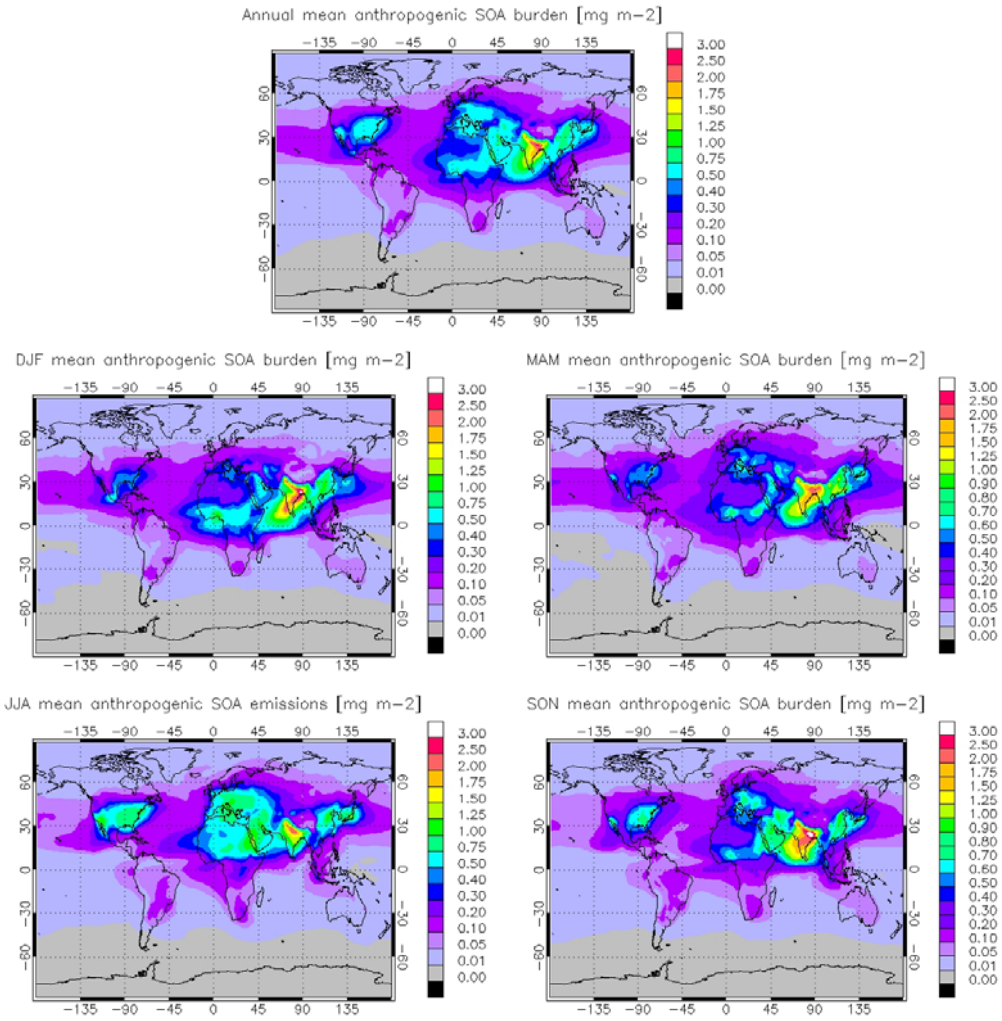

Figure 2.5. Annual and seasonal means of anthropogenic SOA burden

A combination of high emissions and active photochemistry gives a high burden over south and southeast Asia, weakening in the summer with the enhancement of the wet deposition sink in the monsoon season. Low wintertime OH levels north of 45°N lead to very little SOA formation despite substantial precursor emissions from Europe and the north-eastern United States.

The modelled biogenic SOA burdens are shown in figure 2.6.

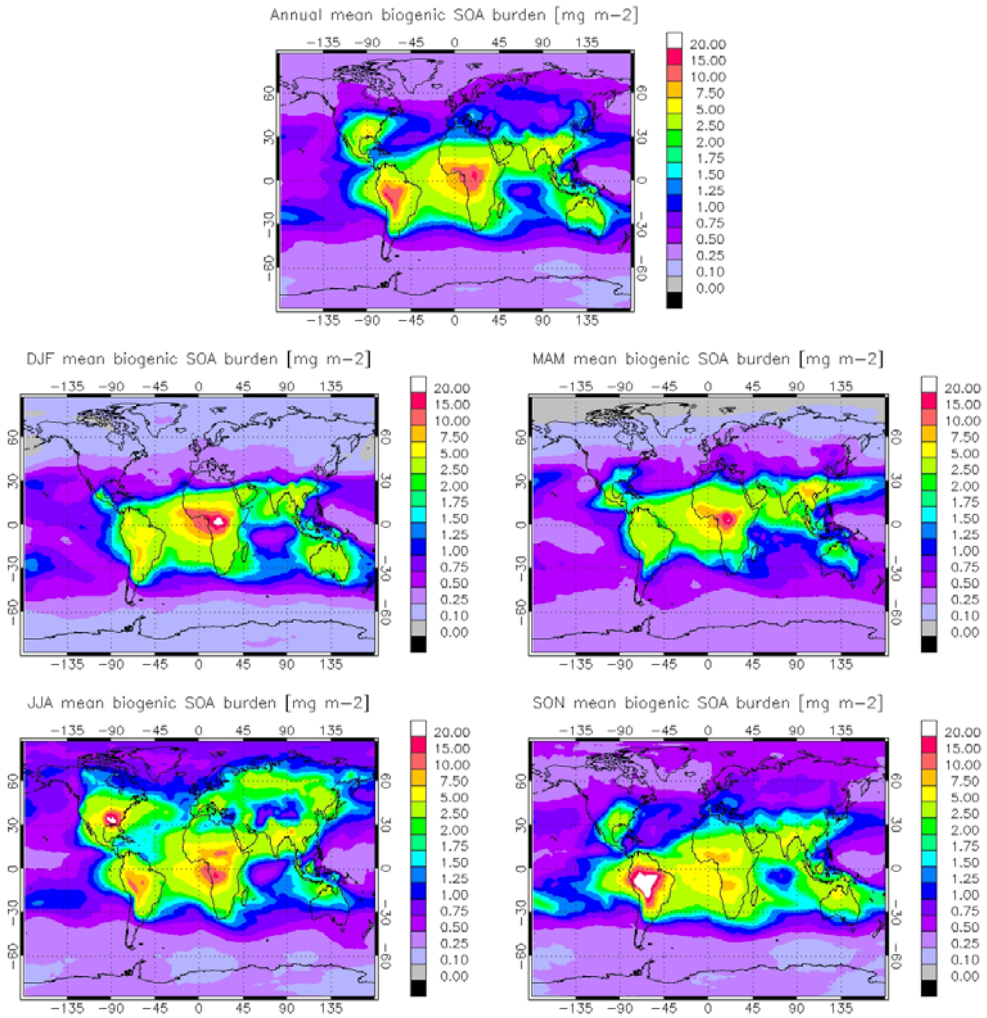

Figure 2.6. Annual and seasonal means of biogenic SOA burden

The biogenic SOA loading is strongly dominated by the contribution of tropical forests, with a comparatively small (on an annualised basis) input from the Boreal forest. In particular, the peak in September-November in the Amazon is related to the biomass burning season. SOA formation is related to the amount of organic absorbing material (M_0) in the ambient aerosol. The high organic loading in the biomass burning season therefore leads to enhanced SOA formation. In reality, this effect will be mitigated by the soil dryness (which reduces plant emissions) and the destruction of biomass, effects that are not accounted for in the model. Elsewhere, the 'biogenic hotspot' in the south-eastern United States is clearly visible in the summer months. Also worth remarking upon is the relatively low burden over the forests of Indonesia and Papua New Guinea, despite the high precursor emissions in those areas. Heavy model precipitation in that region efficiently removes SOA through wet deposition.

2.3.7 *Vertical distribution of SOA*

Vertical transport plays a crucial role in SOA formation. Convection lifts gas-phase condensable species to much colder regions of the atmosphere, where partitioning favours the aerosol phase. The common occurrence of deep convection in the tropics thus enhances SOA formation, already favoured due to high precursor emissions and strong photochemistry.

The simulation without SOA, with values of less than 5 ng m^{-3} above 8km, cannot explain observations of organic aerosols (Murphy et al., 1998; Froyd et al., 2009; Morgan et al, 2009) in the upper troposphere.

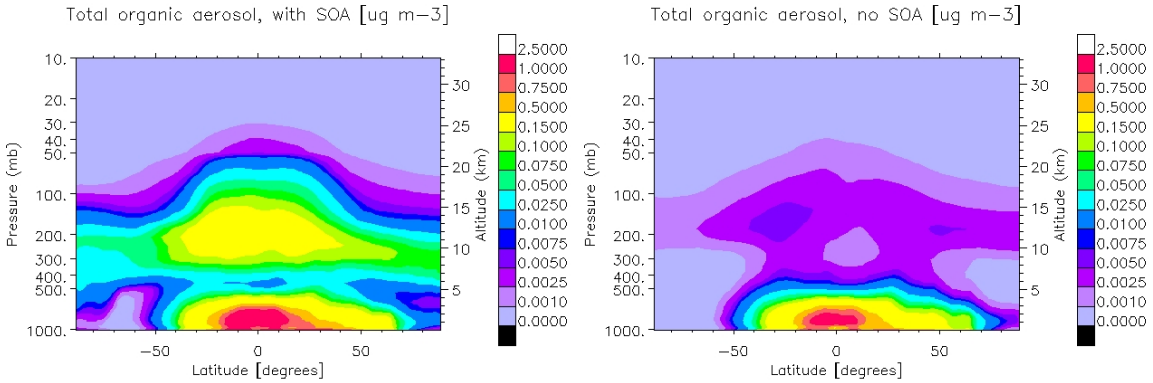

Figure 2.7 Annual zonal mean total particulate organic matter (POM) with SOA (left) and withot SOA (right)

The two-product model of SOA formation is clearly visible in the modelled vertical profile of biogenic SOA. For each modelled biogenic precursor, we have two SOA products of differing volatilities. The more volatile products require lower temperatures for the gas-aerosol partitioning to favour the aerosol phase. The split is clearly visible in the vertical profile, which is shown below as annual mean zonal concentration for each semi-volatile product. In reality, SOA is composed of a range of compounds of differing volatilities, so that the two peaks of the model distribution is unlikely to be an accurate reflection of true vertical distribution.

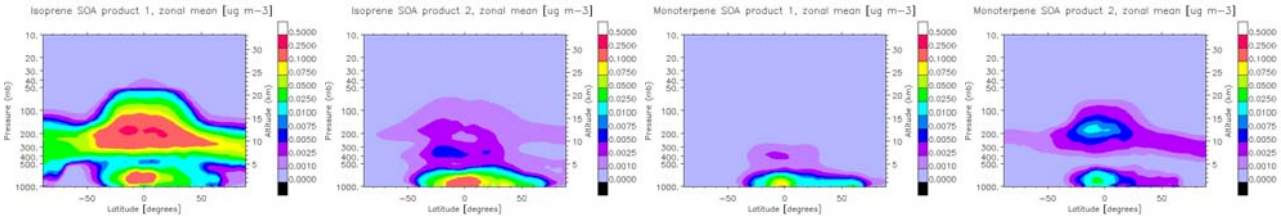

Figure 2.8. Vertical profile of aerosol phase mass of each model semi-volatile compound,

A high-altitude SOA pool is formed mainly in the tropical mid- to upper troposphere at altitudes of approximately 8-16 km, and at temperatures of less than 240K, mainly from isoprene product 1 (the high-volatility product). This pool is subsequently transported worldwide.

The high upper-tropospheric loading of isoprene-derived SOA merits close scrutiny. It comes about as a result of the two-product properties of isoprene-derived SOA, in particular those of product 1, for which the laboratory data chosen (Henze and Seinfeld, 2006) gives a stoichiometric yield of 0.232 and a partitioning coefficient of 0.00862 $m^3/\mu g$ at 295K. The former implies an input to the atmosphere (assuming OH supply is non-limiting) of some 100 Tg/yr condensable gas from the model isoprene emissions of 446 Tg/yr. The latter implies that the compound so formed is highly volatile and favours the gas phase down to very low temperatures (K_p = 1 $m^3/\mu g$ at 228K). The combination of high yield and

high volatility results in an aerosol species that condenses primarily in the upper troposphere, at temperatures too cold for liquid water. The high altitude and lack of wet removal (SOA in the model does not interact with ice) lead to the high modelled burden and extended lifetime. The vertical distribution of this species is shown in more detail below, where the green shading indicates the 0.1 $\mu g/m^3$ (in the aerosol phase) isosurface. Horizontal lines on the right-hand plane bounding the box indicate pressure levels in steps of 50 hPa, with the box top at 100 hPa.

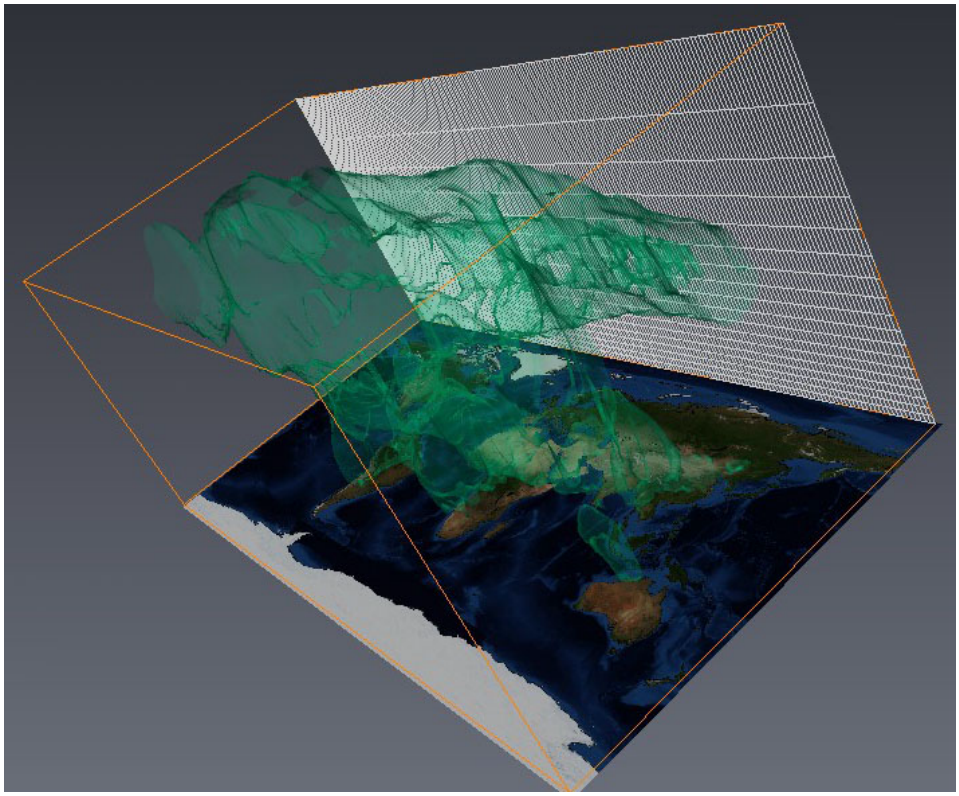

Fig. 2.9. Annual mean vertical distribution of high-volatility isoprene SOA

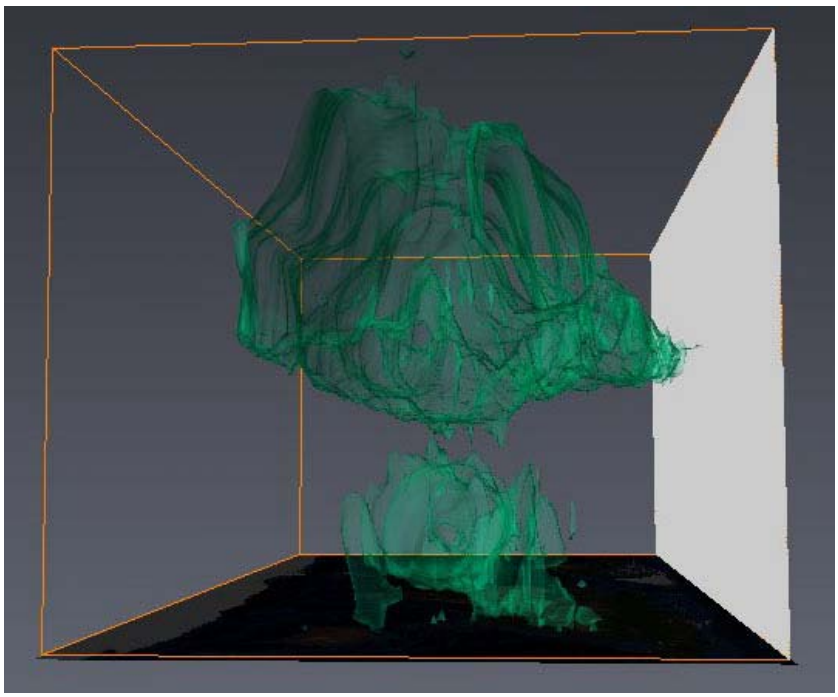

Figure 2.10. As figure 2.9, westward-looking perspective from 180°E.

2.3.8 Impact of SOA on aerosol number concentration

Since SOA condenses onto pre-existing aerosol, one would intuitively expect that the main effect of SOA on aerosol numbers is to boost some of the population of the smaller modes into the larger size ranges. This is indeed so in the zonal and annual mean: in particular the soluble accumulation mode number concentration is increased at the expense of that of the Aitken mode. Numbers are also enhanced in the coarse mode, though the effect is rather small compared to the accumulation mode.

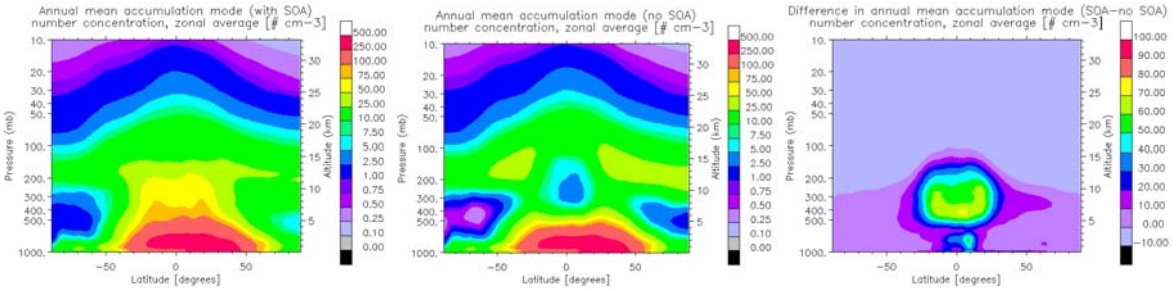

Fig 2.11. Number concentration in the accumulation soluble mode with SOA (left), without SOA (centre) and difference (right)

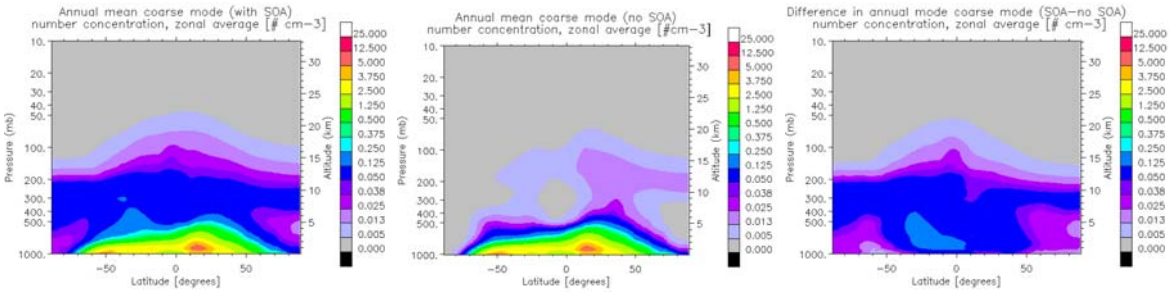

Fig 2.12. Number concentration in the coarse soluble mode with SOA (left), without SOA (centre) and difference (right)

Number concentrations in the nucleation and Aitken modes are depleted in the simulation with SOA compared to that without SOA. For the nucleation mode (which in the model contains only sulphate and water, not SOA) the effect is minor. Aitken insoluble particles are associated with anthropogenic emissions in the model, and converted to soluble by condensation of sulphuric acid and by coagulation with the soluble modes, and hence generally confined to the lower and mid-troposphere. Note that the difference plots in figures 2.13-2.15 represent number *depletion* (no SOA – SOA), as opposed to the number *enhancement* (SOA – no SOA) shown in figures 2.11-2.12.

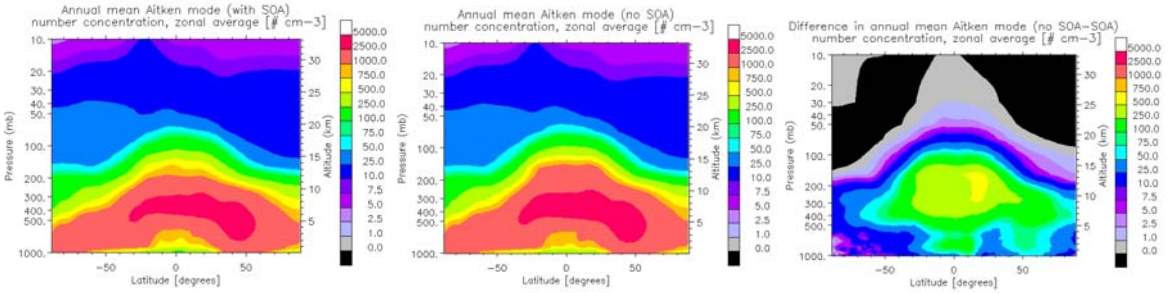

Fig 2.13. Number concentration in the Aitken soluble mode with SOA (left), without SOA (centre) and difference (right)

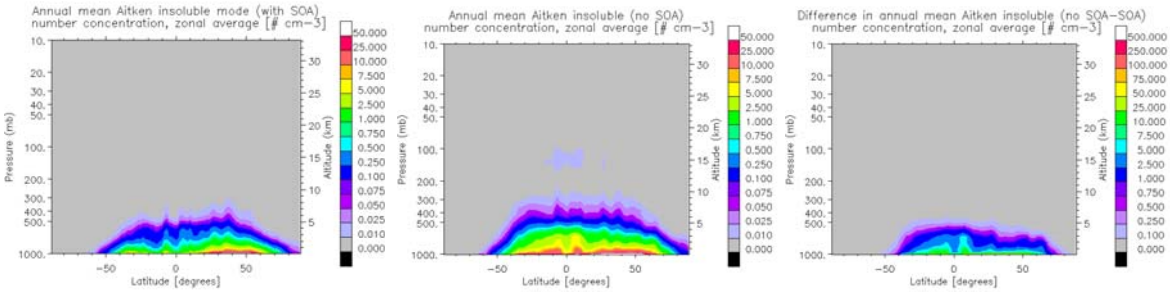

Fig 2.14. Number concentration in the Aitken insoluble mode with SOA (left), without SOA (centre) and difference (right)

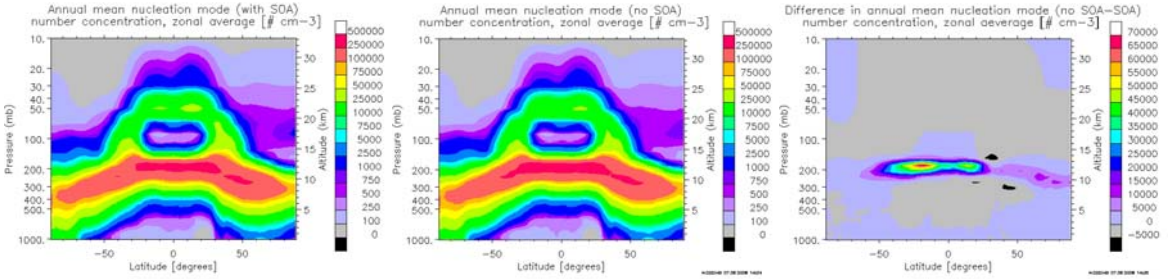

Fig 2.15. Number concentration in the nucleation mode with SOA (left), without SOA (centre) and difference (right)

2.3.9 *Optical Properties*

The model global annual mean aerosol optical depth at 550 nm is 0.13, compared to 0.12 without SOA. Seasonal and regional variations in the difference follow the variations of the SOA burden, discussed in chapter 2.3.3, reaching a local maximum of about 0.2 in the Amazonian basin in the biomass burning season.

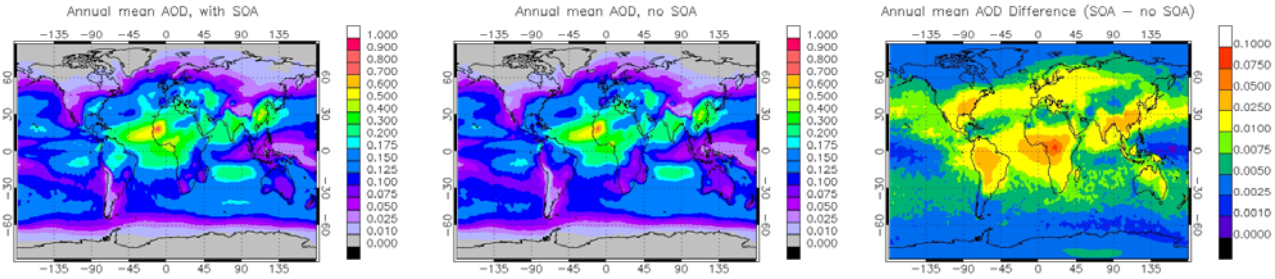

Figure 2.16. AOD at 550nm with SOA (left), without SOA (centre) and difference (right)

The overall single-scattering albedo (SSA) of the aerosol is increased in most areas in the simulation with SOA, particularly in regions with large biogenic SOA loadings, indicating that addition of SOA makes the total aerosol population more scattering and less absorptive in nature. However, the asymmetry factor is increased in the same areas, indicating that scattering increases in the forward direction, as one might expect from the increase in particle size with SOA.

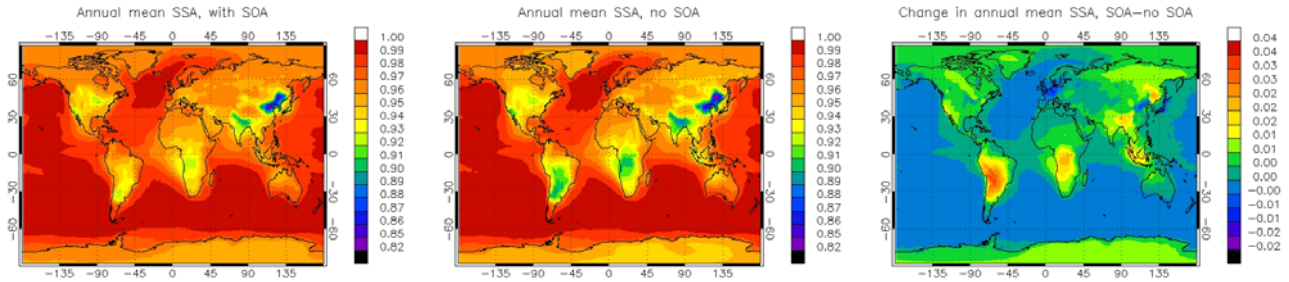

Figure 2.17. SSA at 550nm with SOA (left), without SOA (centre) and difference (right)

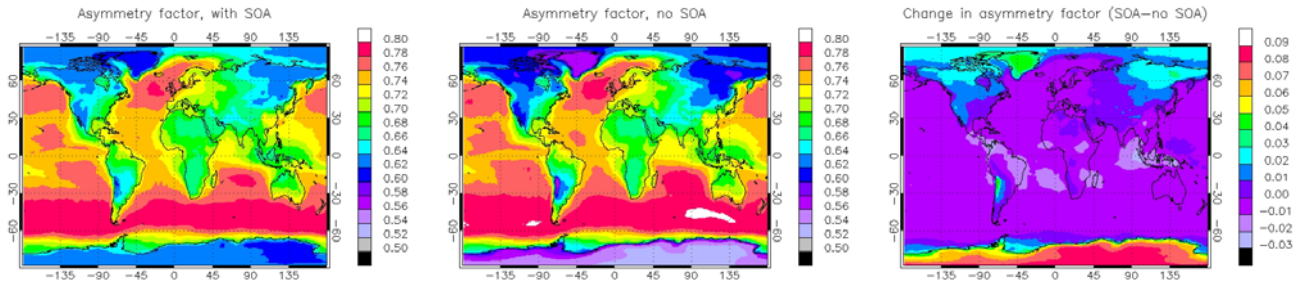

Figure 2.18. Asymmetry factor at 550nm with SOA (left), without SOA (centre) and difference (right)

SOA influences the distribution of optical depth between coarse and fine modes. Optically, the fine mode is dominated by the particles of diameter > 100 nm (the accumulation mode). The accumulation mode fraction of the total AOD is shown in figure 2.19. The significance of this finding lies in the fact that a high fine mode fraction of AOD is used as an indication of anthropogenic aerosol in satellite observations,

whereas the model suggests that regionally, a significant part of the fine mode is biogenic. This is further discussed in chapter 2.6.5.

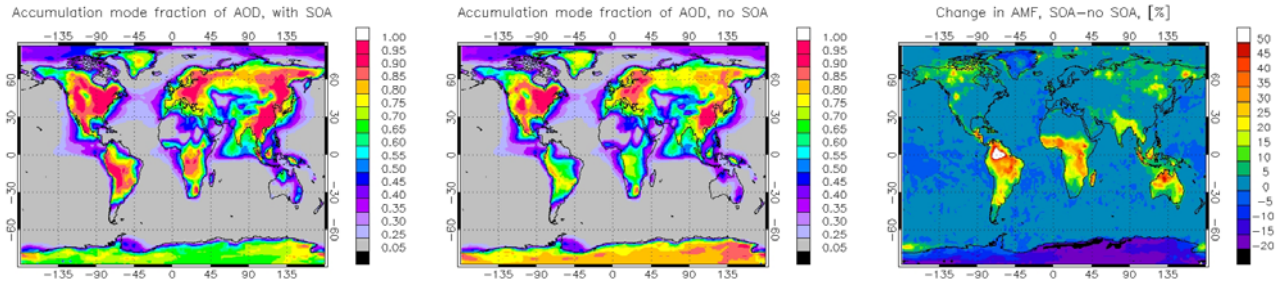

Figure 2.19. Accumulation mode fraction (AMF) of AOD at 550nm with SOA (left), without SOA (centre) and difference (right)

2.3.10 Impact on other aerosol species

SOA has no discernible effect on the emissions, burdens or lifetimes of sea salt and mineral dust. It is also noteworthy that the introduction of SOA has little effect on the total aerosol water burden. The lifetimes of sulphate, black carbon and primary organic carbon are slightly reduced, but the effect is very small. Further simulations, for example simulating different years, would be needed to investigate whether this effect is systematic or just model internal variability.

The sources, sinks, burdens and lifetimes of the model species (other than SOA) are tabulated below for one 1-year model simulation including SOA (subscript 'S') and one not including SOA (subscript 'NS').

Species / Simulation	Prod [Tg/yr]	Wet Dep. [Tg/yr]	Dry Dep. [Tg/yr]	Sed [Tg/yr]	Burden [Tg]	Lifetime [days]
$(SO_4)_S$[1]	71.1	68.1	2.12	1.10	0.884	4.55
$(SO_4)_{NS}$[1]	71.2	68.0	2.17	1.21	0.894	4.60
BC_S	7.72	7.23	0.57	0.026	0.106	5.02
BC_{NS}	7.72	7.20	0.61	0.020	0.113	5.35
OC_S	47.2	44.1	3.24	0.133	0.773	5.99
OC_{NS}	47.2	44.0	3.30	0.115	0.788	6.11
SS_S	4970	2810	844	1320	12.0	0.88
SS_{NS}	4970	2810	845	1320	12.0	0.88
DU_S	726	378	49.1	303	10.0	5.04
DU_{NS}	726	380	49.4	304	10.0	5.04
$(H_2O)_S$	-	-	-	-	46.8	-
$(H_2O)_{NS}$	-	-	-	-	46.7	-

[1] Sulphate figures are in Tg(S)/yr or Tg(S) as applicable

Table 2.4. Impact of SOA on budget of other model species

2.3.11 Direct and Indirect effects of secondary organic aerosols

Finally, we present the modelled influence of SOA upon climate in terms of radiative effects. The direct effect is estimated as the difference in the top of the atmosphere (ToA) net radiative flux under clear-sky conditions between a simulation including SOA and a simulation with zero SOA, with the large-scale meteorology constrained by nudging as described in the introduction to chapter 2.3. The indirect effect is the difference in the TOA fluxes under cloudy (all-sky minus clear-sky) conditions. A third simulation was performed with only biogenic SOA, with results very similar to the simulation including all SOA. Because of the close similarity, results of this simulation are not shown and only briefly quoted.

The clear-sky effect is a cooling of -0.31 Wm^{-2} on the global annual mean, with peak cooling of approximately -2 Wm^{-2} in the southwest of the Amazon basin, where the Andes form a barrier (compare the maximum annual burden in Figure 2.6 in chapter 2.3.6). Some small positive values can be seen, mainly over Greenland and Antarctica. These are connected with the changes in the particle diameter towards the larger size range, which is largest in these regions, as seen from the change in the asymmetry factor in Figure 2.18. Larger particles scatter more radiation in the forward direction, and thus less radiation is lost to space than would be the case with the same number of smaller particles of identical composition. Elsewhere, it is noteworthy that the boreal forest contributes significantly only in the northern hemisphere summer (not shown) and little in the annual mean.

The biogenic SOA only simulation gives a clear-sky effect of -0.29 Wm^{-2}.

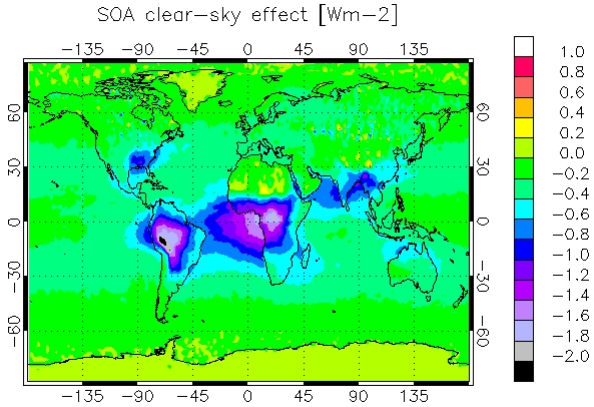

Fig. 2.20: Difference in clear-sky top of atmosphere SW flux (SOA – no SOA)

The model gives a noisy result for the SOA indirect effect. For this reason, the image below has been subject to a 9-point smoothing algorithm. The result is somewhat surprising, in that the modelled indirect effect of SOA is clearly positive in some regions: north-western Europe, especially the North Sea, Japan and the surrounding maritime area, much of South America and the West African coast from approximately the equator to 20°S.

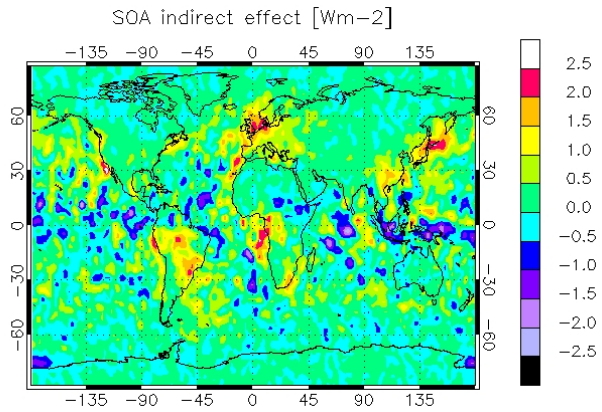

Fig. 2.21. Annual mean SOA indirect effect

This is related to seasonal perturbations of stratus decks in anthropogenically influenced (whether by industry or biomass burning) areas. The mechanism appears to be as follows: in the model, the Lin and Leaitch activation scheme is used, whereby any particle with radius of at least 35 nm can act as a cloud condensation nucleus (CCN). In this model scheme, SOA partitions preferentially to large particles (thus, to those that are already of CCN size). In the presence of a sufficient number of such particles, the condensable SOA supply is essentially exhausted by those large particles, leaving very little growth 'fuel' for small particles, while at the same time enhancing the coagulation sink for the small particles. The net result is a *decrease* in CCN. On the other hand, if there are few large particles available, SOA will drive growth of small particles and this can result in an *increase* in CCN.

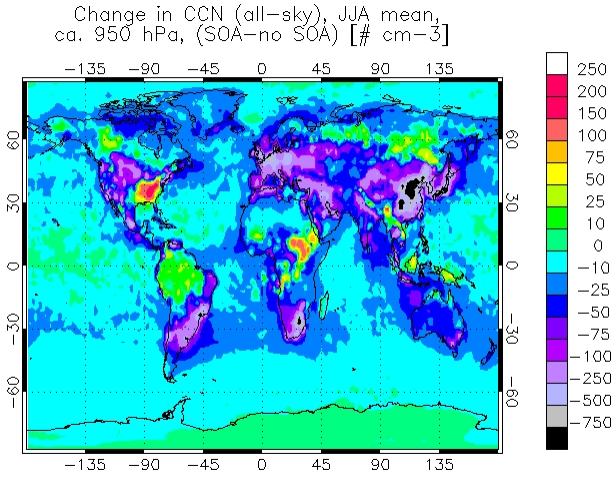

Fig.2.22. Change in JJA CCN (number of particles ot radius > 35 nm).

This is most evident in the NH summertime, when biogenic SOA production from the Boreal forest and from the south-eastern United States hotspot is maximal. Then an increase in CCN–sized particles compared to the 'no SOA' case can be seen in these regions, as well as over the Amazonian and south-east Asian rainforests (with a mixed picture over Central Africa). By contrast, all anthropogenically dominated regions show a decrease in CCN-sized particles.

Of course, in order for such particles to become cloud droplets, we also require supersaturation, so that their influence on clouds follows a different spatial distribution. In figure 2.23 below, the change in cloud droplet number concentration (CDNC) is shown, where the time averaging is done taking into account

only timesteps when clouds are present. The image has also been smoothed. The level of 950 hPa has been chosen because that is the level where the stratus decks off West Africa and off Japan are found (thin stratus are often found only in a single model layer). No effect is seen upon the stratus deck west of South America, most likely because the Andes mountain range forms an effective barrier to low-levels transport of continental aerosols. The effect is much stronger in Europe and China in winter, but the picture is complicated by less stable cloud patterns.

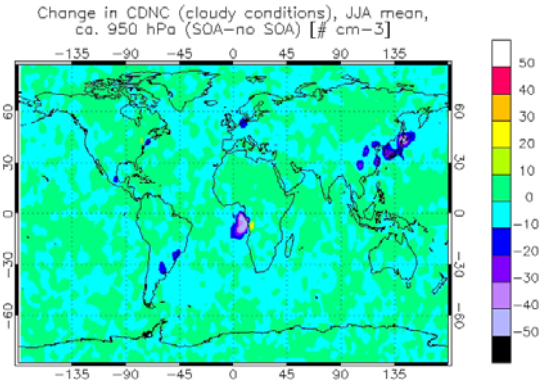

Fig 2.23a Change in JJA CDNC (SOA-no SOA).

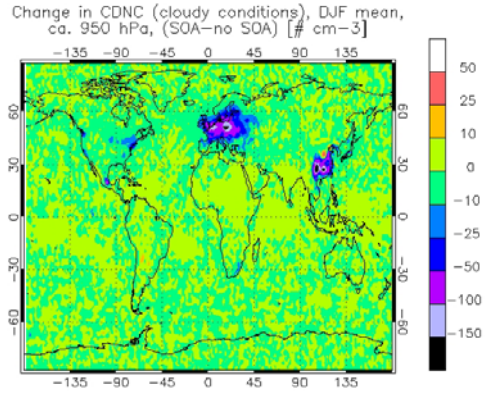

Fig.2.23b Change in DJF CDNC (SOA-no SOA)

Globally, the modelled global mean SOA indirect effect is a warming of +0.23 Wm^{-2}.

Whether this effect should be classified as a feedback of natural aerosols or as an anthropogenic forcing requires some reflection. For the purposes of calculating an overall effect of SOA, it will be treated as a feedback.

Longwave (thermal) radiative effects are small, a global clear-sky total of +0.02 Wm^{-2}, and an indirect effect of -0.03 Wm^{-2}.

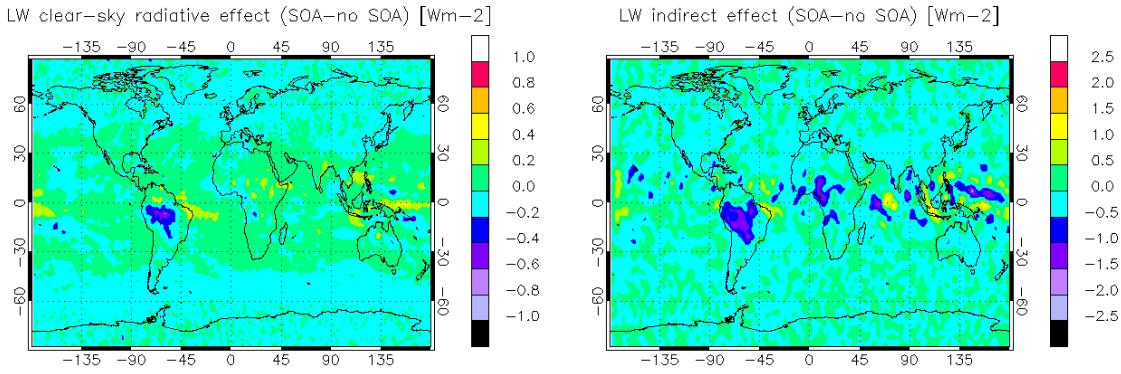

Figure 2.24. LW radiative effects of SOA

The overall model estimate of the climate impact of SOA under year 2000 conditions is therefore -0.09 Wm^{-2}.

2.4 Comparison with measurements

For evaluation of global models, measurements of modelled species over wide areas and long time intervals are desirable. Unfortunately, few such data sets are available as far as organic species are concerned, and none that explicitly provides SOA data. Long-term and wide-area measurements are almost invariably clustered in economically advanced countries, with few measurements available in the tropics, which this study indicates as the most important source region of SOA. In this subchapter, comparison of organic carbon (OC) aerosol mass measurements in Europe and the United States is compared against model calculations at the same points.

The need for in-situ measurements in the free and upper troposphere has been stated in chapter 1.4. Unfortunately, such measurements that can explicitly give organic mass (rather than, for example, an organic to sulphate mass ratio, e.g. Froyd et al., 2009) are very scarce indeed. Some information about the performance of the updated model in the whole atmospheric column may be obtained from optical measurements. To this end the Aeronet (Holben et al., 1998) network of measurement sites is used.

The biogenic emission models are evaluated in the work of Guenther et al. (2006) and Guenther et al. (1995) and this work is not repeated here.

All measurements are quoted in mass of organic aerosol (not mass of organic carbon).

2.4.1 Europe

Measurements of organic carbon aerosol on a wide area and over a long time period – at least one year, to capture seasonal variation – are scarce. One such campaign is the so-called EC/OC campaign carried out by the European Monitoring and Evaulation Programme (EMEP) from July 2002 – June 2003. Twelve stations participated in the campaign. One station (Kosetice, Czech Republic) did not report data for the first two months of the campaign, giving a total of 142 monthly mean observations. For comparison, the model was run for the same time period as the EC/OC campaign (after spinup), nudged to ECMWF analysis, with and without SOA. The graphs below show the measured monthly means and the modelled monthly means for the grid box containing the measurement site for the simulations with and without SOA.

The EC/OC campaign results document PM_{10} (particles of diameter up to 10 μm) measurements only. This is potentially important, since the model is not designed to include large particles, since those particles are less radiatively active and have short atmospheric lifetimes (recall that the coarse mode in the model consists of a lognormal distribution of particles larger than 1 μm diameter). A sample containing a significant proportion of OC mass in particles of the uppermost size range of PM_{10} is therefore not possible to capture with the model.

While the inclusion of SOA increases the total modelled organic mass substantially (by 50% on the average of all sites for the year in question), in general the modelled mass remains well short of the measured OC mass. Only at one site (Kollumerwaard) and for three out of twelve months does the modelled mass equal or exceed the measured mass, and this is the case only for the simulation with SOA. This difference between model and observations is particularly large in the more southerly sites in wintertime, when the large organic peaks observed at Ispra, ISAC Belogna (Italy) and Braganca (Portugal), sites that are located at latitudes between 42°N and 46°N, are absent in the model. Blue circles: measurements, purple squares: model without SOA, green triangles: model with SOA.

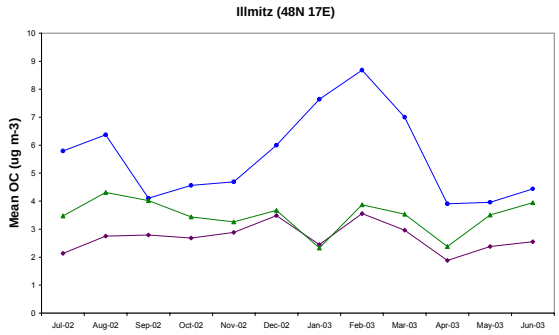
Illmitz (48N 17E)
Mean OC (ug m-3)
Jul-02
Aug-02
Sep-02
Oct-02
Nov-02
Dec-02
Jan-03
Feb-03
Mar-03
Apr-03
May-03
Jun-03

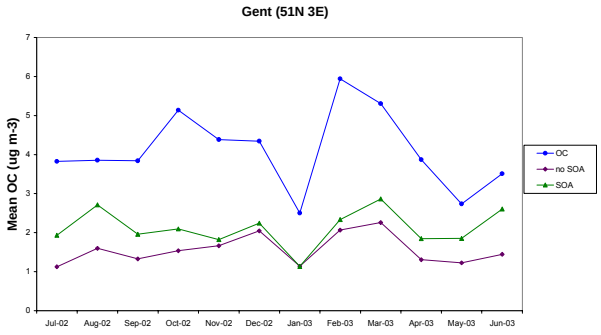
Gent (51N 3E)
Mean OC (ug m-3)
OC
no SOA
SOA

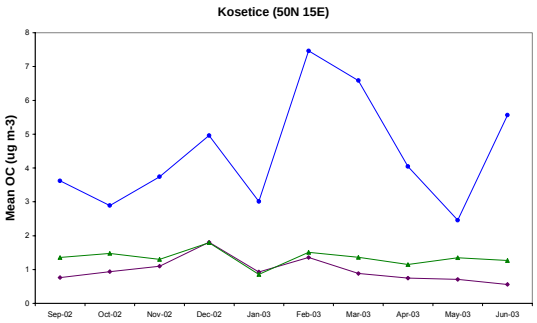
Kosetice (50N 15E)
Mean OC (ug m-3)
Sep-02
Oct-02
Nov-02
Dec-02
Jan-03
Feb-03
Mar-03
Apr-03
May-03
Jun-03

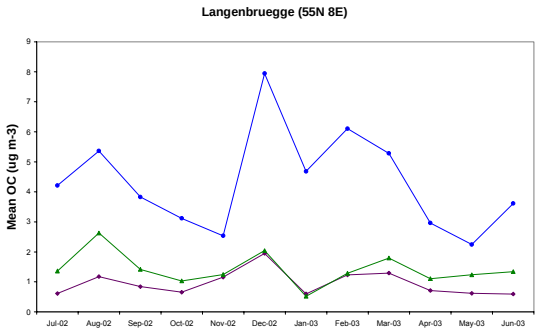
Langenbruegge (55N 8E)
Mean OC (ug m-3)
Jul-02
Aug-02
Sep-02
Oct-02
Nov-02
Dec-02
Jan-03
Feb-03
Mar-03
Apr-03
May-03
Jun-03

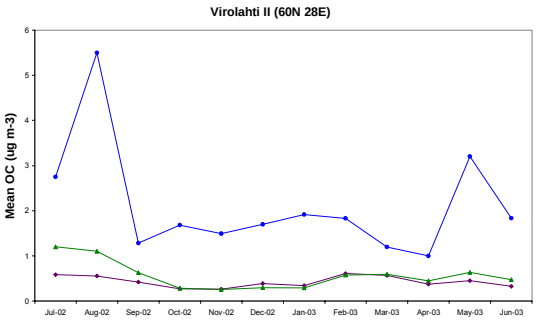
Virolahti II (60N 28E)
Mean OC (ug m-3)
Jul-02
Aug-02
Sep-02
Oct-02
Nov-02
Dec-02
Jan-03
Feb-03
Mar-03
Apr-03
May-03
Jun-03

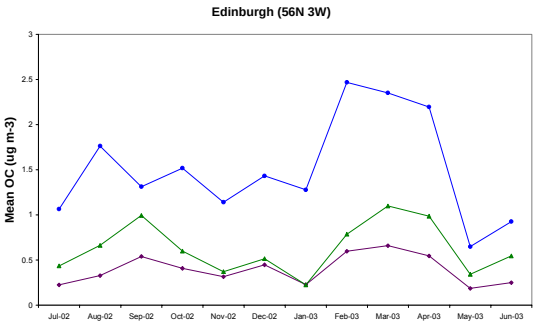
Edinburgh (56N 3W)
Mean OC (ug m-3)
Jul-02
Aug-02
Sep-02
Oct-02
Nov-02
Dec-02
Jan-03
Feb-03
Mar-03
Apr-03
May-03
Jun-03

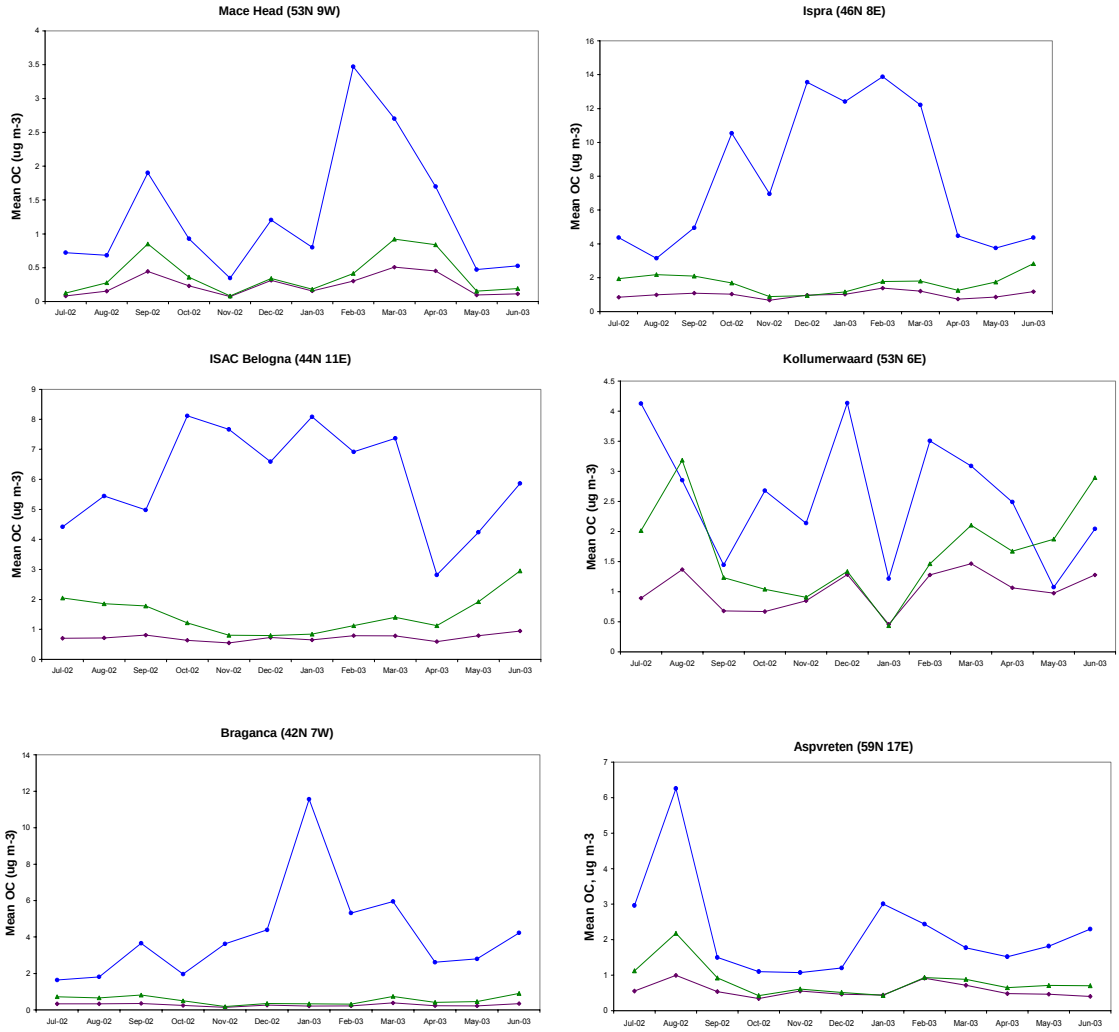

Figure 2.25. Modelled total organic aerosol *vs.* EMEP measurements

Overall, the mean of all OC mass measurements at all stations in the EMEP EC/OC campaign is 3.85 μg/m^3, compared to 0.90 μg/m^3 modelled (without SOA) at the gridboxes containing the relevant stations, and 1.35 μg/m^3 modelled with SOA. The respective median values are 3.49 μg/m^3 observed, 0.69 μg/m^3 modelled without SOA and 1.13 μg/m^3 with SOA.

The model capture of seasonal variation may be measured by the correlation between model and measurements. For Europe this is, as a whole, poor: only 0.42 for the full measurement dataset (without SOA) and even poorer, 0.39, with SOA. Excluding the three southern European stations at Bracanga, Ispra and ISAC leaves better agreement of the variation of model and observations, with a correlation of 0.70 between observations and model without SOA and 0.75 with SOA. The mean of the observations excluding these stations is 3.1 μg/m^3, compared with modelled values of 1.0 μg/m^3 (without SOA) and 1.4 μg/m^3 (with SOA). On this basis, the model seems to reflect the seasonal variation in total OC reasonably well in the northern and central Europe, even though the magnitude remains short of the measurements. In the south, however, the model differs by up to an order of magnitude to observed OC values. In addition, it is temporally anti-correlated to observations in that region.

For most stations in the EMEP network, and particularly for the southern stations, total OC and EC are very strongly related. Overall correlation of EC to OC is 0.83; for measurements excluding the three southern sites, 0.65; and for measurements at the three southern sites, 0.95. This indicates that the OC content is largely anthropogenic throughout the campaign domain, and almost exclusively so in the south.

The distributions of observed and modelled OC mass are presented hereunder as frequency of observed/modelled mass in bins of 0.5 μg/m^3. Note the difference in the y-axis scales.

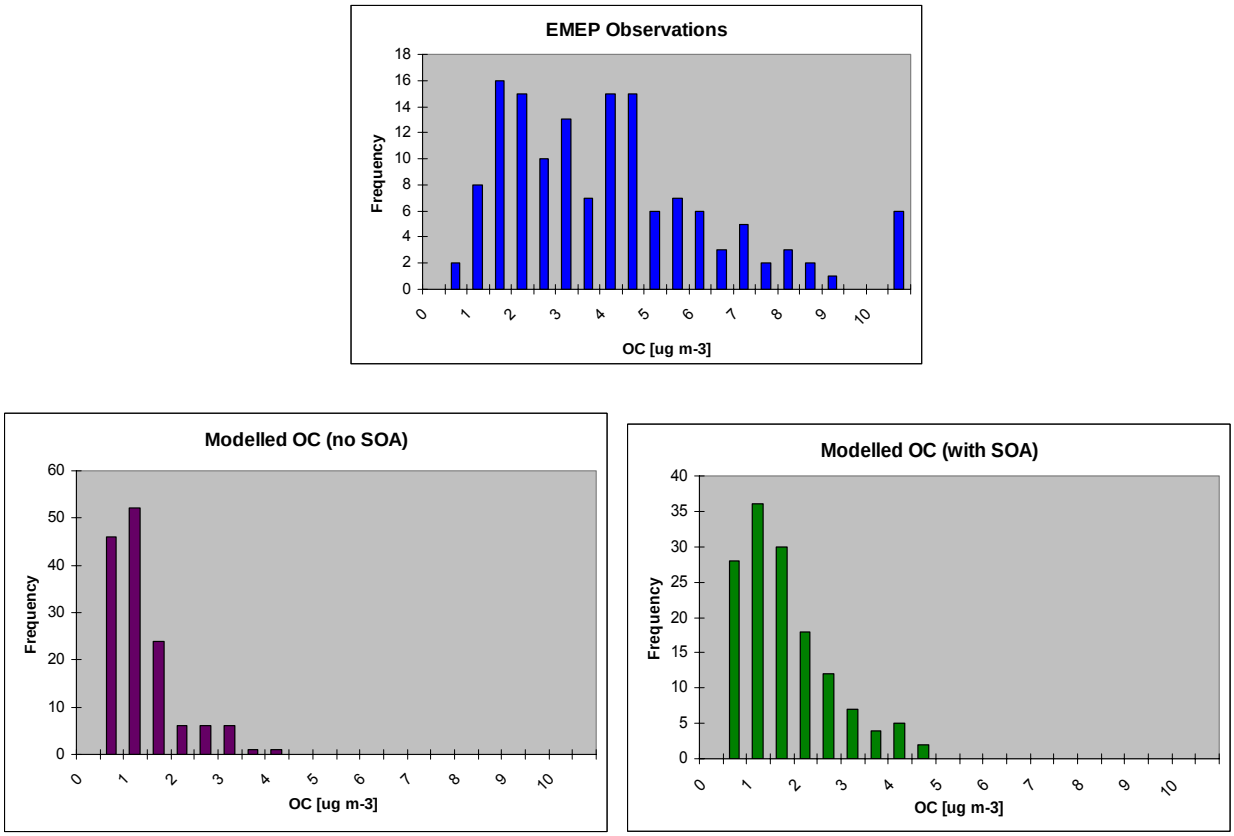

Figure 2.26. Distribution of EMEP observations of and modelled OC aerosol mass

The model exhibits a mass peak in the accumulation mode for both POA and SOA, and hence the distribution of modelled values appears almost mono-modal. The observed distribution is much more complex, and it is not obvious that the observations can be modelled successfully as a superposition of lognormal modes.

2.4.2 North America

The IMPROVE (Interagency Monitoring Protected Visual Environments) network (http://vista.cira.colostate.edu/improve/) has recorded aerosol properties over the contiguous United States since the 1980s, and, as its mission is primarily to monitor visibility at places of outstanding natural beauty, it is a rural network. The network measurement dataset has been analysed for the same period that covers the EMEP EC/OC campaign, which consists of a total of 1915 monthly mean observations from *circa* 160 stations (not all stations reported during each month of this period).

IMPROVE measurements are for $PM_{2.5}$, unlike the EMEP measurements.

The observed monthly mean of all stations and months in the study period is 1.84 μg/m^3. Modelled values at the gridpoints containing the measurement sites are 0.74 μg/m^3 without SOA and 1.21 μg/m^3 including SOA. Median values are 1.46 μg/m^3 observed, 0.36 μg/m^3 modelled without SOA and 0.64 μg/m^3 with SOA. The large number of stations in the IMPROVE network makes it meaningful to examine the mean and median of all stations on a monthly basis.

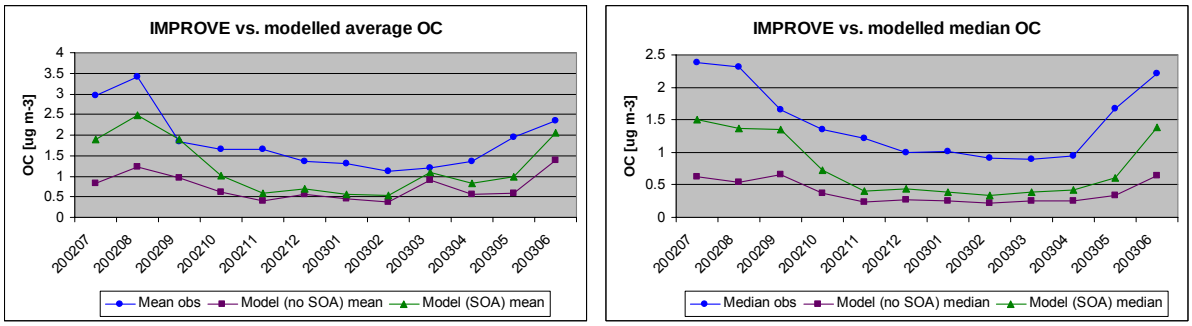

Figure 2.27. IMPROVE measurements of and modelled OC in the average (left) and median (right)

Wildfires are, episodically, a major factor in aerosol loading at some of the IMPROVE stations (observations of organic carbon are as high as 57 μg/m^3 in the monthly mean in the study period), which is not the case in Europe. Real fire events are not always present in the model, and in such cases very large differences between model and observations occur. Another consequence is that the standard deviations of these datasets are very large. These factors destroy any overall correlation between the observations and modelled data. Also, while some improvement in agreement on the large scale between model and observations is visible from Figure 2.27, it is notable that the observations remain consistently higher than modelled OC concentrations, particularly in winter time.

The distribution of IMPROVE OC observations is substantially different from that of the EMEP observations and is shown below, with the modelled distributions without and with SOA for comparison. Again note the differences in the y-axis scales.

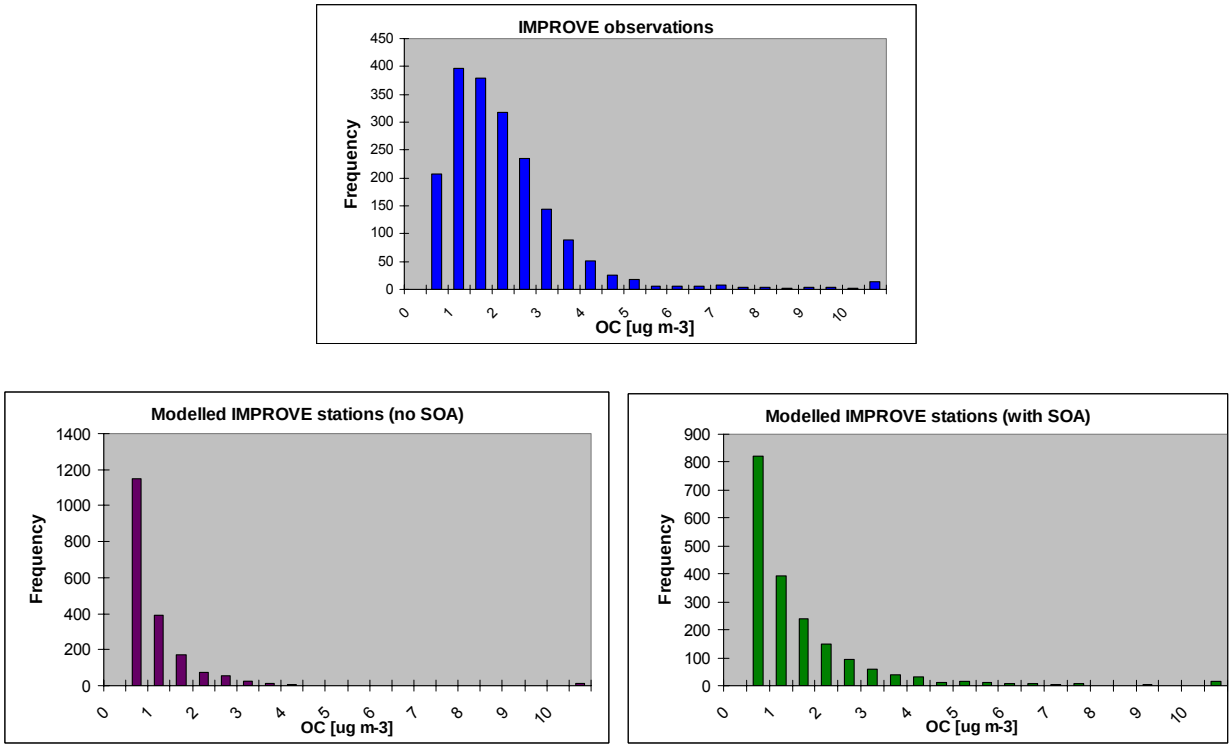

Figure 2.28. Distribution of IMPROVE measured and of modelled OC mass

Unlike the EMEP case, the IMPROVE distribution exhibits a single peak near 1 μg/m^3. Clearly, the simulation with SOA better approaches the observed distribution: however, the occurrence of low total POM is still much higher in the model than in observations.

2.4.3 Aeronet

Aeronet observations over the period of the EMEP EC/OC campaign comprises a total of 845 monthly mean observations at locations spread worldwide (but not uniformly, so that, for example, aeronet means are not comparable to satellite-derived global means). Aeronet observations include aerosol optical depth (AOD) measurements at different wavelengths. The wavelengths measured depend upon the measuring site, but measurements at 500 nm and 875 nm are commonly available. The model diagnostic AOD is calculated at 550 nm and 825 nm, so that while we are not comparing identical quantities, they can be expected to be very closely related.

The distribution of measured and modelled mid-visible AOD at the aeronet sites is shown in figure 2.29. Once again, note that the scales on the y-axes differ.

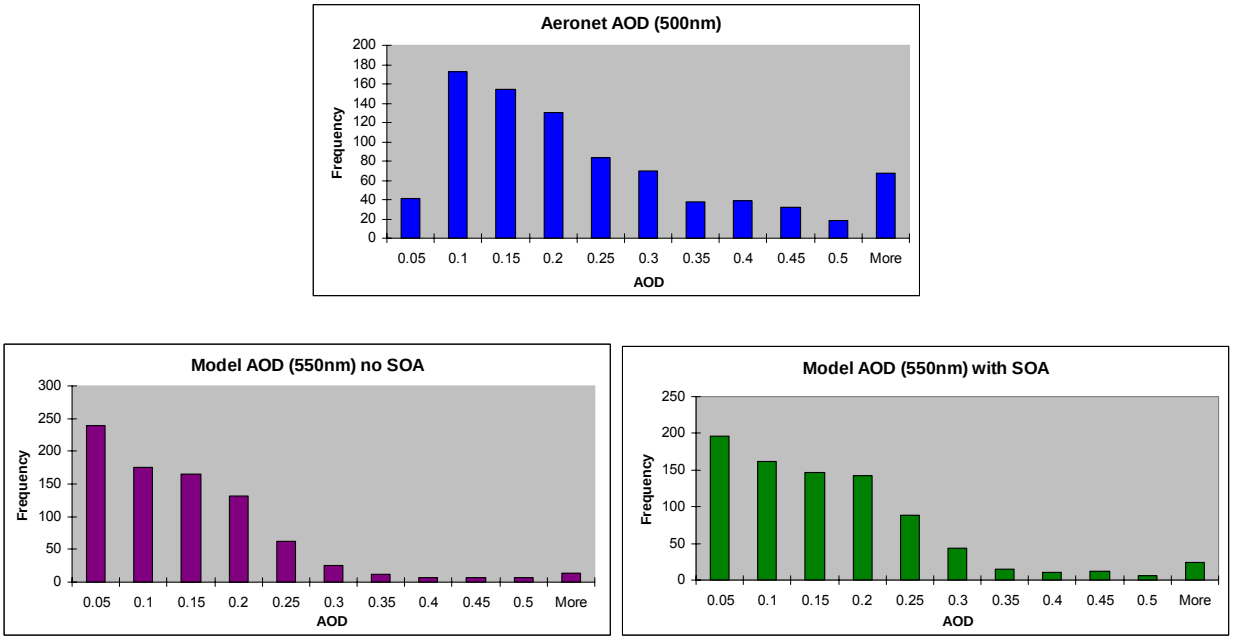

Figure 2.29. Distribution of measured and modelled AOD in the mid-visible

The incidence of very low (less that 0.05) mid-visible AOD in the model is reduced by about 20% in the simulation with SOA compared to that without SOA, but low AOD remains much more common in the model than in the aeronet observations. Otherwise, the distribution is moved slightly in the direction of higher AOD. Overall, the relevant mean (median) values are 0.225 (0.169) observed, 0.125 (0.103) for the model without SOA, and 0.149 (0.120) for the model with SOA.

Results for the near-infrared AOD are broadly similar, with a reduction in the incidence of modelled low AOD and increase in that of high AOD. Here y-axes are equal.

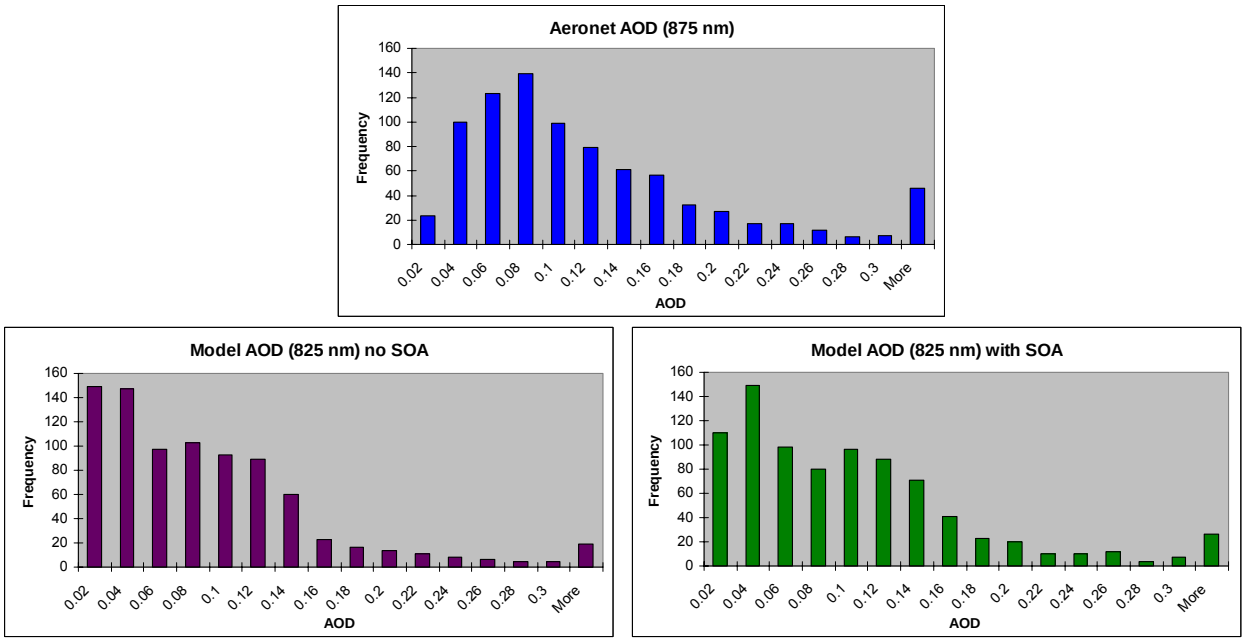

Figure 2.30. Distribution of measured and modelled AOD in the near-infrared

For the near-infrared, the relevant mean (median) AOD values are 0.117 (0.088) observed, 0.082 (0.067) for the model without SOA, and 0.094 (0.077) for the model with SOA.

With the inclusion of SOA, the correlation between aeronet observations and model increases marginally from 0.71 to 0.73 for the mid-visible AOD, and from 0.66 to 0.67 for the near-infrared AOD.

No systematic difference between the simulations with and without SOA is apparent when comparing against the Aeronet-measured Ångström parameter.

2.5 Comparison with other models

Due to the importance of isoprene to the results, this model inter-comparison is limited to those studies which include isoprene as a SOA precursor. In table 2.5, the emissions, production and burdens calculated by previous studies and this study are listed. Emissions of isoprene, monoterpenes and anthropogenics are denoted E_i, E_t and E_a and are given in Tg(C)/yr. Production and burdens of the respective species are denoted P_i, P_t, P_a, B_i, B_t and B_a, and the total SOA burden by B_{tot}. Production figures are in Tg/yr and burden figures in Tg unless otherwise stated.

Reference	Model	E_i	E_t	E_a	P_i	P_t	P_a	B_i	B_t	B_a	B_{tot}
Tsigaridis et al. (2007)	TM3	467	137	16	4.6	12	1.8	0.08	0.69	0.04	0.81
Hoyle et al. (2007)	OSLO CTM2	220	127	17	15	38	2.5	-	-	-	0.52
Henze et al. (2008)	GISS II'	461	121	19	14	8.7	3.5	0.45	0.22	0.08	0.75
Heald et al. (2008)[1]	CAM3	496	43	16	19	3.7	1.4	-	-	-	0.59
This study	ECHAM5/HAM	460	89	17	17	4.0	5.6	0.70	0.06	0.07	0.83

[1] All figures in Tg(C) or Tg(C)/yr as appropriate

Table 2.5. Model estimate of SOA precursor emission, SOA production and atmospheric burden

The ostensibly good agreement in total SOA burden between the models belies the wide differences in SOA production and in burdens of individual species, and any such agreement must therefore be regarded as coincidental. Production figures must be viewed with caution, since, as discussed in chapter 2.2.4, the definition of 'SOA production' is not clear when applied to semi-volatile species, and none of the studies listed specifies how exactly the model in question calculates this diagnostic. There are substantial differences between the model choices of SOA production pathways. For example, Hoyle et al. (2007), following Chung and Seinfeld (2002), assume unity mass yield of SOA from all monoterpenes under NO_3 oxidation (using β-pinene as surrogate species), whereas the study of Tsigaridis et al. (2007) and this study assume zero SOA yield for this case (using α-pinene as surrogate species).

Other key differences include the nature of the models: all models in the listed studies except this study include full chemistry models with prognostic OH, O_3 and NO_3, compared to the highly simplified scheme and prescribed oxidant values in this model. This study is unique in using a size-resolved aerosol model with detailed microphysics and coupling to cloud processes. TM3, GISS II' and OSLO CTM2 are all offline chemistry-transport models (CTMs) that are driven by prescribed meteorological datasets. Tsigaridis et al. (2007) simulated the year 1990, whereas Hoyle et al. (2007) and Henze et al. (2008) simulated the year 2004, but using different datasets. The two online models, Heald et al. (2008) and this study, both simulated the year 2000. The consequent meteorological differences between the models can lead to variations in emissions (of biogenic precursors), in SOA formation, in convective and advective transport, and in sink processes.

The models also differ in resolution in both the horizontal and the vertical. This gives rise to differences in numerical diffusion between models, which causes further variation in the transport of aerosols and gases.

A more rigorous SOA model inter-comparison is planned within the AeroCom framework.

2.6 Discussion

2.6.1 Emissions

Biogenic emissions calculated by the model lie within the range of other models, which have been evaluated against observations. This, however, must be viewed with caution. Firstly, MEGAN and its predecessors, especially Guenther et al. (1995), underlie most global biogenic emission models, and therefore a comparison of ostensibly different models is to a large extent comprised of a comparison of different implementations of the same underlying parameterisation. This can give one the illusion that estimates of global biogenic emissions are well-constrained, when this is not the case. This subject is analysed in more detail by Arneth et al. (2008), who point out that global estimates of biogenic emissions remain poorly constrained, despite seeming agreement between models.

Anthropogenic emissions are derived by assuming that the mix of different species in 2000 is the same as that for 1990. Technological and regulatory changes during the intervening period may have altered the mix. Perhaps more importantly, seasonality is lacking in the emissions. This may play an important role in reconciling the model with observations over, for example, Western Europe in wintertime.

2.6.2 SOA production

2.6.2.1 SOA precursors

There are known SOA precursors, both biogenic and anthropogenic, that are not included the model. These include methyl chavicol and sesquiterpenes, emissions of which remain unquantified. The latter class of compounds may be important in new particle nucleation: this is further discussed in chapter 2.6.3. Furthermore, they have large molecular weight (chemical formula $C_{15}H_{24}$) and are known to give a high aerosol mass yield (Lee et al., 2006).

Several anthropogenic substances that can yield SOA are known, but not included in the model either for lack of emissions estimates, or because they are recent discoveries. It has long been known that alkanes can yield aerosol, but this has been observed for larger (carbon number C_9 and higher) members of the alkanes group: so far emissions estimates exist only for the group as a whole. Certain alkenes are also SOA precursors (Forstner et al., 1997b; Kalberer et al., 2000). A recent discovery is that even the lightest non-methane hydrocarbon (acetylene, C_2H_2) can yield SOA (Volkamer et al., 2009). These compounds may go some way to explaining the large discrepancy between modelled and measured OC in anthropogenically-dominated regions. This topic is further discussed in chapter 2.6.7.

2.6.2.2 SOA in the laboratory and in the real atmosphere

There are some critical differences between the worlds of laboratory experiment and global model. In laboratory experiments, SOA is generated from a single pulse of precursor gas, and the SOA yield measured at the end of the experiment. The time dimension that is the experiment duration is not of primary importance for the purpose. Neither is the fate of the gas-phase moiety of the semi-volatile species at the end of the measurement an important consideration. By contrast, in the atmosphere, precursors are supplied in a continuous flux and thus there is a continuous source of gas-phase semi-volatiles. Experiments are necessarily time-limited (typically not more than 12 hours) due to factors

including wall losses and the need to obtain accurate measurements. In the atmosphere, both aerosol and gas continue to evolve. The gas phase condensable species produced cannot be ignored, since, as long as they are present in the atmosphere, they may ultimately condense to form new aerosol mass. Kroll and Seinfeld (2008) discuss requirements for a more complete representation of semi-volatile species, including:

i) Direct removal from the gas phase through wet and dry deposition
ii) Chemical transformation, which may yield either more (through breaking of the carbon chain) or less (through addition of oxygen) volatile species
iii) Condensation to the aerosol phase and removal from there

The removal processes i) and iii) are represented in this model, although there is considerable uncertainty in the choice of physical properties (solubility, molecular weight) of the model compounds.

The lack of any chemical aging process is potentially more serious. The very large contribution of isoprene-derived SOA product 1 to high altitude aerosol has been discussed in 2.3.7. If this product were subject to reactions that yield only lighter, pure gas phase products, then clearly the final SOA burden can only be reduced. If instead it were subject to reactions that yield less volatile products, then competing effects upon aerosol mass would result. On one hand, it would increase the proportion of mass found in the aerosol phase; on the other, a greater proportion of the aerosol could condense at lower altitudes, where liquid water can exist, thereby strengthening the wet deposition sink, leaving the overall effect unclear.

Finally, the existence of gas-phase condensable species and their transport in the atmosphere implies that atmospheric SOA production should be expected to be greater than measured in the laboratory. In the atmosphere, at least some of the gas-phase mass will inevitably condense onto aerosol. Conversely, some aerosol may re-evaporate: however, since the chemical formation of most modelled SOA takes place mainly in the warmest layers of the troposphere, atmospheric transport (especially convection) will generally move mass to colder regions and therefore the condensation flux should be the greater. For this reason, the model yield (as defined in 2.2.4) and laboratory yield for any given species should not be expected to match.

2.6.2.3 Effect of NO_x on SOA production

The effect of NO_x on production of SOA from isoprene (Kroll et al., 2006), monoterpenes (Ng et al, 2007), and aromatic compounds (Henze et al., 2008) is well documented. These results indicate a reduced SOA yield under high NO_x for all species that are included in this model. This may be of particular importance for anthropogenic species, since NO_x is mainly anthropogenic, and therefore high NO_x levels and high anthropogenic SOA levels are expected to coincide. Omission of the effect of NO_x might, accordingly, be expected to cause an overestimate of anthropogenic SOA yields. Following the discussion in the previous subchapter, however, this is not necessarily the case: the key questions are rather how much condensable gas is produced, at what temperatures that gas will condense, how efficient wet and dry removal processes are for that gas, and how strong is vertical transport from the surface. Thus the overall effect is expected be to overestimate near-surface levels, but the impact on the whole column SOA burden is not clear.

Study with a more sophisticated chemistry model is required to determine the effect of the omission of NO_x.

2.6.2.4 Optical properties of SOA

Optical properties of SOA have been little investigated. Some studies (e.g. Dinar et al, 2008) exist, but fall short of what the model requires for computation of radiative properties, namely complex refractive index measured at several wavelengths for a representative selection of substances occurring in real SOA. Organic aerosols are known to be primarily scattering, but some species exhibit significant absorption in the ultra-violet (Myhre and Nielsen, 2004). In this study, the same optical properties as POA have been assumed (Stier et al., 2005).

2.6.3 Nucleation and the role of SOA in particle number concentrations

In this model, SOA only condenses upon existing particles. Nucleation of new particles is determined by sulphuric acid and water, without reference to organic substances. This is in apparent contradiction to observations (O'Dowd et al. 2002; Smith et al. 2008) of organic compounds in the newly formed particles. Some reflection on the difference between model and observations will show that this is not necessarily the case.

It is worth repeating here that the model nucleation mode extends down to 1nm. Observations, on the other hand, are limited by the detectability limit of (usually) 3nm, which is larger than the model mode median. Thus even the notions of 'particle formation' and 'nucleation mode number concentration' are not the same in the model as in observations. From the observational point of view, 1nm particles are background clusters whose existence is inferred from the detection of larger particles: so that, if a 3nm particle contains organics, then from this standpoint, organics must contribute to new particle formation in some way, and must influence the nucleation mode aerosol number concentration. But if instead, the cutoff limit is only 1 nm, the question of whether organics contribute to the nucleation mode remains unresolved. It is possible, for example, that condensation of organic vapours onto a sulphuric acid/water cluster is not thermodynamically favourable at 1nm, but becomes viable around (for example) 1.4nm (Kulmala et al. 2004b). If that is the case, then from the model viewpoint, organics do not contribute to aerosol number, but only to growth of pre-existing particles. If it is not the case, and organics participate in some way in the formation of clusters from gas-phase species, or begin to condense on clusters smaller than the model cutoff, then from the model viewpoint organics do play a role in formation of new particles.

Thus the question of whether organics contribute to new particle formation may be simply a question of what one defines as a particle and what one defines as a cluster; unless it is true that organics participate in the initial gas-to-cluster formation process, in which case there is no ambiguity.

The proposal of Bonn and Moortgat (2003) and Bonn et al. (2008) therefore has significance beyond that of pure atmospheric chemistry. It is also important to find out if such a mechanism can exist not only for sesquiterpenes, but for other organic precursors.

While nucleation events are well documented at many sites (Kulmala et al., 2004a), it has never been observed (near the surface) at the largest biogenic emission sources, namely the Amazonian and African tropical forests (Capes et al., 2009; Zhou et al, 2002; Rissler et al., 2004).

2.6.4 Vertical distribution, cloud processing and SOA lifetime

It has been noted in chapter 2.3.7 that the vertical distribution of SOA is very substantially affected by the volatility of the compound in question. One may question if the laboratory data chosen to represent isoprene, in particular, are suitable to apply throughout the troposphere for atmospheric studies. There are few published estimates of the two-product parameters that described isoprene-derived SOA (Carlton et al., 2009 and the references therein), but all share the same characteristic high stoichiometric

coefficient (α_1) and low partitioning coefficient ($K_{p,1}$), for one of the products. The existence of substantial quantities of such high-volatility products in laboratory experiments is thus confirmed by several independent sources. However, there is to the author's knowledge no published study of isoprene-derived SOA at low temperatures, so that the temperature dependence of SOA formation from this source can neither be supported nor refuted with any empirical data. For monoterpenes, the data of Saathoff et al. (2008) have been used. That study examined SOA yields from α-pinene ozonolysis at temperatures down to 243K, so for monoterpenes, at least, the model has an empirical base for a much greater fraction of the troposphere.

Vertical distribution is also dependent upon aerosol aging processes and interactions with clouds. In this model, no SOA aging processes exist, and the only interaction with clouds is the wet scavenging of aerosols and gases.

Any overall effect arising from the omission of aging reactions is not possible to gauge, because of the non-linearity of the processes involved. For example, increased production of low-volatility SOA in the particle phase leads to an increase in the absorbing mass, which shifts the gas-aerosol partitioning in favour of the aerosol phase. Depending on where in the atmosphere this occurs, it may deplete the supply of gas phase condensables to the upper troposphere, where, as we have seen, such compounds condense to aerosol with a long lifetime. The total effect on the SOA burden and radiative effect may thus be of either sign.

Omission of aqueous phase reactions also has unclear consequences for the model. Clearly, aqueous phase reactions in the model would have to take place where temperatures exceed the model homogenous freezing threshold of 235K. This is below the level where most isoprene-derived upper tropospheric model SOA is formed, so that while the SOA volatility would decrease (and thus increase the aerosol mass) in the portion of the atmosphere affected by liquid clouds, the supply of gas-phase condensables to the upper troposphere would again be reduced, leading to less SOA there. Once again, considering the difference of aerosol lifetime between the upper and mid-to-lower troposphere, the impact of such a changed distribution remains unclear.

In the last decade, a great deal of effort has been put into understanding the chemical pathways of SOA formation. Unfortunately, comparatively little effort has been expended in characterising anything other than the chemical formation of SOA. Information about the properties that govern the efficiency of the main sink process, wet deposition, is completely lacking. In order to calculate wet deposition from the gas phase of any species, one must know the Henry's Law coefficient for that species. In this study, coefficients have been chosen from http://www.mpch-mainz.mpg.de/~sander/res/henry.html among many possible choices among the products of SOA precursor oxidation. The two-product model thus creates a paradox, whereby the volatility of a wide spectrum of real compounds is represented by two fictitious compounds: yet a complete model requires several physical parameters that must be assigned to the two fictitious compounds using the properties of real compounds. Other than Henry's Law coefficients, this model requires molecular weight and dry reactivity for the dry deposition scheme. Like the Henry's Law coefficient, molecular weights are assigned from among a large number of observed compounds, whereas dry reactivity is simply assumed to be zero for all SOA species.

Finally, the extended lifetime of upper tropospheric organic aerosol, if it is indeed correct that SOA creates substantial amounts of such aerosol, has consequences for other study techniques. Some studies, for example Maria et al. (2003), use the ratio of observed CO to OC as an indicator of aerosol source. The CO/OC ratio of an aerosol sample containing upper tropospheric aerosol will be lower than an equivalent sample containing only lower tropospheric aerosol, since more CO is consumed over the extended aerosol lifetime. This can cause incorrect source apportionment of the aerosol sample. In particular, it may cause incorrect identification of biomass burning as aerosol source, since the observed CO/OC ratio for such aerosol is low (Andreae and Merle, 2001).

2.6.5 *Direct Radiative Effect of SOA*

To the author's knowledge, this is the first study that has attempted to quantify the direct radiative effects (DRE) of SOA including biogenics.

Yu et al. (2006) surveyed model studies of direct radiative effect of several models and compared them against satellite-derived observational estimates. SOA is not explicitly included in any of the models (which do not include ECHAM5-HAM). The observation-based median estimate of DRE is -5.9 Wm^{-2} and that of the models -2.8 Wm^{-2}.

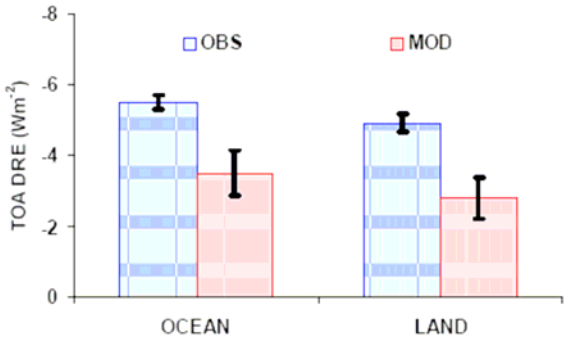

Fig. 2.31. Estimates of TOA median DRE from observations (OBS) and models (MOD). From Yu et al. (2006).

The modelled SOA direct effect over land is -0.35 Wm^{-2} and over ocean -0.29 Wm^{-2}, so that SOA accounts for a sizeable fraction of the model-observation discrepancy. Other reasons for the discrepancy may include the unavailability of satellite observations over high-albedo surfaces such as snow, ice and low clouds, where the true direct effect may even be positive (Quaas et al. 2008).

Forster et al. (2007) compared direct radiative *forcing* of several models against three satellite-derived estimates. Again, the satellite-derived results indicate a higher direct forcing than is modelled.

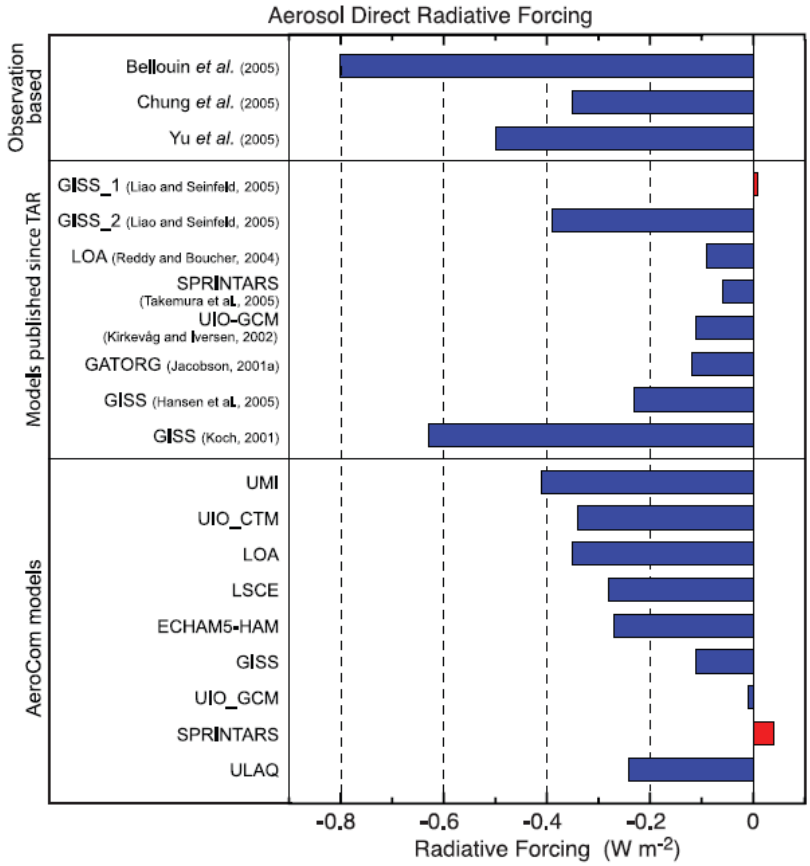

Figure 2.32. Radiative forcing estimated from satellite observations and by models. From Forster et al. (2007)

While this study has not attempted any estimate of total anthropogenic aerosol forcing, the results herein are relevant to the comparison of satellite and models for the following reason. Observations typically classify into fine mode (submicron diameter) and coarse mode (super-micron diameter). The fine mode is regarded as principally anthropogenic. Biogenic aerosols are not taken into account, although this study suggests that the biogenic aerosol mass resides mainly in that fraction. In this model, 88% of biogenic SOA mass resides in the fine fraction in the global annual mean. Particularly over land, the inclusion of biogenic aerosol mass in the anthropogenic fraction in observational studies may cause an overestimation of the anthropogenic forcing, especially when compared against models that do not contain biogenic SOA.

Finally, one can note that Forster et al. (2007) found a direct radiative forcing of just -0.05 Wm^{-2} for OC from fossil fuel. In this light, the estimated radiative effect of SOA may appear large. However, one must bear in mind that the vertical distribution of SOA is completely different from POA and that its mixing state and size distribution are also very different, since it is mostly of biogenic origin and therefore not related to black carbon. Also, the long lifetime of upper tropospheric SOA in this model should be kept in mind.

2.6.6 Indirect Radiative Effect of SOA

Model estimates of the global cloud albedo effect range from -0.5 Wm^{-2} to -1.9 Wm^{-2} in the models surveyed by Lohmann and Feichter, (2005). In recent years, relationships have been derived between

satellite retrievals of cloud properties and aerosol optical depth (Quaas et al., 2008 and the references therein) and used to constrain models. The results indicate that earlier model studies overestimate the cloud albedo effect. Quaas et al. (2008) estimate the cloud albedo effect to be -0.2 ± 0.1 Wm^{-2}. Possible contributors to the model overestimates include the model parameterisation of the autoconversion rate (i.e. the rate of conversion of droplets to raindrops) and whether the model cloud updraft velocity depends on the turbulent kinetic energy (Forster et al., 2007).

This study identifies another possible source of overestimate: secondary organic aerosols. In chapter 2.3.11, it was shown that the CCN concentration can be decreased by SOA (which does depend on the model definition of CCN as any particle of radius > 35 nm). Note that only a model with size-resolved aerosol microphysics can produce this effect, and that it might not occur in models using other cloud droplet activation schemes. Whether this SOA impact is a reasonable reflection of real cloud processes is not possible to state with any certainty, but since (i) it reduces the gap between estimates by model alone and observationally constrained estimates and (ii) the cloud decks affected in the model are observed to be susceptible to aerosol modification (Quaas et al., 2008), some encouragement may be taken from the results.

2.6.7 Model results and surface observations

Comparison of modelled total organic aerosol concentration to surface observations yields mixed results. On the positive side, there is a clear improvement in agreement between model and measurements at the IMPROVE network, but the failure of the model to capture either magnitude or seasonal variability at the southern European EMEP sites remains a major concern, as is the fact that the model remains systematically too low in organic mass compared to nearly all measurements. The very strong correlation of black carbon to total OC measurements at the southern European EMEP sites where the model fails, as well as the better agreement with IMPROVE in summer, when biogenic SOA is high, than winter, points to an anthropogenic (or at least primarily anthropogenic) source for the 'missing' OC.

Possible reasons for the remaining discrepancies include:

1. Constant anthropogenic emissions. Neither POA nor anthropogenic SOA precursor emissions in the model have either diurnal or seasonal cycle. For SOA precursors, night-time emissions are not subject to photochemical conversion to SOA near the source, but instead will be transported away and thereby diluted. Transport is a major user of fossil fuels, and much more of this takes place during the day. Heating and lighting requirements for fossil fuels are also greater in winter. A single annual emission flux, applied throughout each day and throughout the year, is unrealistic.
2. Missing SOA precursors. As has been noted in chapter 1.5, several anthropogenic SOA precursors are known but have not been included in the model either for lack of emission inventories or laboratory data that can quantify the SOA yield and volatility from that precursor.
3. Missing primary organic semi-volatile substances (Robinson et al., 2007)
4. Intermediate compounds. By this is meant compounds that are short-lived but can partition to the aerosol phase. In a smog chamber experiment, where the precursor gas is injected in a single pulse, such compounds will die out quickly, possibly taking no part in the aerosol measurement at the end of the experiment. In the atmosphere, such compounds will be replaced in a continuous flux (Galloway et al., 2009)
5. Missing particle and aqueous phase chemistry.
6. Adsorptive uptake of SOA.
7. Measurement artefacts. The possibility of SOA condensation onto filters has been mentioned in chapter 1.4. Contamination of organic aerosol measurements by ambient organic vapours could explain the systematic gap between model and measurements, although the fact that this gap widens in winter does not seem to support the idea.

2.7 Summary and Conclusions

Secondary organic aerosol (SOA) has been introduced into the global aerosol-climate model ECHAM5-HAM. The SOA submodel treats both anthropogenic and biogenic sources of SOA. SOA is formed in the atmosphere from gas-phase oxidation reactions of precursor gases. Anthropogenic precursor gases include toluene, xylene and benzene. Emissions of anthropogenic precursors are prescribed. Biogenic precursor gases included in the model are isoprene and monoterpenes. Individual monoterpene species are not distinguished from one another, but treated as a single species using the properties of α-pinene as a surrogate. Biogenic emissions are calculated online, depending on temperature and leaf area index (for both isoprene and monoterpenes) and photosynthetically active radiation (for isoprene), following the widely used parameterisations of Guenther et al., (2006) and Guenther et al., (1995).

The model calculates SOA formation from the precursor gases using a highly simplified chemistry scheme, which uses the two-product model of SOA formation developed by Odum et al. (1996). Prescribed monthly values for the concentrations of the atmospheric oxidants OH, O_3 and NO_3 are used. Only the major SOA production for each precursor is considered to form SOA (ozonolysis of monoterpenes, and OH oxidation for all other species). Other oxidation reactions serve to consume precursor gas, but not to produce SOA.

SOA may be either semi-volatile or non-volatile (fixed per species): for semi-volatile species the gas-aerosol partitioning is calculated at each timestep using the equilibrium partitioning model of Pankow (1994a, 1994b). This method only describes the partitioning of SOA into gas and aerosol, whereas the SOA model requires partitioning into several size modes. A simple theory of how to extend the Pankow model to describe size-resolved partitioning has been developed and it has further been shown that the Pankow model describes a unique gas-aerosol equilibrium among multiple organic compounds. This theory predicts that SOA condenses preferentially on large particles.

The SOA submodel takes advantage of the tracer transport, convection and diffusion processes of ECHAM and the aerosol microphysics and gas and aerosol sink processes (wet deposition and dry deposition for gases and aerosols, and sedimentation of aerosols) of HAM, as well as the HAM radiation module that permits size- and composition-resolved calculation of the radiative influence of the aerosol population. In order to allow the hygroscopic growth of organic aerosols, a new water uptake parameterisation (Petters and Kreidenweis, 2007) has been implemented.

The results of two simulations, where the large-scale climate was constrained by nudging to the same reference meteorology, one simulation with SOA and one without, are presented and compared.

Calculated biogenic emissions under year 2000 conditions are 446 Tg/yr isoprene and 89 Tg/yr monoterpenes. The prescribed anthropogenic SOA precursors amount to 17 Tg/yr. Aerosol production is estimated as 21 Tg/yr from biogenic sources and 5.6 Tg/yr from anthropogenic precursors. This compares with 47 Tg POA emissions and 71 Tg(S) sulphate aerosol production.

Column burdens of SOA are highest over the source regions, with biogenic SOA present especially over the tropical forests of Africa and South America. Anthropogenic SOA is largest over the Indian subcontinent, due to high benzene emissions. The modelled atmospheric lifetimes of SOA derived from anthropogenic precursors and from monoterpenes, at 4.8 days and 5.8 days respectively, are comparable to those of other fine-mode aerosol species (e.g. sulphate, 4.6 days; POA 6.0 days); but for isoprene-derived SOA, the lifetime reaches over 15 days. This has been shown to be a result of the laboratory data describing the SOA yield from isoprene oxidation in terms of the two-product model. One such product is described as being produced with a high yield, but highly volatile, favouring condensation to the aerosol phase only at very low temperatures. This leads to large amounts of SOA condensing in the upper troposphere, to which the gas-phase semi-volatiles are transported by tropical convection. Far

from the surface, where temperatures are lower than the homogenous freezing temperature of water (-35°C in ECHAM5) there is effectively no sink of SOA (which, in the model, does not interact with cloud ice), which leads to the extended atmospheric lifetime. It is a matter of concern that isoprene-derived SOA at low temperatures has, to the author's knowledge, never been the subject of any published study.

Aerosol optical depth increases only modestly due to SOA, increasing the global mean AOD by just 0.01 between the simulations without SOA and with SOA. Regionally and seasonally, the increase in AOD can be much larger, with increases of up to 0.2 modelled for the Amazon region in the biomass burning season.

A comparison of model results against measurements has been performed, with the emphasis on wide area and longer term (measurement data over one year were used), with the aim of evaluating the distribution of model results against that of the measurements, rather than concentrating on point-by-point comparison of single stations or short field campaigns. Simulation results both with and without SOA were analysed. Comparison of simulated total organic aerosol concentration against the IMPROVE network of rural stations in the United States, where biogenic SOA can be expected to play a significant role at least in summertime, showed significantly better agreement with the simulation including SOA, especially in the summer months. For a network of stations in western and central Europe, the model performance was much poorer, especially southern Europe. Analysis of correlation between measured organic and elemental carbon (a marker of anthropogenic activity) showed that times and places of poorest model performance are strongly dominated by anthropogenic OC. Whether this is primary or secondary material is not known. In general, the model underestimates organic aerosol mass. While the underestimation is reduced in the simulation with SOA, it is clear that the SOA species included for in the model do not account for all the 'missing' OC. Comparison of modelled AOD values against measurements from the AERONET network showed a modest improvement in the simulation with SOA, but again the modelled values remain systematically too low. The study does reveal, though, that observations (AERONET, IMPROVE) are not normally distributed and that the respective median quantities may be better metrics for model evaluation than the traditionally-used mean values.

Finally, estimates of the direct and indirect effects of SOA have been presented: to the author's knowledge, no previous study has included biogenic aerosols in an analysis of aerosol radiative effects. The direct SW radiative effect of SOA is estimated as -0.31 Wm^{-2}, concentrated over the biogenic source regions. The indirect SW effect is, surprisingly, positive, amounting to +0.23 Wm^{-2}. Analysis of the distribution of particles that can act as cloud condensation nuclei (CCN) shows that the model SOA can act to increase or to decrease CCN. In pristine areas, condensation of SOA boosts growth of small particles, increasing CCN. However in polluted areas, where particles are present in sufficient numbers, the stronger effect is the strengthening of the coagulation sink as particles grow larger, decreasing CCN. In such areas, SOA acts to counteract the indirect effect of anthropogenic aerosols, leading to the positive radiative effect. LW radiative effects are estimated to be close to zero: the net result of all effects is a weak net cooling of -0.09 Wm^{-2}.

The model development herein described represents a second step in modelling of atmospheric organic aerosols, a vast and diverse array of compounds (the first step being the modelling of primary organic particles). Subsequent steps may include the addition of further SOA precursors as laboratory data and emission inventories allow; integration of the scheme with a fully-featured atmospheric chemistry model; development of further chemistry of SOA formation, which may include particle phase, aqueous and acid-catalysed reactions; atmospheric aging of SOA; and possibly parameterisation of the role of SOA in new particle nucleation and interaction with cloud ice, when knowledge of those processes reaches a sufficient level. Although much progress has been made in recent years, the path to a sound level of scientific understanding of atmospheric organic particles remains a long one.

A p p e n d i x 1

SIMPLE CHEMISTRY MODEL

The simplified scheme can be written as:

$$MT + OH \xrightarrow{k_1} X$$

$$MT + O_3 \xrightarrow{k_2} \alpha_{M1} S_{M1} + \alpha_{M2} S_{M2}$$

$$MT + NO_3 \xrightarrow{k_3} X$$

$$IS + OH \xrightarrow{k_4} \alpha_{I1} S_{I1} + \alpha_{I2} S_{I2}$$

$$IS + O_3 \xrightarrow{k_5} X$$

$$IS + NO_3 \xrightarrow{k_6} X$$

$$TOL + OH \xrightarrow{k_7} \alpha_T S_T$$

$$XYL + OH \xrightarrow{k_8} \alpha_X S_X$$

$$XYL + NO_3 \xrightarrow{k_9} X$$

$$BENZ + OH \xrightarrow{k_{10}} \alpha_B S_B$$

where:

- *MT, IS, TOL, XYL, BENZ* denote the precursors monoterpenes, isoprene, toluene, xylene and benzene respectively,
- '*X*' denotes "don't care", meaning that such products are ignored by the model,
- S_i denote condensable SOA species with the subscript *i* denoting the precursor and, where the products are semivolatile, distinguishing the two putative products of the reaction
- α_i are the mass-based stoichiometric coefficients of the reaction, taken from laboratory studies. The α_i used in this study are given in Table 2.1.
- k_i, i = 1,…,10 are reaction rate constants. The k_i used in this study are given in Table 2.1.

For example, for monoterpenes we have, for the precursor gas:

$$\frac{d[MT]}{dt} = -[MT]\left(k_1[OH] + k_2[O_3] + k_3[NO_3]\right) \tag{A1.1}$$

Since the terms in parentheses are constant over a model timestep, we can immediately see the solution for *[MT]* (*t*) as a function of time

$$[MT](t) = [MT](0)\exp\left\{-\left(k_1[OH] + k_2[O_3] + k_3[NO_3]\right)t\right\} \tag{A1.2}$$

Hereafter for brevity the notation

$$k_i[OX_i] = k_1[OH] + k_2[O_3] + k_3[NO_3] \quad \text{(A1.3)}$$

is adopted

The change in monoterpene concentration over a model timestep Δ*t* are

$$\Delta MT = \left([MT](\Delta t) - [MT](0)\right) = -[MT](0)\left(1 - \exp\left\{-\left(k_i[OX_i]\right)\Delta t\right\}\right) \quad \text{(A1.4)}$$

For SOA production, we have for product 1 of the monoterpene-ozone reaction:

$$\frac{d[S_{M1}]}{dt} = k_2\alpha_{M1}[MT][O_3] \quad \text{(A1.5)}$$

Substituting for [*MT*] from above,

$$\frac{d[S_{M1}]}{dt} = k_2\alpha_{M1}[O_3][MT](0)\exp\left\{-\left(k_i[OX_i]\right)t\right\} \quad \text{(A1.6)}$$

Integrating,

$$[S_{M1}](t) = \alpha_{M1}k_2[O_3][MT](0)\left(\frac{-1}{k_i[OX_i]}\right)\exp\left\{-\left(k_i[OX_i]\right)t\right\} + C \quad \text{(A1.7)}$$

where *C* is a constant of integration, evaluated as usual by setting *t* = 0, whence

$$C = [S_{M1}](0) + \alpha_{M1}[MT](0)\left(\frac{k_2[O_3]}{k_i[OX_i]}\right) \quad \text{(A1.8)}$$

So we can write down the concentration of SOA product 1 of this reaction by combining (A1.7) and (A1.8):

$$[S_{M1}](t) = [S_{M1}](0) + \alpha_{M1}[MT](0)\left(\frac{k_2[O_3]}{k_i[OX_i]}\right)\left(1 - \exp\left\{-\left(k_i[OX_i]\right)t\right\}\right) \quad \text{(A1.9)}$$

The change in mass of SOA product 1 over one model timestep is

$$\Delta S_{M1} = \left[S_{M1}\right](\Delta t) - S_{M1}(0) = \alpha_{M1}\left[MT\right](0)\left(\frac{k_2\left[O_3\right]}{k_i\left[OX_i\right]}\right)\left(1 - \exp\left\{-\left(k_i\left[OX_i\right]\Delta t\right)\right\}\right) \quad \text{(A1.10)}$$

Substituting from (A1.4)

$$\Delta S_{M1} = -\alpha_{M1}\left(\frac{k_2\left[O_3\right]}{k_i\left[OX_i\right]}\right)\Delta MT \quad \text{(A1.11)}$$

and the change in mass of product 2 follows simply from the stoichiometry:

$$\Delta S_{M2} = \left(\frac{\alpha_{M2}}{\alpha_{M1}} \right) \Delta S_{M1} \qquad 8\text{(A1.12)}$$

Likewise for isoprene, which is also consumed by all three oxidants and produces SOA from OH:

$$\Delta S_{I1} = -\alpha_{I1} \left(\frac{k_4 [OH]}{k_j [OX_i]} \right) \Delta IS \,, \quad j = 4,5,6. \qquad \text{(A1.13)}$$

$$\Delta S_{I2} = \left(\frac{\alpha_{I2}}{\alpha_{i1}} \right) \Delta S_{I1} \qquad \text{(A1.14)}$$

The same procedure gives, for the aromatics:

$$\Delta S_T = \alpha_T \Delta TOL, \qquad \text{(A1.15)}$$

$$\Delta S_X = \alpha_X \left(\frac{k_8 [OH]}{k_8 [OH] + k_9 [NO_3]} \right) \Delta XYL, \qquad \text{(A1.16)}$$

$$\Delta S_B = \alpha_B \Delta BENZ \qquad \text{(A1.17)}$$

A p p e n d i x I I

UNIQUENESS OF GAS-AEROSOL EQUILIBRIUM

We begin by writing (2.10) as a simple algebraic equation in one variable x, corresponding to M_0 in (2.10), with other terms regarded as constants written as a_i and b_i. We have

$$x = a_0 + \sum_{i=1}^{n} \frac{a_i x}{1 + b_i x} \tag{A2.1}$$

Examining the sum term on the right hand side of (A2.1), let us define

$$f_i(x) = \frac{a_i x}{1 + b_i x} \tag{A2.2}$$

This has first and second derivatives with respect to x:

$$f_i'(x) = \frac{a_i}{(1 + b_i x)^2}, \qquad f_i''(x) = \frac{-2 a_i b_i}{(1 + b_i x)^3} \tag{A2.3a, A2.3b}$$

respectively. We observe that, for solutions that have physical meaning ($x \geq 0$):

i) $f_i(x)$ has no singularities.
ii) $f_i(0) = 0$
iii) $f(x) > 0$ for all $x > 0$, since $a_i \geq 0$, $b_i > 0$.
iv) $f'_i(x) > 0$ (except for the trivial case $a_i = 0$)
v) $f''_i(x) < 0$ (except for the trivial case $a_i = 0$)
vi) $\lim_{x \to \infty} f_i'(x) = \frac{a_i}{b_i}$ and $\lim_{x \to \infty} f_i'(x) = 0$

i) – iv) mean that each $f_i(x)$ is monotonically increasing from zero and has no local maximum or minimum. Thus for each x there is one and only one value of $f_i(x)$ and vice-versa. v) and vi) show that each $f_i(x)$ tends asymptotically to a finite limiting value.

Since these deductions are true for each $f_i(x)$, they are true for their sum.

Considering the left and right hand sides of (A2.1), the left hand side (lhs) can be written as the line

$$y = x \tag{A2.4}$$

which has the value zero at x = 0 and is unbounded as $x \to \infty$. The right hand side can be written as the function

$$y = a_0 + \sum_{i=1}^{n} f_i(x) \tag{A2.5}$$

which is non-negative at x = 0 and bounded as $x \to \infty$. Therefore equality of the y of (A2.4) and (A2.5) must exist for some x, and, since y is single-valued in both (A2.4) and (A2.5), this x must be unique. This is graphically illustrated below.

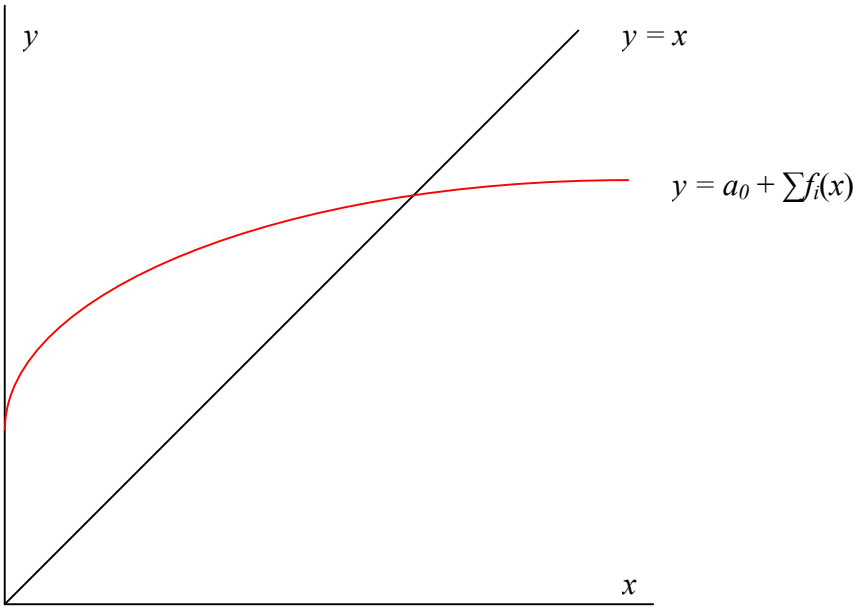

Appendix III

GAS-AEROSOL PARTITIONING AMONG DIFFERENT SIZE MODES

Suppose we have two sets of numbers x_i and y_i such that the ratio of each pair of numbers is the same.

$$\frac{x_i}{y_i} = k \tag{A3.1}$$

where k is a constant. Then

$$\frac{x_i + x_j}{y_i + y_j} = \frac{ky_i + ky_j}{y_i + y_j} = k \tag{A3.2}$$

This can be iterated as many times as we wish, so that we can write

$$\frac{\sum_{i=1}^{n} x_i}{\sum_{i=1}^{n} y_i} = k \tag{A3.3}$$

Now consider semi-volatile aerosol of different size classes (modes) in phase equilibrium. Let A_{ij} denote the mass concentration of species *i* in mode *j*, M_{NVj} and M_{0j} the mass concentrations of non-volatile SOA absorbers and total SOA absorbers respectively in mode *j*. Let A_i, M_{NV} and M_0 be the corresponding total quantities. G_i is the gas-phase masss concentration of species *i* and $K_{p,,I}$ it partitioning coefficient. Equilibrium of the total is given by (2.4); to reiterate,

$$A_i = K_{p,i} M_0 G_i \tag{A3.6}$$

Equilibrium of each mode specifies the same gas phase, and further, it has been shown that the same partitioning coefficient may be used for all size modes. Then

$$A_{ij} = K_{p,i} M_{0j} G_i \tag{A3.7}$$

The fraction of SOA species *i* in mode *j* is, by dividing (A3.7) by (A3.6):

$$\frac{A_{ij}}{A_i} = \frac{M_{0j}}{M_0} \tag{A3.8}$$

Observe that the right hand side is *independent of i*, so (A3.8) is true for all *i*, which is as one would expect, since there is no reason to assume that different species would behave differently for a given mode (as we have neglected activity coefficients). Because the ratio of A_{ij} to A_i is the same for all *i* for a given *j*, we can, following (A3.1)-(A3.3), write

$$\frac{A_{ij}}{A_i} = \frac{\sum_{i=1}^{n} A_{ij}}{\sum_{i=1}^{n} A_i} \tag{A3.9}$$

Substituting (A3.9) in the left hand side of (A3.8) and expanding the M_0 terms on the right hand side into their non-volatile and semi-volatile components (2.9)

$$\frac{\sum_{i=1}^{n} A_{ij}}{\sum_{i=1}^{n} A_i} = \frac{M_{NVj} + \sum_{i=1}^{n} A_{ij}}{M_{NV} + \sum_{i=1}^{n} A_i} \tag{A3.10}$$

The product of sums terms cancel on cross-multiplying, leaving

$$\frac{\sum_{i=1}^{n} A_{ij}}{\sum_{i=1}^{n} A_i} = \frac{M_{NVj}}{M_{NV}} \tag{A3.11}$$

Or, using (A3.9) again,

$$\frac{A_{ij}}{A_i} = \frac{M_{NVj}}{M_{NV}} \tag{A3.12}$$

Chapter 3

3 On biogenic emissions in different climate states and the possibility of a 'biogenic thermostat'

ABSTRACT

The coupling between climate and biogeochemical processes remains an area where considerable progress remains to be made in order to advance our understanding the interactions between the many components of the global climate system. Among these many processes, the emission of aerosol precursor gases from plants has been the subject of extensive study over the past two decades. Many studies have shown that emissions of identified precursors from plants – in particular, isoprene and monoterpenes – are sensitive to ambient temperature, as well as, at least in the case of isoprene, to photosynthetically active radiation (PAR). These dependencies are accounted for in models of biogenic emissions, and such models have been deployed within global climate models to generate estimates present-day estimates and future projections of biogenic precursor emissions and secondary organic aerosol (SOA) formation. Several such studies indicate a large increase in future emissions and SOA burden, due to the observed sharp increase of emissions with increasing temperature. Furthermore, the hypothesis has been advanced that such an increase can constitute a negative feedback in a warming climate, through the cooling effect of organic aerosols. However, there is now a body of evidence that biogenic precursor emission is negatively correlated to CO_2 concentration. In this study, we apply two different models, one representative of the present generation of global models of biogenic emissions, and one process-based dynamic vegetation model to the study of biogenic emissions in different climate states. Present-day climate and a warmer, high-CO_2 climate are studied. In the model that does not take the CO_2 effect into account, emissions in a warmer climate increase substantially. In contrast, results from the process-based model indicate that biogenic emissions and biogenic SOA loading may decline in a warmer, high-CO_2 climate. If this is the case, then the reaction of the biosphere is a positive feedback rather than a negative feedback.

3.1 Introduction

Plants emit a number of volatile compounds, collectively known as biogenic volatile organic compounds (biogenic VOCs or BVOCs). BVOCs include isoprene, monoterpenes, sesquiterpenes, alkanes, alkenes, alcohols, carbonyls, esters, ethers and acids (Kesselmeier and Staudt, 1999). The flux of such compounds to the atmosphere is estimated to be of the order of hundred of teragrams per year (Guenther et al. 1995; Guenther et al. 2006). Many of these species are readily oxidised in the atmosphere, and certain reaction products are known to condense into the aerosol phase. Aerosol so formed is known as secondary organic aerosol (SOA), and the particular case of aerosol formed from biogenic VOC precursors as biogenic SOA (BSOA). Known BSOA precursors include isoprene (Claeys et al., 2004) and many different monoterpenes and sesquiterpenes (Griffin et al., 1999). Emission of each of these species is influenced by leaf temperature. Isoprene emission takes place only under leaf illumination by photosynthetically active radiation (PAR). This is also true of monoterpenes in some plant species, although more commonly monoterpene emission takes place independently of light. Other factors include soil moisture and leaf age (Guenther et al. 2006). Sesquiterpene emissions are also influenced by temperature, but can also take place in intense bursts as a plant response to herbivory or other stress. Sesquiterpene emissions exhibit high variablility, even between individuals and at different environmental and phenological states (Dhul et al. 2008). No global estimate of sesquiterpene emission is yet available, and for this reason this work is confined to the study of isoprene and monoterpenes.

Organic carbon aerosol is estimated to have a net cooling influence on the Earth's climate (Forster et al. 2007). Thus we see a bi-directional relationship between plant emissions and climate: climate influences plant emissions through variation in temperature, PAR and soil moisture, whereas plant emissions influence climate through formation of SOA and the radiative and cloud effects of these aerosols.

This link between climate and emissions from vegetation has been the subject of a number of studies, mainly focused on the effects of global warming (e.g. Turner et al., 1991; Sanderson et al., 2003; Lathière et al., 2005; Liao et al., 2006; Heald et al., 2008). All these studies concur in the conclusion that biogenic emissions will rise sharply in a warmer climate. Furthermore, it has also been hypothesised that in a warming climate, biogenic emissions operate a negative feedback (Kulmala et al. 2004b). The basis of this hypothesis is that increased ambient temperatures will lead to sharply increased biogenic emissions, which in turn will lead to increased BSOA production and thus to an enhanced aerosol-induced cooling effect. This hypothesis is sometimes called the 'biogenic thermostat' hypothesis.

There is, however, one more known factor at work in the interaction between climate and emissions from vegetation, namely the ambient CO_2 concentration. This is not taken into account by any of the above-cited works, although such a dependency has long been known to exist, at least for isoprene (Sanadze, 1991). Observations of plants grown in differing ambient CO_2 levels clearly indicate an inverse relation between isoprene emission and CO_2 concentration (Arneth et al. 2007 and the references therein). Fewer studies have addressed the response of monoterpene emissions to varying CO_2 levels, but there is some evidence (Loreto et al., 2001; Staudt et al., 2001; Baraldi et al., 2004) that monoterpene emission is also inhibited under elevated CO_2 concentration. The existence of such a relation between isoprene and monoterpene emissions and CO_2 levels requires that the conclusion that future warmer-climate emissions will increase sharply must be re-examined. So far, only one study (Heald et al., 2009) has modelled the CO_2 effect on isoprene emissions with the result that a decline was projected for year 2100 conditions. No study has addressed emissions of other BSOA precursors or BSOA formation in this context. The application of a process-based dynamic vegetation model to the study question is also new.

In this study, we apply two different approaches to biogenic emission modelling. The first is an empirically-based model (MEGAN: Guenther et al., 2006; Guenther, 2007) that takes into account temperature, PAR and leaf area index (LAI), but not CO_2 concentrations. The second is a process-based model (Arneth et al., 2007; Schurgers et al., 2009) that calculates emission rates based on in-leaf processes and ambient conditions including temperature, PAR and CO_2 concentrations. Each model in turn is used as input to the global aerosol-climate model ECHAM5-HAM. Two climate states are studied: firstly, present-day conditions, and secondly, a warmer, high-CO_2 climate state with CO_2 levels according to the SRES scenario A2. Emissions for both climate states and both models are examined, as well as the resulting aerosol effects. In this way, we can assess whether the conclusion that biogenic SOA will greatly increase in a warmer climate is sustainable in the light of the CO_2 dependency of emissions, and whether modelling supports the notion of a 'biogenic thermostat'.

It should be emphasised that this study aims to examine a biosphere-climate feedback mechanism via organic aerosol. It is not the intention of this study to make any future projection. Neither is it the purpose of this study to make any inter-comparison of, or evaluation of, different approaches to the modelling of biogenic emissions.

3.2 Method

In this set of simulations, we use two different biogenic emission models, in conjunction with the aerosol-climate model ECHAM5-HAM (Stier et al. 2005) The MEGAN model (Guenther et al. 2006; Guenther, 2007) has been implemented as an integral (but optional) part of ECHAM5-HAM. This configuration calculates biogenic emissions online, as a function of temperature, PAR and LAI. The influence of soil moisture and of leaf age, which are also quantified in (Guenther et al. 2006), are not included in this

MEGAN implementation. As an alternative, ECHAM5-HAM can be supplied with prescribed monthly biogenic emissions. To investigate the impact of CO_2 on biogenic emissions and upon the climate effects of biogenic SOA, biogenic emissions are caculated offline using the dynamic vegetation model LPJ-GUESS (Smith et al., 2001; Sitch et al., 2003), which includes process-based calculation of isoprene (Arneth et al., 2007) and monoterpenes (Schurgers et al., 2009) emissions, and which takes the ambient CO_2 concentration into account. The emissions calculated by LPJ-GUESS are then taken as prescribed input to ECHAM5-HAM.

Two climate states are investigated, firstly near present-day conditions, and secondly a warmer, high-CO_2 climate. The climate state in each of these simulations is constrained on the large scale by using prescribed sea surface temperatures (SSTs). The SSTs used are 30-year means of monthly means of SST calculated by the coupled atmosphere-ocean model ECHAM5/MPI-OM as part of the modelling community effort for IPCC AR4. For near present conditions, the mean conditions 1971-2000 are used. For the warmer climate state, we use SSTs for the years 2071-2100 as calculated for SRES scenario A2.

The atmospheric CO_2 concentration is also prescribed according to the A2 scenario. No other A2 greenhouse gases or emissions are used. Emissions of all carbonaceous aerosol species, other than biogenics, are identical between all simulations. Neither is any land use change supposed. This is done to minimise the number of variables that affect the biogenic aerosol loading, since, in addition to the emission flux, the formation of biogenic SOA depends on the pre-existing organic aerosol mass as outlined in chapter 1.6. This means that, all other things being equal, an increased POA loading will by itself give rise to an increased SOA loading. In addition, varying emissions lead to responses in column burdens and radiative effects that are non-linearly related to those emissions (Stier et al., 2006). Of course, we seek to extract unambiguous cause-effect relationships from these simulations, and for the foregoing reasons this can best be done if additional perturbations to the aerosol system are avoided as far as possible.

Six simulations were performed: for both climate states and for both biogenic emission models as well as without any biogenic emissions. Each model run simulates five years, following a three-year spinup period. These simulations are hereafter designated as per the table below. 'A2' in the CO_2 concentration column means 'according to SRES scenario A2'. 'NB' signifies 'no biogenics'.

Name	Climate State	Emission Model	SST	[CO_2] (ppmv)
Lo-NB	Near-present	None	1971-2000	370
Lo-MEG	Near-present	MEGAN	1971-2000	370
Lo-LPJ	Near-present	LPJ	1971-2000	370
Hi-NB	Warmer, high-CO_2 climate	None	2071-2000	A2
Hi-MEG	Warmer, high-CO_2 climate	MEGAN	2071-2100	A2
Hi-LPJ	Warmer, high-CO_2 climate	LPJ	2071-2100	A2

Table 3.1. List of simulations related to biogenic emissions in different climate states

The LPJ-GUESS model requires temperature, precipitation, surface shortwave (SW) radiation and CO_2 concentration. The former three are derived from the same ECHAM5/MPI-OM model runs as the SST for the corresponding climate state. As the MEGAN simulations in this suite are run for five years, the input data for LPJ-GUESS are taken as the monthly means of same time period. The output from LPJ includes the monthly mean emissions of isoprene and monoterpenes. These results, for each climate state, are then used as input to the aerosol model in the Lo-LPJ and Hi-LPJ simulations.

The MEGAN simulations are standalone ECHAM5-HAM simulations.

One should note that the simulations described in this chapter are all free model runs, not nudged runs, as simulation of a different climate state is required. The resulting differences in meteorology give rise to considerable differences in horizontal and vertical tracer transport, and the results are therefore not directly comparable to those presented in other chapters.

Differences in the meteorological inputs to the LPJ-GUESS model (temperature, surface shortwave radiation and precipitation) are shown in figures 3.1. The difference in cloud cover is also presented, since it aids understanding of the change in surface SW radiation.

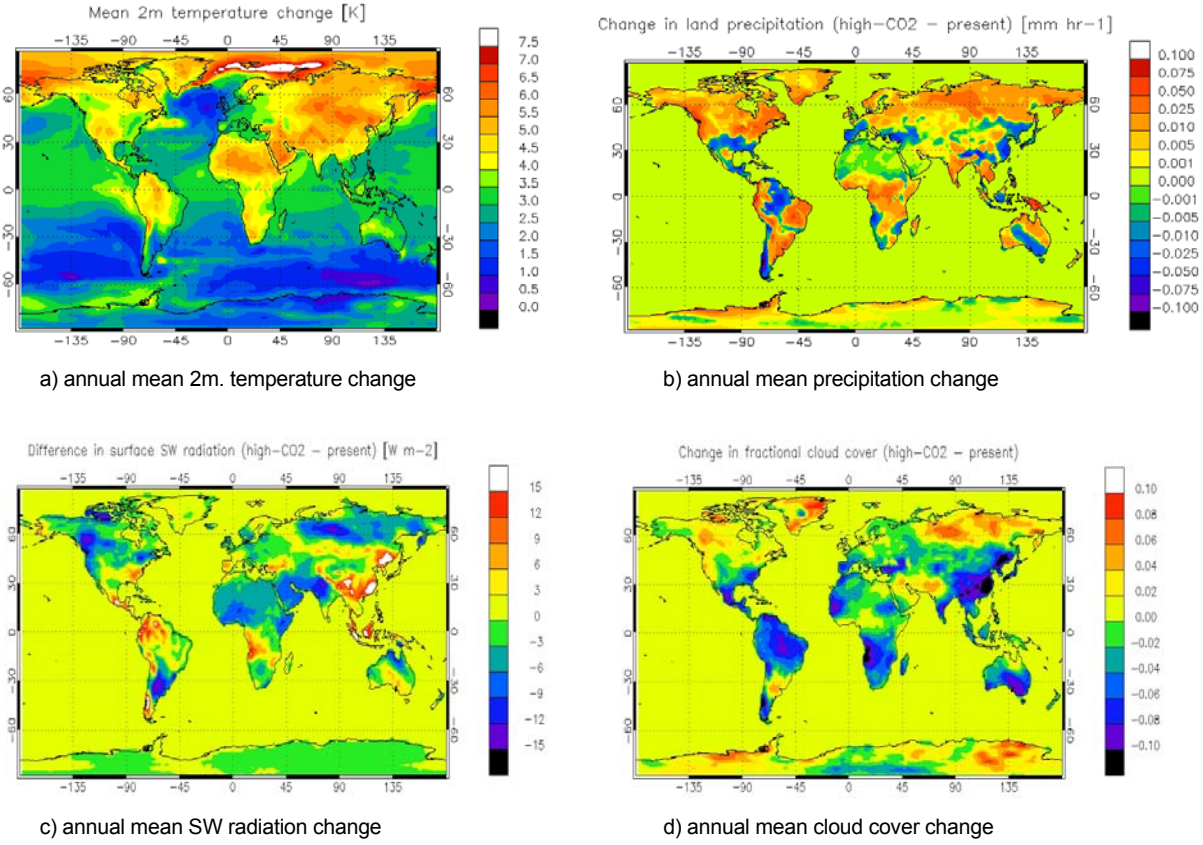

a) annual mean 2m. temperature change

b) annual mean precipitation change

c) annual mean SW radiation change

d) annual mean cloud cover change

Figure 3.1. Changes in meteorological input data (warmer climate minus near-present climate)

Temperature in the most important emitting regions, the tropical forests of South America and Africa, increases by a factor of 3.5 – 5 K in the annual mean. SW surface radiation also increases in these regions. The temperature increase over the boreal forest is even higher, although this is mitigated by a decrease in annual mean SW radiation over most of the region, which can be attributed to an increase in cloud cover (the anti-correlation between the change in cloud cover and the change in surface SW radiation is clear from figures 3.1c) and 3.1d). Precipitation increases over the boreal forest and the central African rainforest, but is reduced over much of the Amazonian rainforest, and over the biogenic hotspot in the south-eastern United States.

3.3 Results and discussion

3.3.1 Emissions of isoprene and monoterpenes

Global annual mean emissions of isoprene are calculated using MEGAN as 460 TgC/yr in near-present, rising to 752 TgC/yr in the warmer climate scenario. Using LPJ, the near-present figure is 365 TgC/yr, falling to 311 TgC/yr in the warmer climate. For monoterpenes, MEGAN calculates the annual mean emission as 88 TgC/yr in near-present, and 130 TgC/yr in the warmer climate. The corresponding totals calculated by LPJ are 25.5 TgC/yr and 20.5 TgC/yr.

The two vegetation models are in reasonable agreement – within a margin less than 30% - in their calculations of isoprene emissions under near-present conditions. However, this not the case for monoterpenes, where under these conditions the models differ by a factor of more than 3. LPJ lies at the low end of the spectrum of modelled monoterpene estimates: this is further analysed in Schurgers et al. (2009).

Isoprene emissions calculated by MEGAN increase in all regions in the warmer climate. With LPJ, isoprene emission declines throughout the tropical forests. A few areas show an increase: these are arid areas such as the western United States and West Australia, where the increased CO_2 levels allow plants to become more water-efficient through reduced stomatal opening, leading to increased vegetation in those areas.

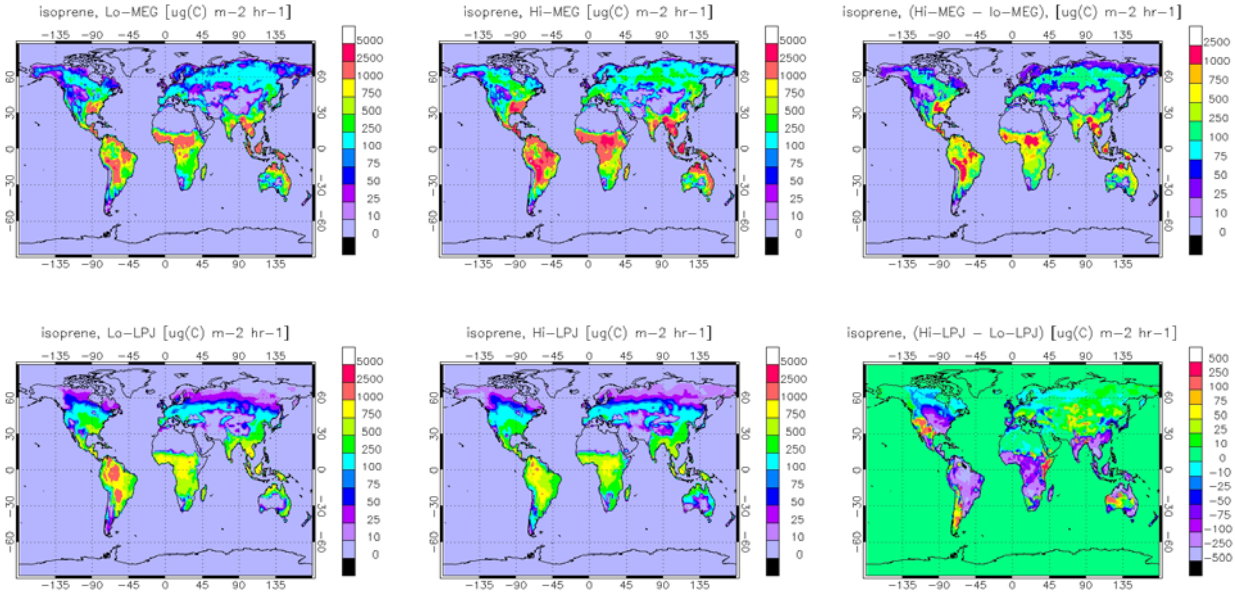

Figure 3.2. Isoprene emissions calculated by MEGAN (above) and LPJ (below), for near-present conditions (left), warmer climate (centre) and the difference (warmer climate minus near-present), (right)

Monoterpene emissions follow a similar pattern, with large increases in the MEGAN-calculated emissions, especially in the Amazonian rainforest, and declines in the LPJ-calculated emissions, with a marked decrease in emissions from tropical broadleaf and temperate deciduous trees.

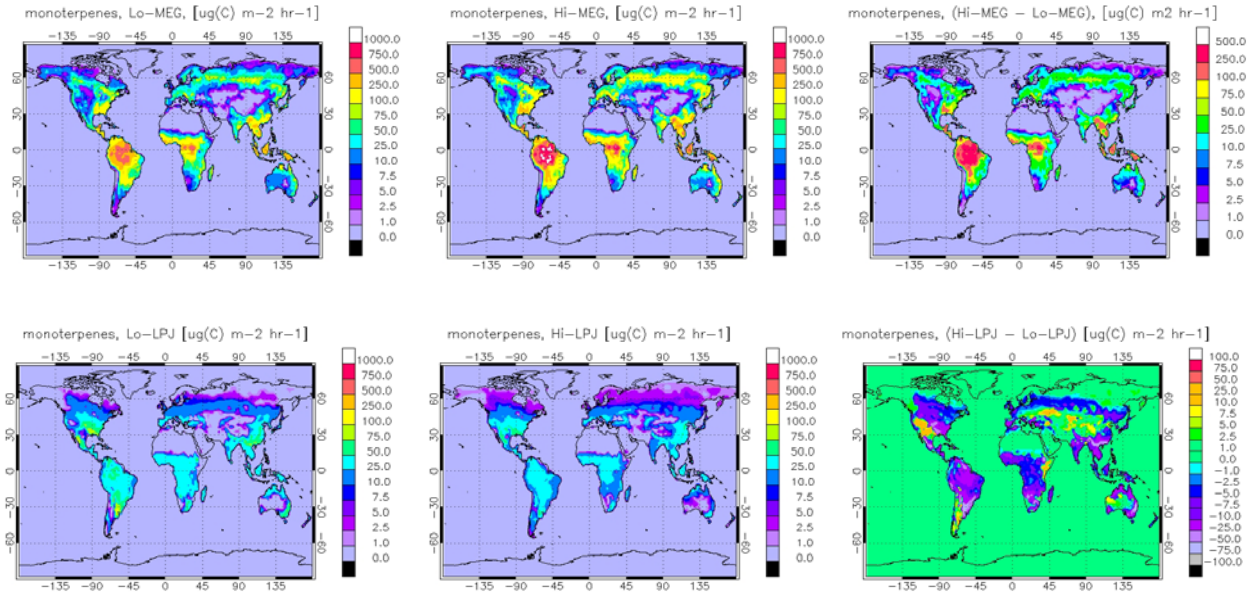

Figure 3.3. Monoterpene emissions calculated by MEGAN (above) and LPJ (below), for near-present conditions (left), warmer climate (centre) and the difference (warmer climate minus near-present), (right)

Comparisons with other models that have studied biogenic emissions in present climate states requires some caution, since there are differences in the warmer states studied (for example, using SRES scenario A1B versus A2) and in the climate sensitivities of the models, so that different models using the same scenario result in different model climates. Nonetheless, the perspective obtained by such a comparison is still valuable. In table 3.2, 'ISOP' denotes isoprene, 'MT' monoterpenes, 'NP' near-present and 'WC' warmer climate and 'CO_2' the source of CO_2 data or the prescribed concentration used.

Reference	GCM	CO_2	ISOP NP [TgC/yr]	ISOP WC [TgC/yr]	MT NP [TgC/yr]	MT WC [TgC/yr]
Sanderson et al. (2003)	HadCM3	IS92a	484	649	-	-
Lathière et al. (2005)	LMDz	560 ppmv	402	638	131	265
Liao et al. (2006)	GISS II'	A2	438	680	117	185
Heald et al. (2008)	CAM3	A1B	496	607	43	51
Heald et al. (2009)	CAM3	A1B	523	479	-	-
This study, MEGAN	ECHAM5	A2	460	752	88	130
This study, LPJ	ECHAM5	A2	365	311	25.5	20.5

Table 3.2. Biogenic emission studies in present and warmer climates

The relatively small variation between models in calculation of isoprene under near-present conditions compared to monoterpenes is more likely to be due to similarity of parameterisations than to well-constrained knowledge of the processes and biome emission factors, as discussed by Arneth et al. (2008).

It should also be borne in mind that the number of studies of plant emissions under varying CO_2 conditions is limited, especially for monoterpenes. Tropical species, in particular, require further study. While there is *a priori* no reason to suspect that the processes of isoprene and monoterpene emissions should be affected in different ways in such species than in those species whose response has been documented, the possibility cannot be categorically excluded.

Because only a single altered climate state has been examined, this result does not prove that CO_2 inhibition always has a stronger effect than temperature stimulation on biogenic emissions: it is possible

that a different choice of boundary conditions would result in an increase in emissions in that model. Its significance is rather that, based on known leaf-level processes, it shows that one conclusion of earlier studies, namely that biogenic emissions would rise sharply in a warmer climate, cannot be regarded as robust in the light of the effect of CO_2 on those emissions.

3.3.2 Biogenic SOA production and atmospheric burden

The production of SOA from each of the biogenic precursors, in each climate state, is shown in figure 3.4.

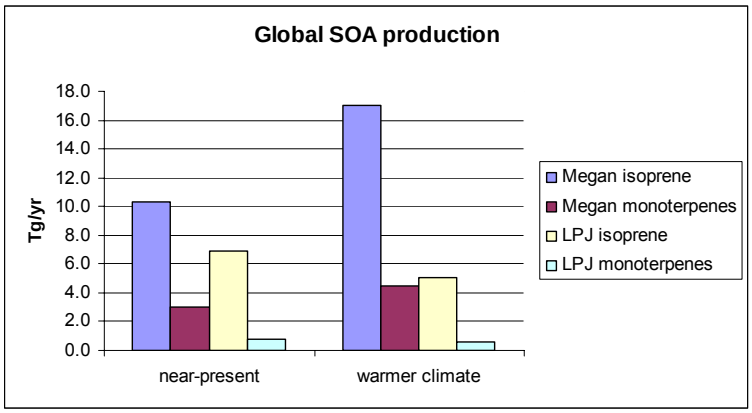

Figure 3.4. Global biogenic SOA production in near-present and warmer climate states

In the near-present climate state, the global annual mean biogenic SOA burden using emissions calculated by MEGAN is 0.75 Tg and 0.46 Tg using LPJ-calculated emissions. In the warmer climate state, the mean biogenic SOA burden climbs to 1.1 Tg (+50%) with MEGAN, but falls to 0.30 Tg (-35%) using LPJ. The largest changes in each case lie over the precursor source regions

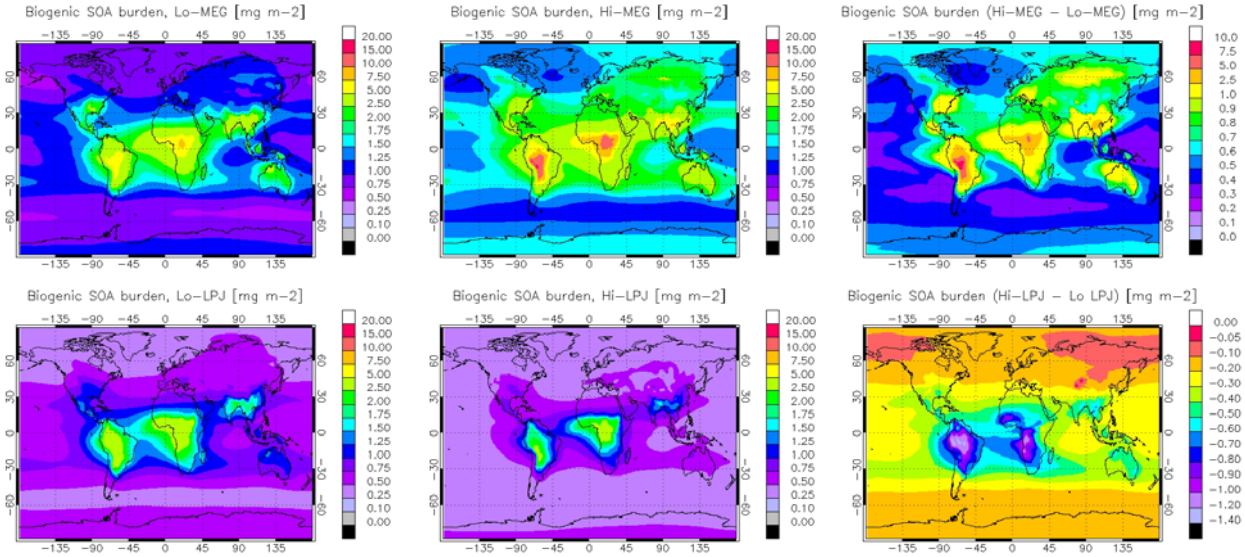

Figure 3.5. Biogenic SOA burden calculated by MEGAN (above) and LPJ (below) for near-present (left), warmer climate state (centre) and the difference between them (right)

In comparison with other models that have computed BSOA burdens, Tsigardis and Kanakidou (2007) used prescribed emissions totalling 467 TgC/yr (near-present) and 639 TgC/yr (future) for isoprene and 137 TgC/yr (near-present) and 301 TgC/yr (future) for monoterpenes. They calculated a SOA production increase from 4.6 Tg/yr to 12.6 Tg/yr from isoprene and from 12 Tg/yr to 40 Tg/yr from the sum of other biogenic sources. The resulting biogenic SOA burden was 0.8 Tg in the annual mean for near-present conditions and 2.0 Tg for future conditions. In that study, anthropogenic organic emissions for the future scenario were substantially increased, whereas in this study they have been held constant.

Liao et al. (2006) performed an simulation for a future climate driven by SRES scenario A2, with anthropogenic aerosol emissions held constant at year 2000 levels. Isoprene was not considered to be a SOA precursor in that study. They calculated a modest increase in total SOA, from 0.35 Tg to 0.38 Tg.

In the study by Heald et al. (2008), production of SOA was calculated as 19 TgC/yr from isoprene and 3.7 TgC/yr from monoterpenes for near-present conditions. For future (A1B) conditions, the corresponding figures are 23 TgC/yr and 4.9 TgC/yr. A breakdown of the column burden by origin (biogenic/anthropogenic) was not presented in that paper, but the total SOA burden was given as 0.59 Tg(C) for near-present conditions and 0.80 Tg(C) for year 2100 conditions. Applying the commonly used conversion factor of 1.4 to convert mass of carbon to organic aerosol mass gives figures for the column burden of of 0.83 Tg and 1.1 Tg, very similar to the results of the MEGAN simulations in this study. This does not, however, indicate close agreement between the models, rather that they have differences of opposite sign in SOA production and SOA lifetime.

There is no published model study of SOA production under warmer climate conditions that takes the effect of CO_2 on biogenic emissions into account. The figures of 5.6 Tg/yr SOA production and 0.30 Tg annual mean biogenic SOA burden, calculated using LPJ in a warmer climate, are lower than those in any published study.

3.3.3 Aerosol Properties

Aerosol optical depth at 550nm is 0.15, 0.16 and 0.17 in the global annual mean for near-present climate for the simulations Lo-NB, Lo-MEG and Lo-LPJ respectively. For the warmer climate state, corresponding results are 0.15, 0.17 and 0.16. The differences in these results are not purely attributable to SOA, however, since internal model variability gives rise to differences in meteorology that are absent when the model is constrained by nudging. Meteorological differences lead in turn to differences in emissions of dust and sea salt, in transport of aerosols, and in clouds and precipitation, which are the main sinks of aerosol and of condensable organic gases. In particular, differing dust emissions are responsible for much of the AOD difference between the simulations. However, we can estimate the contribution of biogenic SOA by its volume weighting. On this basis, the estimated contribution of BSOA to the aerosol optical depth is shown in figure 3.6.

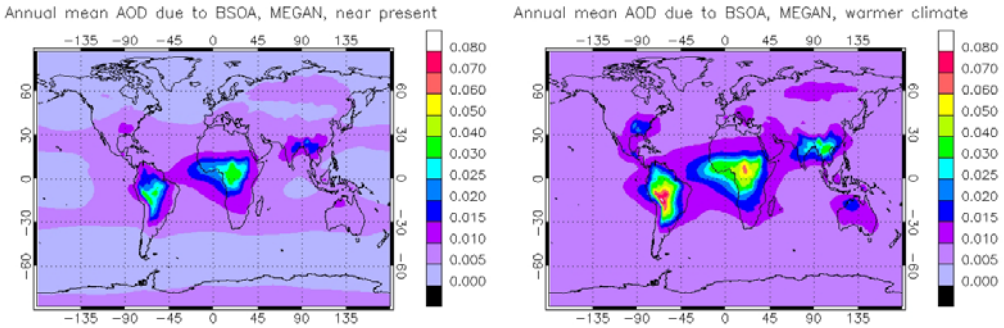

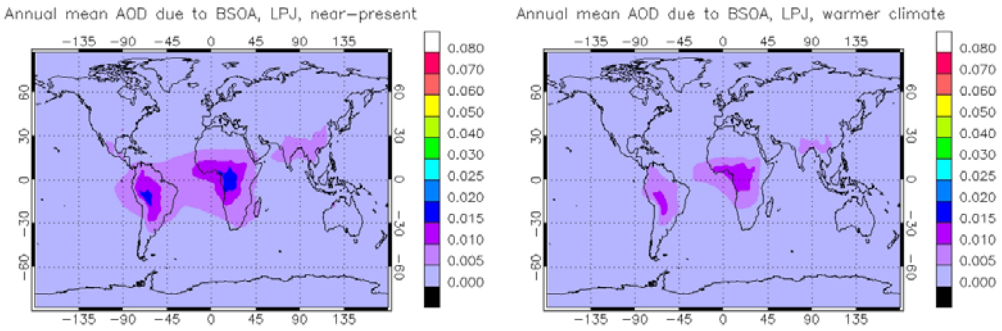

Figure 3.6. Estimate of AOD due to BSOA in the MEGAN (above) and LPJ (below) simulations, in near-present (left) and warmer climate states (right)

The global means of the respective contributions are 0.0066 and 0.010 in the MEGAN simulations for near-present and warmer climate respectively, with corresponding values of 0.0038 and 0.0024 for the LPJ simulations.

3.4 Summary and conclusions

Emissions of certain biogenic SOA precursors, namely isoprene and monoterpenes, have been examined using different vegetation modelling techniques, and in different climate states, and the resulting BSOA production and atmospheric loading calculated with the global aerosol-climate model ECHAM5/HAM, with the goal of re-examining, in the light of the CO_2 effect on emissions, the results of previous studies, that conclude that biogenic emissions and BSOA loadings would increase in a warmer climate. The idea that a negative temperature feedback mechanism exists, whereby increasing temperatures lead to increased BSOA production and thus to a cooling effect is also examined.

Simulations have been performed applying two approaches to modelling of biogenic emissions in two different climate states. These climate states were constrained on the large scale by the use of prescribed sea surface temperatures, in the first case representative of late 20th century (near-present) conditions, and in the second derived from ECHAM5/MPIOM simulations of late 21st century climate under SRES scenario A2. CO_2 concentrations for the respective climate states was fixed at 370 ppmv for the former and prescribed according to the A2 scenario for the latter. In order to minimise the number of non-climatic variables that can influence the formation of BSOA, concentrations of greenhouse gases other than CO_2 were kept constant, as were emissions of all anthropogenic aerosols, for all simulations. For each of these climate states, biogenic emissions were calculated using two different models, the widely-used MEGAN model and the dynamic vegetation model LPJ. MEGAN does not take CO_2 concentration into account when calculating emissions, whereas LPJ does so.

In common with previous studies of biogenic emissions in warmer climates that do not consider CO_2 levels, calculation with MEGAN indicates a large temperature-driven increase in emissions of isoprene and monoterpenes. Calculation with LPJ results in a decrease in emissions, indicating that, for the CO_2 levels and temperatures studied, that the CO_2 inhibition of isoprene and monoterpene emissions outweighs the effect of temperature stimulus. In both models, BSOA loadings move in tandem with biogenic emissions, so that the sign of the biogenic aerosol temperature feedback is negative between the MEGAN simulations and positive between the LPJ simulations. The amplitude of the emission response to temperature is smaller in the simulations using LPJ, as biogenic emissions in these simulations are subject to one major stimulus (temperature) and one major inhibitor (CO_2), compared to the MEGAN simulations which have no significant inhibitor.

The simplified change of conditions between the different climate states in this study means that it cannot be taken to be a real-world projection of the future evolution of climate-biosphere interactions. This study has assumed no human-induced changes in vegetation through agriculture or deforestation/afforestation. Furthermore, since formation of BSOA depends upon the pre-existing organic aerosol mass, actual evolution of the BSOA burden clearly depends upon the evolution of other primary organic as well as anthropogenic SOA species. The fate of organic aerosols in the atmosphere further depends upon the inorganic species, which in turn depend on factors including anthropogenic activities, wind (dust and sea salt), volcanism, and oceanic phytoplankton (emissions of the sulphate aerosol precursor DMS). Atmospheric chemistry is also important, and concentrations of OH, O_3 and NO_x are species of known importance in BSOA formation. A complete model future projection should therefore incorporate land, ocean biogeochemistry, atmosphere, aerosol and chemistry modelling over the duration of the period, which is beyond the scope of this study.

A principal result of this study is that emissions of BSOA precursors and BSOA loadings decline when using a dynamic vegetation model that can model the effect of CO_2 on biogenic emissions. This model study thereby does not support the existence of a negative 'biogenic thermostat' feedback. However, it cannot be said that this study establishes that the CO_2 effect is dominant. If the climate sensitivity to CO_2 is higher than that in this study, the temperature stimulus may be greater than modelled here and then may still prove to be the dominant factor. Nevertheless, the results indicate that the effect of CO_2 upon biogenic emissions is a key factor that cannot be ignored in modelling these species in different climate states.

Chapter 4

4 Towards understanding of the influence of the terrestrial biosphere on a pristine atmosphere

ABSTRACT

The radiative effect of atmospheric aerosols is strongly dependent on aerosol size and composition. Mie theory shows that the extinction (the sum of absorption plus scattering) of radiation by a spherical aerosol particle is a function of the ratio of the particle diameter to the wavelength of radiation incident upon it. It further shows that the scattering of radiation by such particles is in general directionally asymmetric, with a higher proportion of radiation scattered backwards in the direction of the radiation source by smaller particles. Consequently, particles larger than size range as the wavelength of visible light have proportionally less influence on the solar radiation budget than smaller particles of the same composition. Natural sources of aerosols include wind-driven sea salt and mineral dust, which consist mainly of larger (diameter > 1μm) particles and volcanoes. Aerosols are also formed in the atmosphere from precursor gases. Naturally-occuring precursors include SO_2, which is emitted in seismically active areas, dimethyl sulphide (DMS), of which phytoplankton are the largest source, and gases emitted by plants, including isoprene, monoterpenes and sesquiterpenes.

The human race, through biomass burning, and latterly through industrialisation, has brought with it large-scale emissions of carbonaceous and sulphate aerosols, which have fundamentally altered the composition and size distribution of the tropospheric aerosol population. A much greater fraction of anthropogenic aerosol is emitted as submicron diameter particles than is the case for natural aerosols. Although the global tropospheric burden natural aerosols is greater than that of all anthropogenic aerosols by an estimated order of magnitude, anthropogenic aerosol contains a much greater fraction in the radiatively important submicron range. The aerosol size distribution also influences the properties of clouds. Clouds have traditionally been classified as continental or maritime, with continental clouds being associated with much higher cloud droplet number concentrations (CDNC) and smaller droplet radii. Recent measurements over pristine Amazon rainforest in the wet season, which is devoid of anthropogenic disturbance in the form of forest clearing fires, have shown that clouds in unpolluted continental areas have CDNCs comparable to those in clean maritime regions. Since these measurements show that there is no fundamental reason why clouds over continents should have higher CDNC, the traditional classification of clouds into continental and maritime has been challenged, and it has been proposed that the continental class is in fact an anthropogenically polluted class.

In this study, the global aerosol-climate model ECHAM5/HAM is applied to the study of tropospheric aerosol and clouds in the absence of, and in the presence of, anthropogenic emissions of aerosols and aerosol precursors. The role of vegetation in both cases is also studied.

Model results support the idea that 'continental' clouds are in fact anthropogenically polluted clouds. In the pristine atmosphere, the biosphere exerts a stronger influence than in the polluted atmosphere, with a direct shortwave radiative effect of biogenic secondary organic aerosols at the top of the atmosphere estimated as -0.28 Wm^{-2}, with very small indirect and thermal radiative effects.

4.1 Introduction

Aerosols influence climate through the absorption and scattering of shortwave and longwave radiation, and through their impact on the microphysical properties of clouds. Mie (1908) showed that the scattering and extinction of radiation by a spherical particle can be quantified in terms of the particle complex refractive index and a *size parameter* $x = 2\pi r / \lambda$, where r is the particle radius and λ the wavelength of the incident radiation. Complex refractive index is determined by composition. The effect of an aerosol population upon radiation of a given wavelength is thus a function of the aerosol composition and particle size relative to that wavelength. Particles extinguish radiation most efficiently when their radius is close to the wavelength of the incident radiation. Mie theory further shows that, for a given wavelength, the backscattered fraction of total scattering decreases with increasing particle size. For atmospheric aerosols backscattered radiation, unless it is absorbed or scattered again, is lost to space, and thus gives a cooling effect.

For these reasons, the submicron fraction (measured by diameter) is of particular interest for study of the radiative effects of aerosols on climate.

Natural sources of aerosols and aerosol precursor gases include wind-driven sea salt and mineral dust emissions, DMS from phytoplankton, and plant emissions of isoprene, monoterpenes and sesquiterpenes. Sulphate aerosols are formed from volcanic emissions, but also gas-phase atmospheric oxidation of DMS followed by condensation onto existing particles, and by nucleation of new particles. Biogenic emissions also give rise to condensable gases through atmospheric oxidation reactions. Aerosol formed by the condensation of gases formed by oxidation reactions in the atmosphere are known as secondary organic aerosols (SOA). Organic particles of biogenic origin are also emitted from the ocean (O'Dowd et al., 2004). This source still lacks a quantified emission estimate and will therefore not form part of this study.

Natural contributions to the fine mode fraction come mainly from sulphate and organic compounds, since sea salt and mineral dust occur mainly in the super-micron range. Other than active volcanoes, sources of terrestrial sulphate (DMS emissions) are minor. This leaves the biosphere as the major terrestrial source of fine mode aerosol, through natural fire and biogenic emission of SOA precursor gases.

Major quantified anthropogenic sources of particle emissions include production and use of fossil fuels and biomass burning. While vegetation burning also occurs naturally, most fires are presently anthropogenically ignited. Combustion sources generate great numbers of fine particles, and model studies (Bellouin et al., 2005) and observations (Remer et al., 2008) indicate that the fine mode fraction of aerosol is greatly enhanced in anthropogenically polluted regions. Guyon et al. (2003) found that Amazonian particle number concentrations in the wet season (when large-scale biomass burning is absent) were around 400 cm^{-3} in the median, which is comparable to those (100-300 cm^{-3}) found in the remote marine boundary layer (Raes et al., 2000). The onset of the dry season and the consequent weakening of the wet deposition sink increased the observed number concentrations to a median of *circa* 600 cm^{-3}. Biomass burning later in the dry season raised observed particle concentrations to ~4000 cm^{-3} in the median, even though the fires were approximately two days' airmass travel time from the measurement site. Observed particle numbers are higher, ca. 1000 cm^{-3} in the median, in the Boreal forest, where nucleation events are observed (Mäkelä et al., 2000; Heintzenberg et al., 2008). Such nucleation events have been observed to depend on the ambient concentration of sulphuric acid vapour (Sihto et al., 2006), which is largely anthropogenic, so even these environments are anthropogenically perturbed to some degree.

The anthropogenic influence upon the aerosol optical depth observed by satellite is clear.

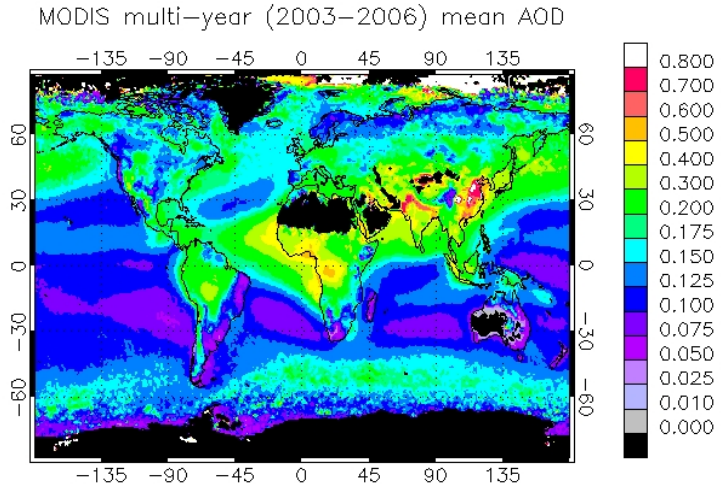

Figure 4.1. Multi-year mean AOD derived by MODIS (Aqua) for 2003-2006. Black indicates no data.

In addition to the direct effects of radiative extinction, aerosols can influence climate by altering the microphysical properties of clouds, in particular by changing the concentration of cloud condensation nuclei (CCN). Andreae (2009) synthesised the results of observations of *in-situ* CCN concentrations in polluted continental, polluted marine, clean continental and clean marine environments.

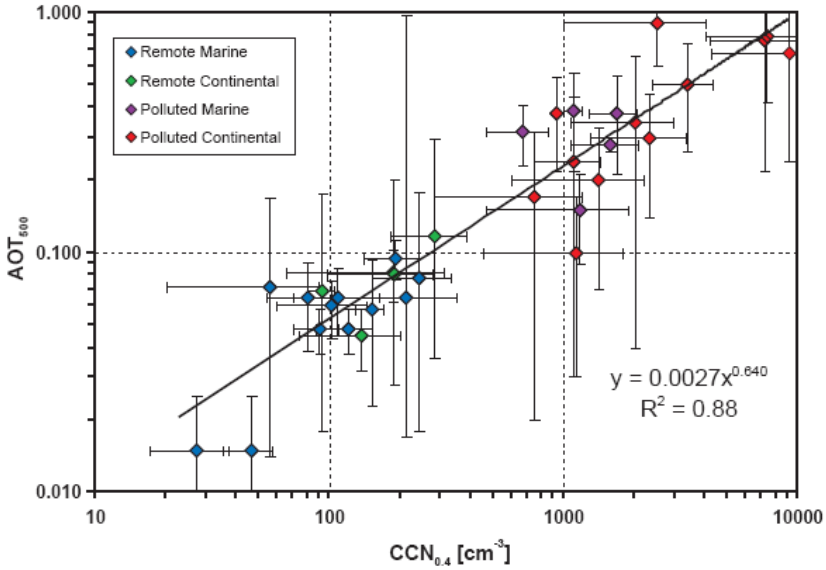

Figure 4.2. Relationship between AOD at 500nm. and CCN at 0.4% supersaturation from investigations where these variables have been measured simultaneously, or where data from nearby sites at comparable times were available. The error bars reflect the variability of measurements within each study (standard deviations or quartiles). Dust-affected areas not included. From Andreae (2009).

Average CCN concentrations for each of these classifications are approximately 100 cm^{-3} for clean marine, 200 cm^{-3} for clean continental, 1000 cm^{-3} for polluted marine and 3000 cm^{-3} for polluted continental environments. It is clear that it is pollution that introduces an order of magnitude change in CCN concentrations, rather than the shift from marine to continental regime.

Satellite measurements also provide evidence of positive correlation between aerosol optical depth and cloud droplet number concentration (CDNC) (Quaas et al., 2008 and the references therein).

These observations raise many questions about the anthropogenic influence on climate, but also about what the biospheric influence on climate might be in the absence of human activities. The model results set out in chapter 2 indicate that the cooling direct effect of SOA is largely offset by a warming indirect effect that depends upon anthropogenic pollutants. The question therefore arises whether a 'biogenic thermostat' exists in nature but is largely suppressed by anthropogenic aerosol.

This study will address the following specific aspects:

i) characterisation of the tropospheric aerosol in terms of number, composition, geographical distribution and optical depth in the absence of any anthropogenic input
ii) characterisation of water clouds in terms of cloud droplet number concentration, liquid water path and cloud optical depth in the absence of anthropogenic aerosol,
iii) estimation of the role of the terrestrial biosphere in shaping the continental aerosol population and the properties of continental clouds.

Ice clouds are not included because our understanding of ice clouds and how they may be influenced by aerosol is insufficient (Forster at al., 2007).

Humans influence the climate system in many other ways, especially through emissions of greenhouse gases and land use change. Since the goals of this study involve only aerosols and clouds, these factors are regarded as constant throughout and kept at values representative of present-day conditions. No attempt is made to simulate climate at any particular point in the past.

4.2 Method

This study is conducted as a set of global modelling simulations, in one of which input of anthropogenic aerosols to the climate system is included, and excluded in the others. The global climate model ECHAM5-HAM (Stier et al., 2005) is used, with the double-moment cloud microphysics scheme of Lohmann et al. (2007). The aerosol model predicts mass and number mixing ratios of aerosol as well as the mixing state in size-resolved classes, assuming a lognormal distribution of prescribed geometric standard deviation for each class. Modelled species are sulphate, black carbon (BC), organic carbon (OC), sea salt and dust. The cloud microphysics scheme uses the information on the aerosol size and composition as input to the calculation of mass mixing ratio and number concentration of cloud droplets.

ECHAM5-HAM uses globally gridded emission inventories of natural and anthropogenic sulphate particle emissions, and of the sulphate aerosol precursors SO_2 and DMS. Anthropogenic emissions of black carbon and of organic carbon are described by gridded emission datasets of Bond et al. (2004). Wildfire emissions of SO_2, black carbon and organic carbon follow van der Werf (2003). Sea salt and dust emissions are calculated online as functions of wind speed and surface parameters.

For this study, online calculation of biogenic emissions of the secondary organic aerosol (SOA) precursor gases isoprene and monoterpenes has been implemented as a model option. Isoprene emissions follow the MEGAN version 2 model of Guenther et al. (2006), (with the corrigendum of Guenther, 2007) and the earlier work of Guenther et al. (1995) is used for monoterpenes. The model has been complemented with a simplified chemistry parameterisation of SOA formation and the necessary methods to handle gas-aerosol partitioning of SOA as well as SOA sink processes, as outlined in chapter 2.2.

For calculation of biogenic emissions, the model requires gridded emission factors for isoprene and for monoterpenes. These are provided through the MEGAN data portal, accessed via http://cdp.ucar.edu. The requirement for an emission factor rather than a plant functional type (PFT), limits the model to present-day vegetation cover. Thus while the pristine atmosphere simulation described herein contain no direct anthropogenic emissions, an indirect anthropogenic effect on emissions is present through human-cultivated plant species. These include both low-emission species (for example, food crops) and high-emission species (for example, oil palms) (Guenther et al., 2006).

Simulation of the climate system without anthropogenic aerosols or aerosol precursors is easily done by replacing the anthropogenic emission datasets with datasets containing only zeros. It is less clear how the case of wildfire emissions should be handled, since no observational information is available on which fires are natural and which anthropogenic. Preindustrial fire emissions have been estimated in the Aerocom study (Dentener et al., 2006), taking into account both increased ignition and increased fire suppression in the presence of human population. While this is not the same as pre-human fire emissions, in the absence of any published estimate of the latter, the Aerocom preindustrial fire emissions are adopted as an estimate of natural fire emissions. Aerocom annual total wildfire emissions of emissions of black carbon, organic carbon and SO_2 in the preindustrial dataset are 1.0 Tg, 13 Tg, and 1.4 Tg respectively, compared with present day climatological values of 3.0 Tg, 35 Tg and 4.1 Tg respectively. The geographical distribution of wildfire emissions is shown in figure 4.3 (for organic carbon: emissions of other species are of course co-located).

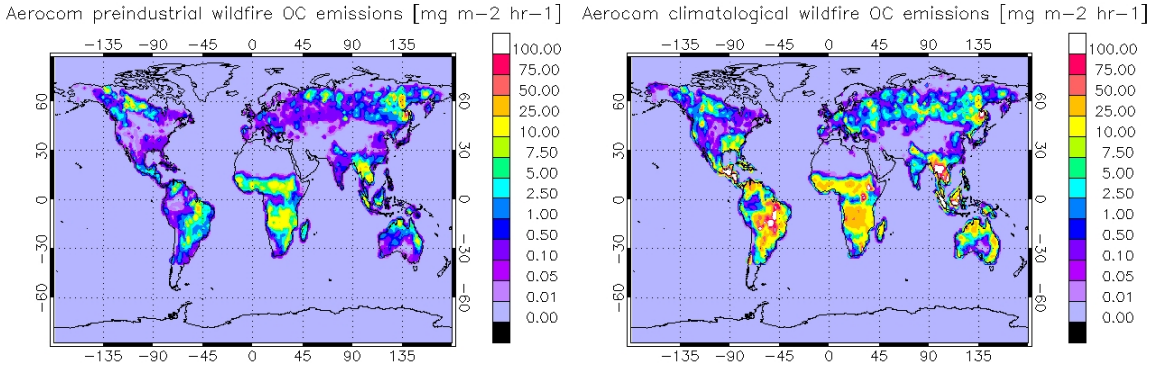

Figure 4.3. Preindustrial (left) and present-day (right) wildfire emissions of organic carbon

Likewise, no information on global pre-human ozone, OH or NO_3 concentrations is available. These oxidant species are needed for calculation of SOA formation. These are identically prescribed for each run, following Stier et al. (2005) for O_3 and OH, and using the mean of each month computed for the period 1961-2000 by the RETRO project (http://retro.enes.org/index.shtml) for NO_3.

Three simulations have been performed for this study: one with all anthropogenic and biogenic emissions, and two for the pristine atmosphere. For the latter case, in order to estimate the effect of biogenic aerosol in a pristine atmosphere, one simulation is performed with and one simulation without biogenic emissions and SOA. (The simulation of the anthropogenically-influenced case is the same simulation as the simulation with SOA described in chapter 2).

To achieve comparability of aerosol properties and of aerosol-cloud interactions between simulations, model meteorology is constrained on the large scale by nudging to the same observations. ECMWF re-analysis data for the year 2000 are used for this purpose.

Each simulation is of one year's duration, following a three-month spinup period.

4.3 Results and Discussion

Since the tropospheric aerosol population simulated in the absence of anthropogenic aerosols can be expected to be radically different from observed global aerosols, the presentation of results will firstly concentrate upon the differences between the simulations with and without anthropogenic pollution. When a picture of the unperturbed (or pristine) atmosphere in terms of aerosols and clouds has been built up, the discussion will turn to the role of biogenic SOA in the pristine atmosphere.

All figures presented in this section are annual means or annual totals.

4.3.1 Atmospheric aerosol budgets

The mass budget for each species and for each simulation is presented in Table 4.1. The simulations are denoted 'anthropogenically polluted' (AP), 'pristine' (PR) and 'pristine including SOA' (PR+S).

Species / Simulation	Prod[1] [Tg/yr]	Wet Dep. [Tg/yr]	Dry Dep. [Tg/yr]	Sed [Tg/yr]	Burden [Tg]	Lifetime [days]
$(SO_4)_{AP}$[1]	71.1	68.1	2.12	1.10	0.88	4.6
$(SO_4)_{PR}$[1]	30.7	29.2	0.68	0.70	0.43	5.1
$(SO_4)_{PR+S}$[1]	30.7	29.3	0.66	0.64	0.42	5.0
BC_{AP}	7.72	7.23	0.57	0.026	0.106	5.0
BC_{PR}	1.02	0.96	0.064	0.002	0.020	7.1
BC_{PR+S}	1.02	0.96	0.060	0.002	0.018	6.4
OC_{AP}	47.2	44.1	3.24	0.133	0.77	6.0
OC_{PR}	12.8	12.0	0.78	0.022	0.22	6.3
OC_{PR+S}	12.8	12.0	0.76	0.027	0.21	6.0
$BSOA_{AP}$	21.1	20.0	1.02	0.039	0.78	13.6
$BSOA_{PR+S}$	20.8	20.1	0.70	0.042	0.55	9.6
SS_{AP}	4970	2810	844	1320	12.0	0.88
SS_{PR}	4960	2800	843	1320	11.9	0.88
SS_{PR+S}	4960	2820	841	1310	12.0	0.88
DU_{AP}	726	378	49.1	303	10.0	5.0
DU_{PR}	737	389	49.4	304	10.3	5.1
DU_{PR+S}	737	389	48.9	303	10.4	5.2
$(H_2O)_{AP}$	-	-	-	-	46.8	-
$(H_2O)_{PR}$	-	-	-	-	44.2	-
$(H_2O)_{PR+S}$	-	-	-	-	44.3	-

[1] Figures for sulphate are in Tg(S)/yr or Tg(S) as appropriate

Table 4.1. Aerosol species budgets for each simulation

Sea salt and dust are, as expected, very similar in sources, sinks, burdens and lifetimes between all simulations and these species are not further discussed in this study. Likewise, number concentrations in the pure dust modes (accumulation and coarse insoluble modes) are little changed and are not discussed either.

Sulphate aerosol production and global mean column burden are cut by a factor of more than two in the pristine atmosphere simulations. Sulphate aerosols are exceeded only by sea salt in contributing to hygroscopic growth of aerosols in the model, and the decline in sulphate is most likely to be the reason behind a 2Tg decline in the global mean aerosol water burden.

Black carbon virtually disappears as an aerosol species of global importance in the pristine atmosphere, with a mean column burden of less than 40ng m^{-2}.

Biogenic emissions of SOA precursors are similar between the simulations (446 Tg isoprene and 89 Tg monoterpenes for the polluted simulation, 452 Tg isoprene and 90 Tg monoterpenes in the pristine simulation). The increase in BSOA production in the polluted atmosphere is expected (because of the presence of substantially more organic carbon that can absorb SOA in the polluted atmosphere), but its small magnitude is not. The BSOA lifetime is considerably shorter in the pristine atmosphere simulation. The overall BSOA lifetime, as seen in chapter 2.3.7, is largely determined by the more volatile of the isoprene oxidation products. In the pristine simulation, upper tropospheric concentrations of this compound are reduced compared to the polluted simulation. Reasons for this are not fully clear, but one such reason may be the greater wet deposition from the gas phase in the pristine simulation (53 Tg/yr *cf.* 48 Tg/yr in the polluted atmosphere simulation).

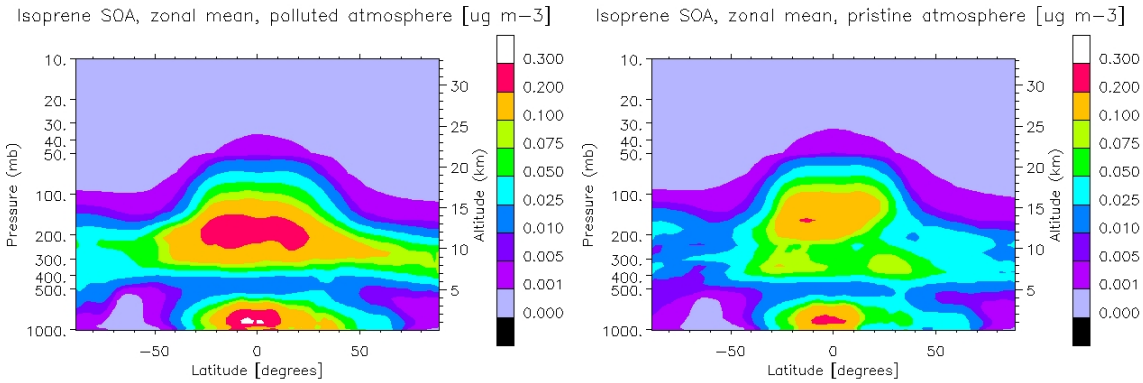

Figure 4.4. Vertical distribution of high-volatility isoprene oxidation product in polluted (left) and pristine (right) atmosphere simulations

Geographical distributions of sulphate, black carbon, POA and SOA for polluted and for pristine atmospheres are shown in figures 4.5-4.8.

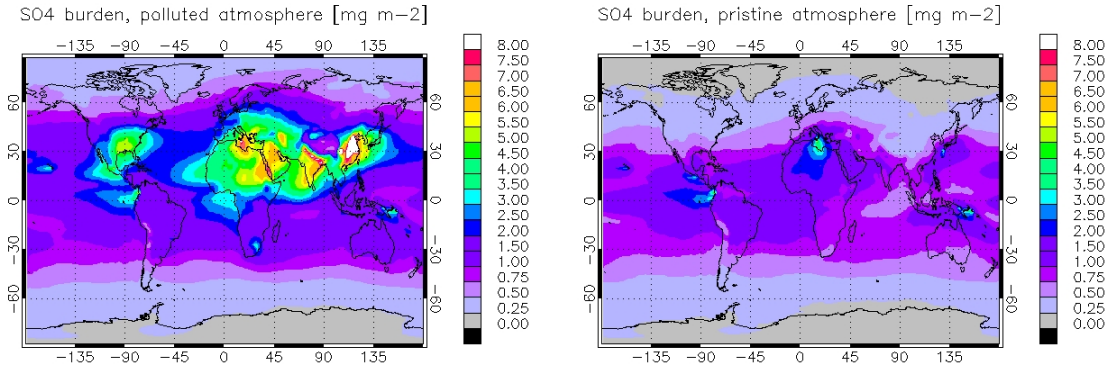

Figure 4.5. Distribution of sulphate aerosol in polluted (left) and pristine (right) atmosphere simulations

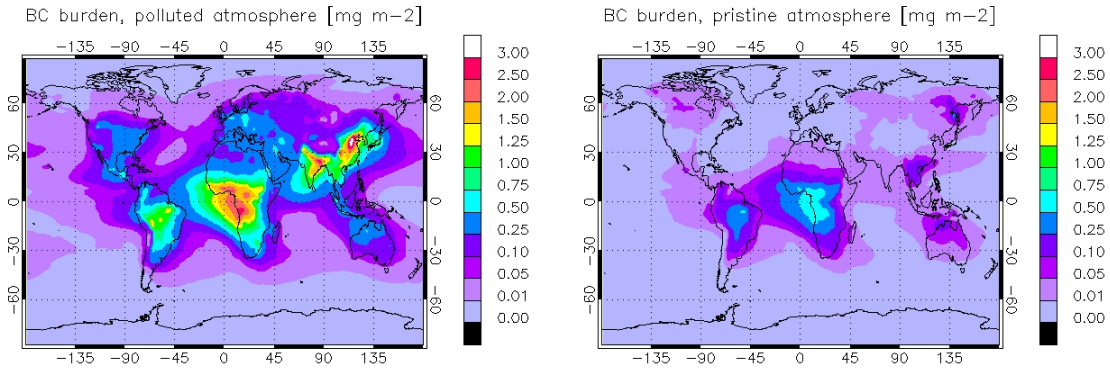

Figure 4.6. Distribution of black carbon aerosol in polluted (left) and pristine (right) atmosphere simulations

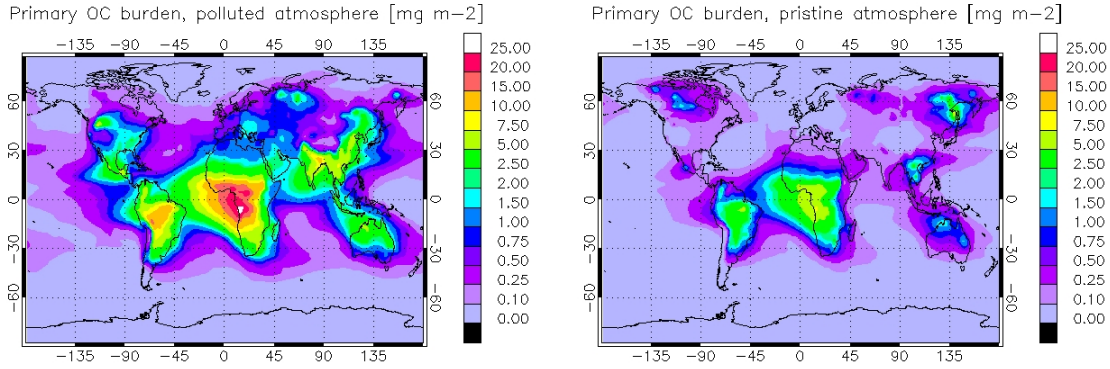

Figure 4.7. Distribution of POA in polluted (left) and pristine (right) atmosphere simulations

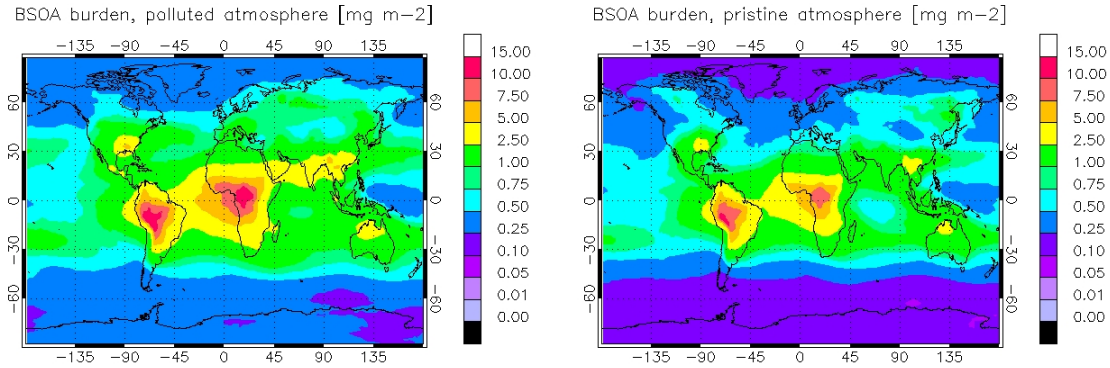

Figure 4.8. Distribution of biogenic SOA in polluted (left) and pristine (right) atmosphere simulations

For number concentrations, nucleation mode is surprisingly, given the changed sulphate burden, little changed. This suggests that sulphate in the model upper troposphere, where most nucleation mode particles are found, is mainly volcanic in origin. Insoluble Aitken mode particles, into which anthropogenic BC and POA from fossil fuel and biomass burning activities are emitted, are almost completely absent in the simulations of the pristine atmosphere. Soluble Aitken mode particles are dominated by sulphate mass in both simulations, with numbers are somewhat higher in the polluted free troposphere. The accumulation mode maximum lies clearly within the tropics, with the maximum now seen south of the equator, consistent with a large biogenic SOA content. In the polluted atmosphere, African biomass burning and industrial pollution move the accumulation mode peak north of the equator, and extend it

into the extratropics. Coarse soluble mode particles remain dominated by near-surface sea salt and dust concentrations, with very low numbers in the free and upper troposphere.

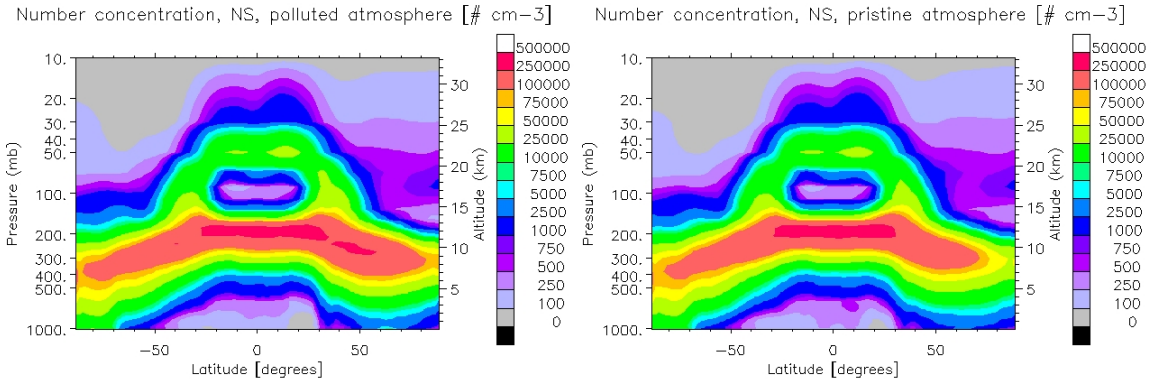

Figure 4.9. Vertical profile of nucleation mode particles in polluted (left) and pristine (right) atmosphere simulations

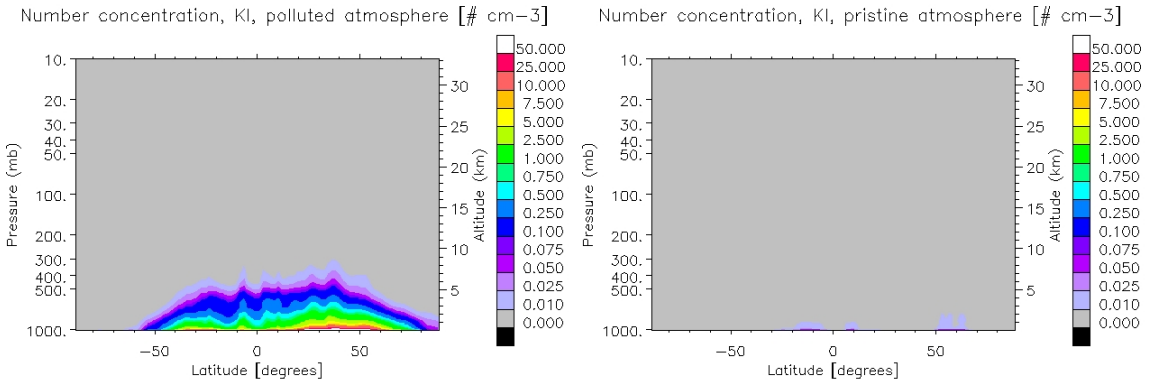

Figure 4.10. Vertical profile of Aitken insoluble mode particles in polluted (left) and pristine (right) atmosphere simulations

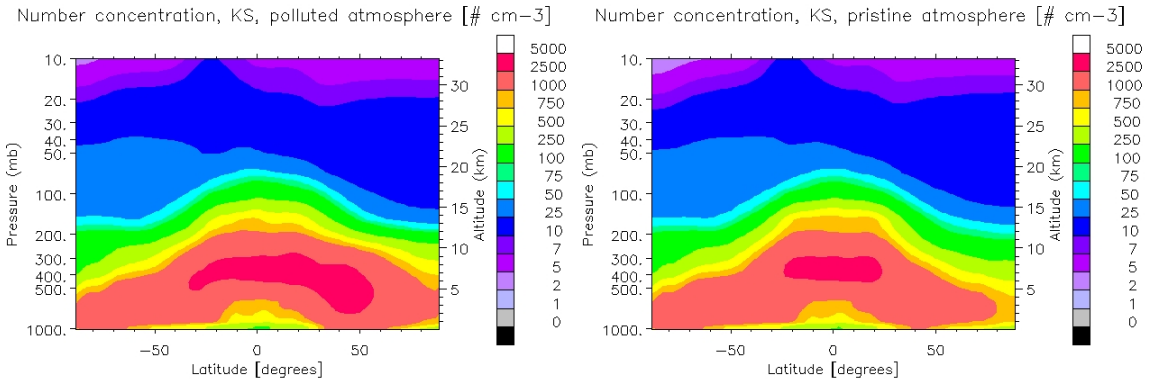

Figure 4.11. Vertical profile of Aitken soluble mode particles in polluted (left) and pristine (right) atmosphere simulations

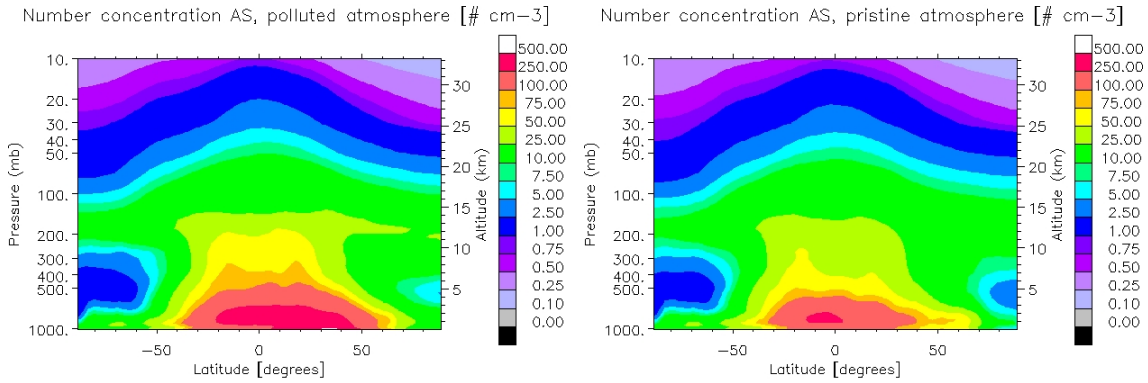

Figure 4.12. Vertical profile of accumulation soluble mode particles in polluted (left) and pristine (right) atmosphere simulations

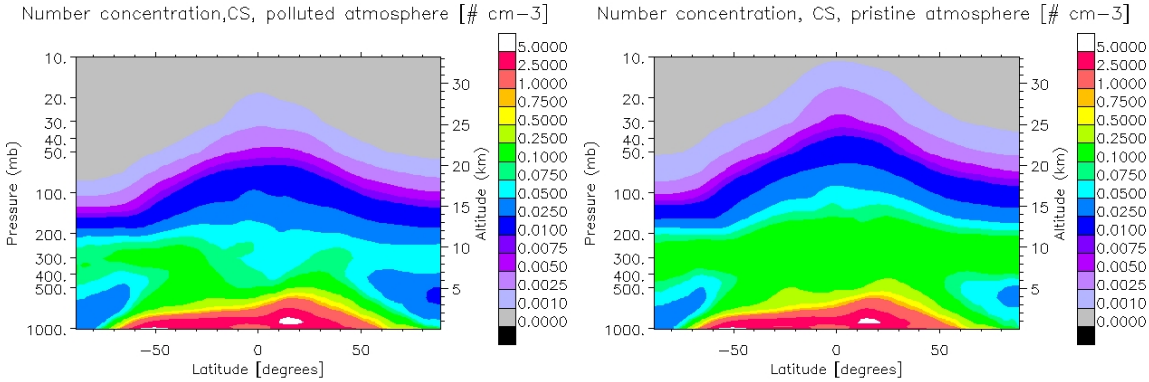

Figure 4.13. Vertical profile of coarse soluble mode particles in polluted (left) and pristine (right) atmosphere simulations

4.3.2 Aerosol Optical Properties in the Pristine Atmosphere

Aerosol optical depth at 550nm in the pristine atmosphere is 0.098 in the global mean, compared with 0.13 for the polluted case. In the polluted atmosphere simulation, the average AOD over the Northern Hemisphere (0.14) is greater than that over the Southern Hemisphere (0.11) due to the much larger anthropogenic contribution. In the pristine atmosphere simulation, this is no longer true; the average AOD is slightly higher (0.10 *cf.* 0.095) over the Southern Hemisphere than over the Northern Hemisphere.

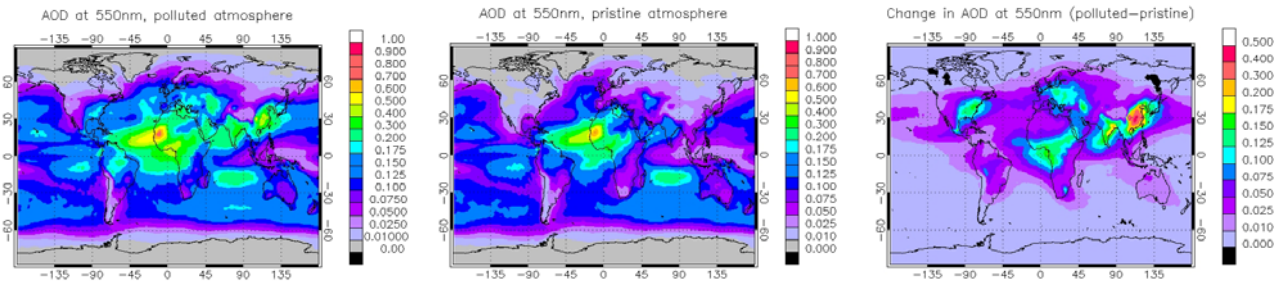

Figure 4.14. AOD at 550nm in polluted (left) and pristine (centre) atmosphere simulations and the difference between them (right)

The fine mode fraction of the aerosol optical depth at 550nm dominates over land in the polluted atmosphere simulation, except near dust sources, whereas in the pristine atmosphere only regions of

high biogenic emissions and some regions where the total AOD is very low (Antarctica, eastern Siberia, north-west Canada and Greenland) show a fine mode fraction of > 0.5.

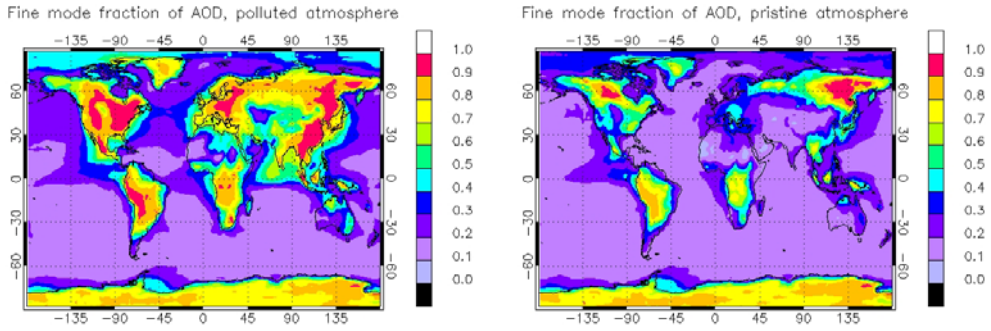

Figure 4.15. Fine mode fraction of AOD at 550nm in polluted (left) and pristine (right) atmosphere simulations

Aerosols over land are much more scattering than absorbing at mid-visible wavelengths in the pristine atmosphere simulation. The global mean absorption optical thickness at 550nm is just $8.6x10^{-4}$ for the pristine atmosphere, compared with $2.8x10^{-3}$ in the polluted atmosphere. The pristine atmosphere simulation shows single scattering albedo values at 550nm of 0.96 or greater almost worldwide, compared to values as low as 0.85 in the most polluted regions of the atmosphere in that simulation. Over land, SSA increases from 0.956 in the polluted atmosphere to 0.969 in the pristine atmosphere.

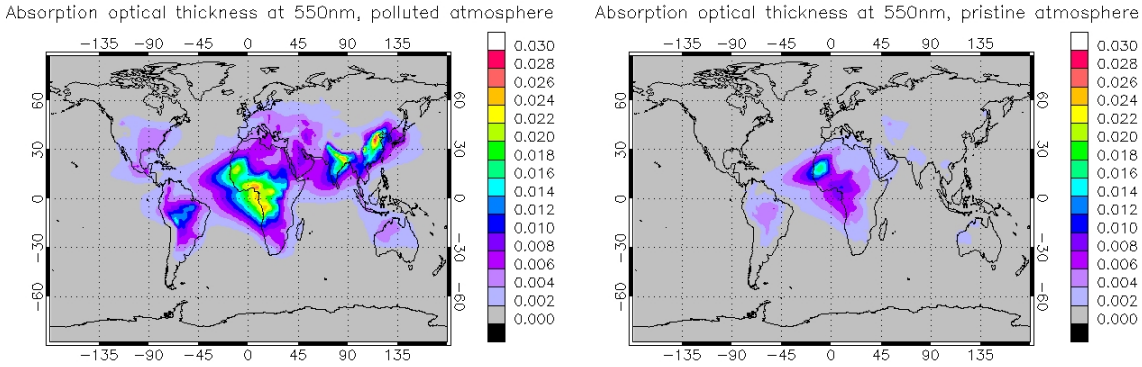

Figure 4.16. Absorption optical thickess at 550 nm in polluted (left) and pristine (right) atmosphere simulations

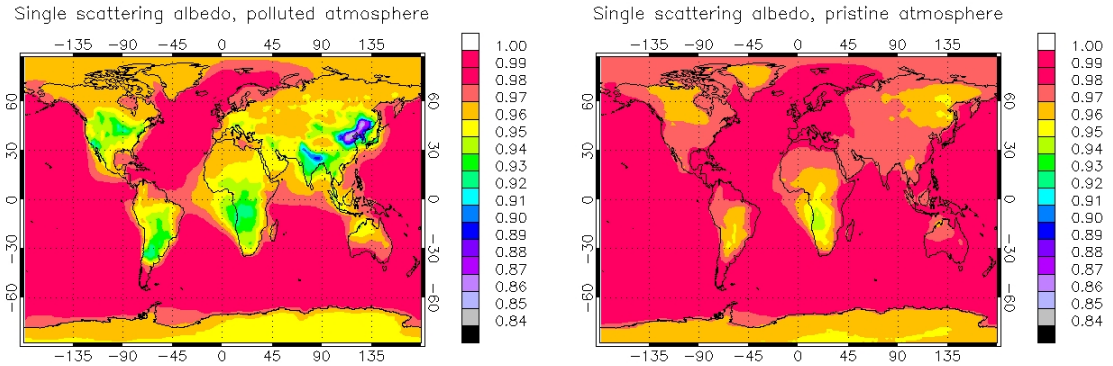

Figure 4.17. Single scattering albedo at 550 nm in polluted (left) and pristine (right) atmosphere simulations

4.3.3 *Changes in cloud cover and precipitation*

Significant differences in cloud cover and precipitation exist between the modelled polluted and pristine atmospheres. Fractional cloud cover is increased in the polluted atmosphere simulation by more than 1% over much of central Europe. Global cloud cover increases by 0.4% in the global mean, with the Northern Hemisphere accounting for most of the increase. Precipitation in the model shows a marked decrease in East Asia, with small decreases in other polluted regions of North America and Europe. Modelled precipitation changes in the tropics are of the order of cm per year and may be considered negligible.

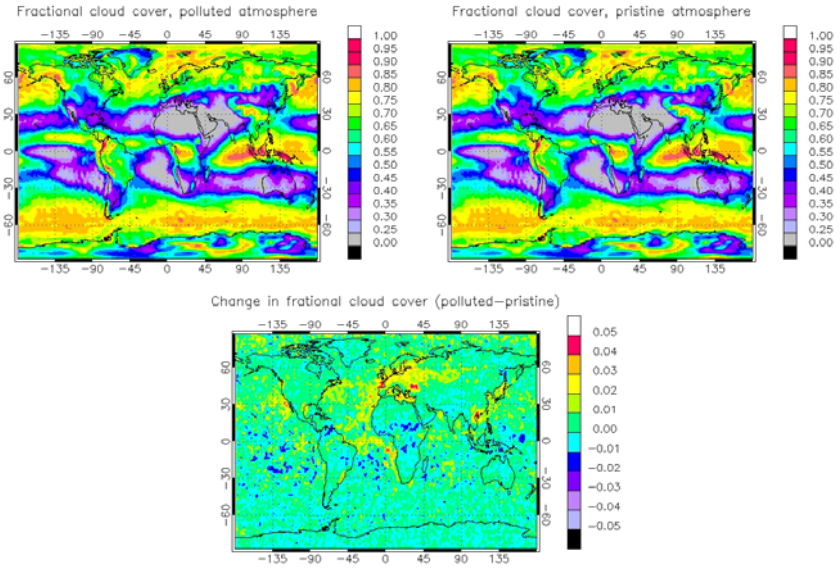

Figure 4.18. Cloud cover in polluted (left) and pristine (centre) atmosphere simulations, and the difference between them (right)

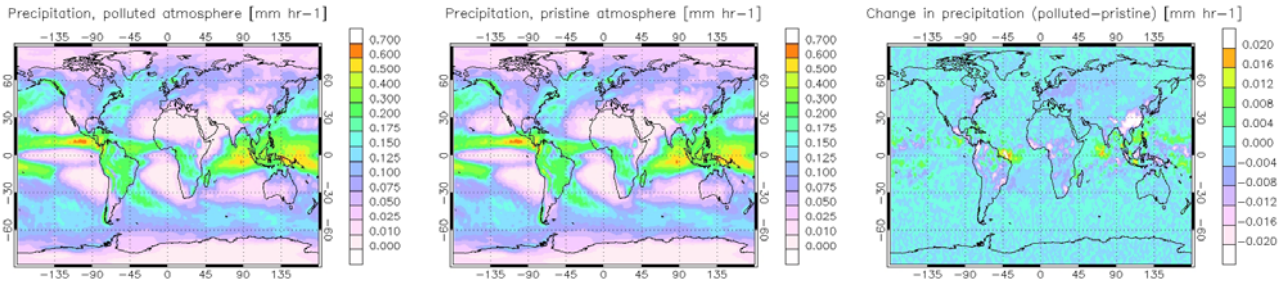

Figure 4.19. Precipitation in polluted (left) and pristine (centre) atmosphere simulations, and the difference between them (right)

Cloud properties are also significantly changed in the polluted atmosphere simulation. The model supports the contention of Andreae (2009) that the traditional classification of clouds into continental and maritime reflects anthropogenic pollution of continental clouds more than any fundamental process in nature. In the Northern Hemisphere, modelled CDNC column burdens in the polluted Northern Hemisphere atmosphere exceed those of the pristine atmosphere by a factor of two or more between approximately 20°N and 55°N, while there is a much smaller impact in the Southern Hemisphere. Figure 4.20 shows the zonally averaged column-integrated CDNC burden for the polluted (black) and pristine (red) simulations. The figures count only time when cloud is present.

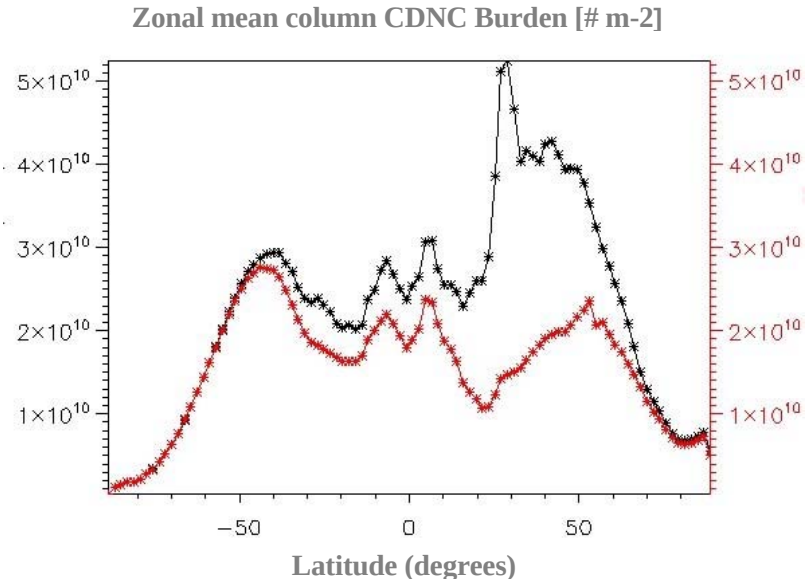

Figure 4.20. Zonal mean column CDNC burdens for polluted (black) and pristine (red) atmosphere simulations.

Cloud liquid water is enhanced along the main Northern Hemisphere pollution tracks, which is clearly reflected in the shortwave cloud optical thickness (figure 4.21).

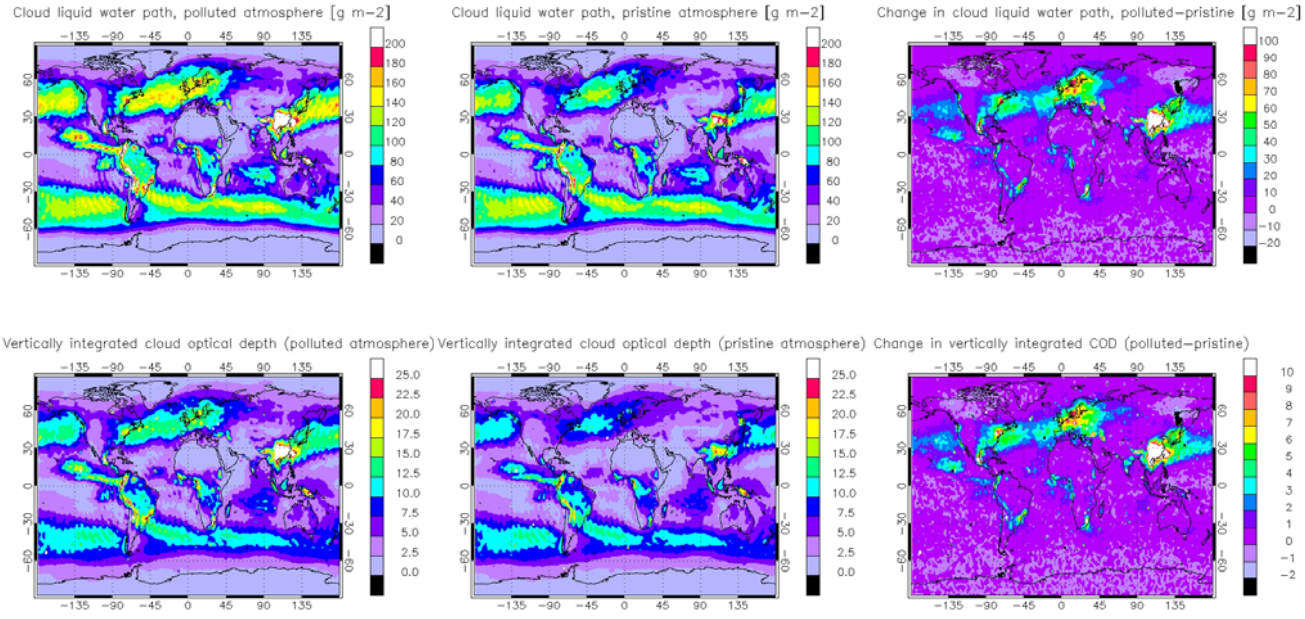

Figure 4.21. Vertically integrated cloud liquid water path (above) and SW cloud optical depth (below) in polluted (left) and pristine (centre) atmosphere simulations, and the difference between them (right).

This completes the characterisation of the atmospheric aerosol population and of liquid clouds in an atmosphere free of human perturbation in the form of aerosols and aerosol precursors.

4.3.4 SOA in a pristine atmosphere

In the foregoing chapters, results of simulations of atmospheres with and without anthropogenic pollution, but including SOA in both cases, were discussed. The study now turns to SOA in the pristine atmosphere, and simulations of the polluted atmosphere will be temporarily left aside.

Without SOA, the global mean aerosol optical depth falls to 0.090, compared to 0.098 with SOA. The contribution of SOA to AOD is essentially negligible outside the tropics, with the exception of the south-eastern United States hotspot.

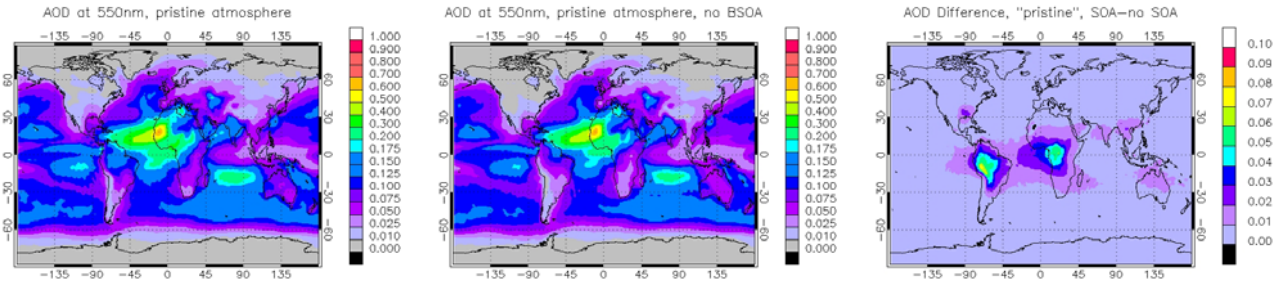

Figure 4.22. AOD at 550nm, pristine atmosphere simuloations, with SOA (left), without SOA (centre) and the difference between them (right).

Changes in the single scattering albedo are positive over land, with very small negative numbers over the oceans. Since BSOA is found mainly over land, the direct effect of SOA is thus still expected to be one of cooling, despite the fact that the low SSAs found in the polluted atmosphere are no longer present. Over land, the mean SSA is slightly larger with SOA, 0.973 compared to 0.969.

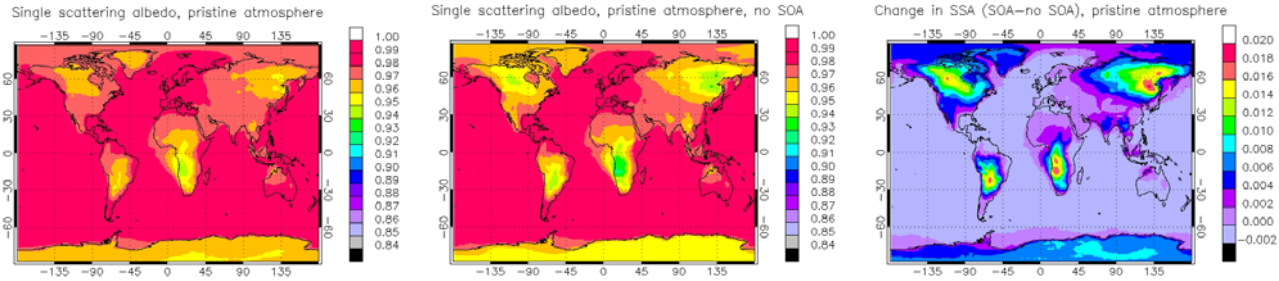

Figure 4.23. Single scattering albedo at 550nm, pristine atmosphere with SOA (left), without SOA (centre) and the difference between them (right).

SOA appears to have a small impact on the modelled cloud cover and precipitation in the Amazon region. Only the differences are presented, since mean cloud cover and precipitation in the simulations with and without SOA are visually indistinguishable (see figures 4.18 and 4.19, centre, for cloud cover and precipitation in the 'with SOA' simulation). The images in figure 4.24 have been subject to a 9-point smoothing algorithm because of the high noise in the raw data. One must however, be cautious about drawing such conclusions, since comparable variations in cloud cover are found in regions that have small SOA concentrations. The application of a smoothing algorithm might also aid the impression of a clear regional signal where in fact only stochastic variations exist.

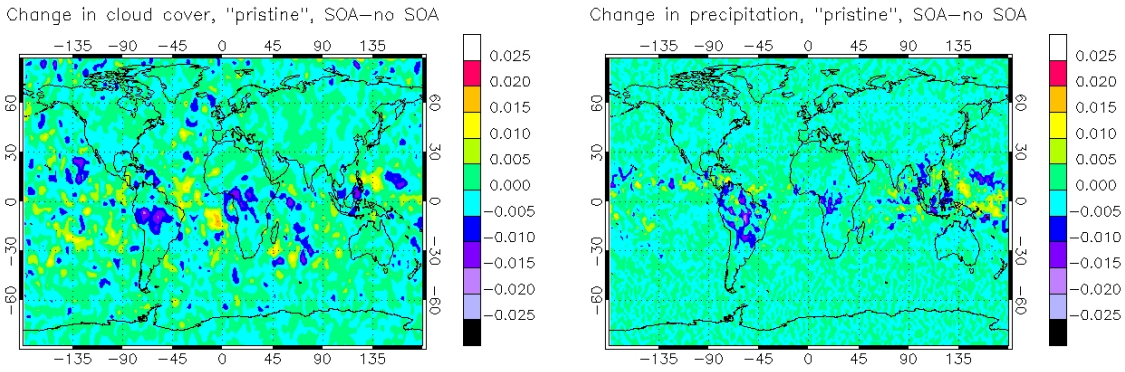

Figure 4.24. Change in cloud cover (left) and precipitation (right), (SOA –no SOA) in the pristine atmosphere simulations.

The global direct SW radiative effect at the top of the atmosphere of biogenic SOA in a pristine atmosphere is estimated as -0.25 Wm^{-2}. The geographical distribution is similar to that found for SOA in the present atmosphere, with the exception of the northern Indian Ocean, where the additional effect of anthropogenic SOA visible in figure 2.19 is no longer present. The SW indirect effect is estimated as -0.03 Wm^{-2}, which represents a change of sign of the indirect effect compared to the present atmosphere. No effect on Northern Hemisphere maritime cloud decks is apparent, as is the case in the present atmosphere (see figure 2.20). SW SOA radiative effects are presented in figure 4.25, where once again smoothing has been applied to the depiction of the indirect effects. The lack of any indirect effect in the pristine atmosphere simulations indicates that the indirect effect of SOA considered in chapter 2.3.11 is in fact an anthropogenic forcing.

In the long wave, effects are minor. The loss in cloud cover in the Amazon allows for the escape of LW radiation, but the global effect is minor, with a mean of +0.02 Wm^{-2}. As for the SW, the LW indirect effect is very noisy, and no clear reason for the appearance of areas of both positive and negative effect in the tropics has been found. Globally, the LW indirect effect is also small, amounting to -0.01 Wm^{-2}.

The overall estimate of SOA radiative effects in a pristine atmosphere is therefore -0.27 Wm^{-2}.

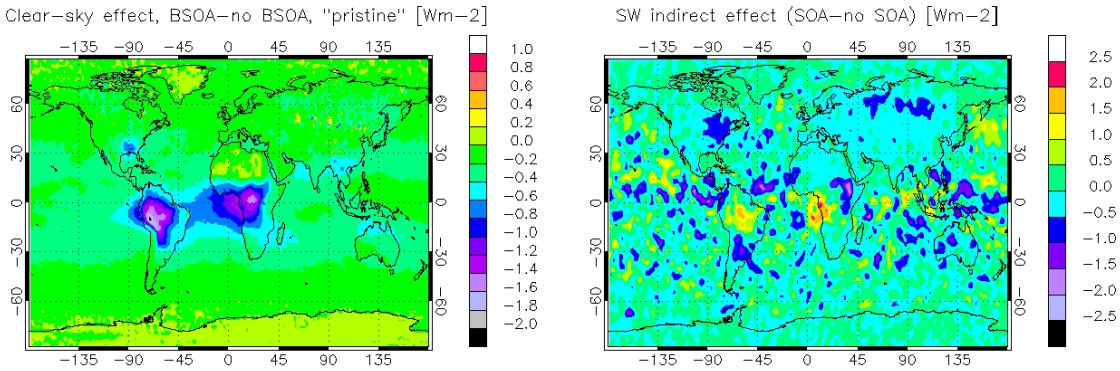

Figure 4.25. SOA SW direct (left) and indirect (right) effects in a pristine atmosphere.

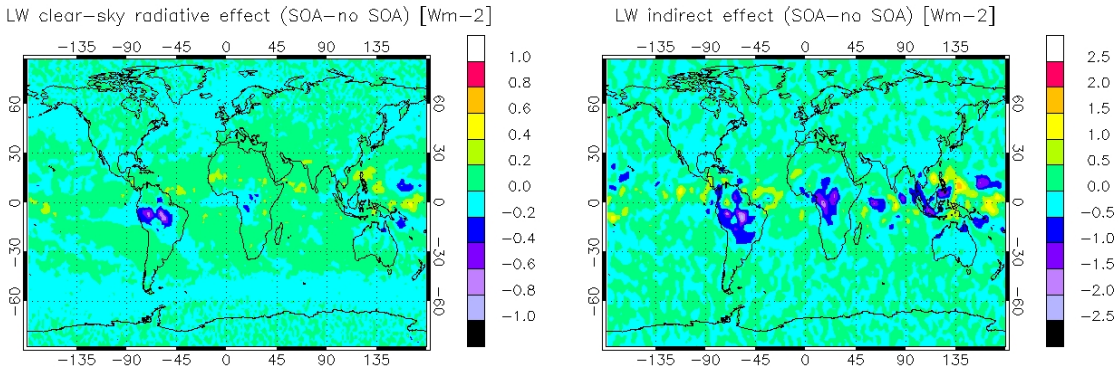

Figure 4.26. SOA LW direct (left) and indirect (right) effects in a pristine atmosphere.

4.4 Summary and conclusions

A global modelling investigation of a pristine atmospheric state, devoid of human disturbance, has been carried out with the goals of identifying possible large-scale human influence on clouds and of investigating the influence of the biosphere upon radiation and clouds, via biogenic aerosols, in the absence of human activities. The global aerosol-climate model ECHAM5-HAM has been used, with extensions that calculate the biogenic emission of aerosol precursor gases as a function of meteorological conditions, and simulate the formation of secondary organic aerosols from those precursors as well as the necessary transport and sink processes.

Rather than attempt any kind of paleo-modelling of ancient pre-human climates, the study has supposed a pristine atmosphere similar to the present atmosphere. Likewise, the present distribution of vegetation has been assumed to remain unaltered.

Three model simulations were performed, one of the anthropogenically perturbed (or polluted) atmosphere and the other two using only natural emissions into the atmosphere. The anthropogenically perturbed simulation included all human emissions that the model is able to simulate, namely sulphate, black carbon, primary organic carbon and, additionally for this study, precursors of secondary organic aerosols. The other two simulations included no anthropogenic emissions. Wildfires have been considered partly natural and partly anthropogenic in this study. In the absence of any known estimate of fire emissions from naturally-ignited fires only, a dataset that estimates global pre-industrial fire emissions has been used as an estimate of natural emissions from wildfires for the simulation of the pristine atmosphere. Of the two simulations in the pristine atmospheric state, one was run with biogenic emissions of isoprene and monoterpenes and the other without. The simulations in the pristine state aim to assess the influence of the biosphere on such an atmosphere and to compare the results with those obtained for the present atmosphere in chapter 2 of this work. Simulation of the anthropogenically perturbed atmosphere is used to understand how the presence of anthropogenic pollutants modifies the influence of the biosphere through interactions of biogenic and anthropogenic aerosols and through modifications of cloud properties.

The large-scale climate in all simulations was constrained by nudging to the same reference meteorology.

Results show considerable differences in the tropospheric aerosol population and in the properties of clouds in the pristine atmosphere. The sulphate burden is greatly increased and its geographical distribution radically altered in the polluted atmosphere simulation compared to those of the pristine atmosphere. Biogenic SOA forms a much more significant portion of the total aerosol in the pristine atmosphere.

The global mean aerosol optical depth falls from 0.13 for the polluted atmosphere to 0.098 for the pristine atmosphere including SOA and further to 0.090 if SOA is excluded from the pristine atmosphere. The aerosol fine mode that is ubiquitous over continents in the present day is much less prevalent in the modelled pristine atmosphere, and only dominates (as measured by aerosol optical depth) in the areas affected by the remaining wildfires and those with high biogenic emissions. The mean aerosol single scattering albedo shifts towards the scattering regime over land and is almost unaffected over ocean.

Liquid cloud properties differ substantially in the Northern Hemisphere between the polluted atmosphere and pristine atmosphere simulations. In particular, the modelled cloud droplet number concentration is up to three times greater in the zonal and annual mean in the industrial belt of the Northern Hemisphere. Clouds in the major pollution transport paths of the Northern Hemisphere exhibit higher liquid water content and higher optical thickness than those in the pristine atmosphere. Total cloud cover is also increased in some industrialised regions in the polluted atmosphere, with the largest effect over Europe and its adjoining seas. Regional suppression of precipitation also occurs in industrialised areas, with the largest effect in south-east Asia. This indicates the presence of an anthropogenic cloud lifetime effect in the model. No large-scale change in cloud properties or precipitation is discernible between the pristine atmosphere simulations with and without SOA.

Cloud ice is not within the scope of the study.

The global direct radiative (SW+LW) effect of biogenic SOA in the pristine atmosphere is estimated as -0.26 Wm^{-2}. Indirect effects of BSOA in both SW and LW are estimated to be very small, with a total all-sky radiative effect of -0.27 Wm^{-2}.

The absence of any substantial indirect effect in this study, and clearly no indirect effect in the extratropics, shows that the model finds little to no natural effect of biogenic SOA on clouds. In contrast, the SW indirect effect of +0.23 Wm^{-2} found in the work described in chapter 2, was attributable to mid-latitude stratiform cloud decks. This supports the explanation of SOA effects on clouds in polluted atmosphere as a result of interactions between SOA and anthropogenic aerosols and thus such an effect should be classed as an anthropogenic forcing.

Thus, the model results point to a considerable natural cooling effect of biogenic aerosols, but one that is, in the polluted atmosphere, mitigated by interaction with anthropogenic aerosols. The idea of a significant negative feedback in the climate system through increased production of biogenic SOA in a warmer climate is therefore possible to support in a pristine atmosphere: however, the presence of anthropogenic pollution weakens any such feedback.

Chapter 5

5 Conclusions and Outlook

5.1 Conclusions

The work herein described has two principal axes of investigation. The first is the modelling of secondary organic aerosols (SOA) in the atmosphere, whose role in the climate system has, to date, remained without any level of quantitative assessment. The second is the elucidation of the connection between the biosphere and the atmosphere that arises from the emission of aerosol precursor gases from vegetation.

To the first end, the global aerosol-climate model ECHAM5-HAM has been extended with a suite of parameterisations that describe the complete life cycle of secondary organic aerosols, starting from emission of the precursor gases, proceeding through the chemical formation of condensable species, the partitioning of those species between the aerosol and gas phases, the microphysics of the aerosol phase and finally to the sink processes that remove both gases and aerosols from the atmosphere. The model treats primary and secondary, organic and inorganic aerosols, prognostically resolves their composition, size distribution and mixing state, and computes their impact on both the shortwave and longwave radiation budget. The model is coupled to the ECHAM5-HAM double-moment cloud scheme that calculates cloud droplet number concentration and mass concentration as prognostic variables as functions of (inter alia) aerosol properties. The model thus contains the elements necessary for estimation of the effects of SOA on radiation and on liquid water clouds.

To the second end, a global model of vegetation emissions of precursor gases has been implemented and linked to the aforementioned SOA extension to the ECHAM5-HAM model. As an alternative, the possibility to use externally-generated sources of biogenic emission data has been added, making it possible to use the output of, for example, a dynamic vegetation model as input to the SOA suite. With these tools, biosphere-atmosphere interactions via biogenic emissions have been investigated in a number of simulations, both in the present atmospheric state, and in hypothetical atmospheric states, that are conceived to examine interactions between anthropogenic activities, biogenic emissions and climate.

5.1.1 Progress towards research goals

Progress towards each of the goals set out in chapter 1.10 may be summarised as follows.

What is the contribution of SOA to the aerosol direct effect?
In the first part of this study, model simulations of the present atmosphere, without SOA, with only biogenic SOA and with both biogenic and anthropogenic SOA were performed. From these simulations, a global mean estimate of SOA direct effect of -0.31 Wm^{-2} for the direct effect of all SOA, and of -0.29 Wm^{-2} for biogenic SOA only were derived.

What is the contribution of SOA to the aerosol indirect effect?
Using the same set of simulations, differences in the properties of marine stratus decks were found in the presence of SOA, amounting to a radiative effect of +0.23 Wm^{-2}. Investigation of the source of the perturbation of cloud properties showed it to be related to interactions between anthropogenic aerosols and SOA, which are mainly biogenic, rather than by direct influence of SOA on the cloud properties. In the third set of simulations, where all anthropogenic aerosols were eliminated from the atmosphere, no such effect was found. Therefore this seemingly purely natural interaction (or lack thereof) between

biogenic aerosols and clouds has been anthropogenically perturbed, and a 'pure' interaction between atmosphere and biosphere via biogenic SOA without reference to humans no longer exists in the polluted atmosphere.

Can the inclusion of SOA in a model explain the under-prediction of organic carbon and aerosol optical depth compared to observations?
In the first part of this work, model simulations were performed with and without SOA over the same time period as a year-long campaign of measurement of elemental (EC) and organic carbon (OC) in Europe, for which time measurements from a large American measurement network of those species are available, as are optical measurements from the AERONET ground-based remote sensing network. While the model with SOA was closer to observations than the model without SOA, substantial under-estimates remain in the model estimates of both organic carbon concentrations and in aerosol optical depth, particularly at remote sites. Further analysis showed that the worst mismatches between model and observation are characterised by high correlation between observed EC (an anthropogenic signature species) and OC, strongly suggesting that the source of the additional OC in these measurements is anthropogenic.

Are published projections of large future increases in SOA loading viable in the light of the dependence of biogenic emissions on CO_2?
In the second part of this work, different biogenic emission models were employed, one an empirically-based model lacking any CO_2 response, the other a dynamic vegetation model with leaf process-based calculation of emissions includes CO_2 concentration in its calculation of biogenic emissions. Both models were used to drive the SOA model in two different climate states, one present day, and one warmer climate state, each climate state being constrained on the large scale by fixed sea surface temperatures. The warmer climate state used SRES scenario A2 CO_2 levels, and sea surface temperatures previously calculated for that scenario by the coupled ECHAM5/MPI-OM atmosphere-ocean model in the context of IPCC AR4 scenario runs. When driven with the empirically-based emission model, the SOA model, in common with published studies, predicts a large increase in biogenic SOA in the warmer climate state. However, when driven with the process-based model the biogenic emissions and SOA loading in the warmer climate state decrease below those of the present state. This shows that there is reason to doubt the published findings that such biogenic emissions and SOA would increase in such a climate.

Does modelling of biogenic aerosols support the "biogenic thermostat" hypothesis?
The "biogenic thermostat" is predicated on the idea that the net radiative effect of biogenic aerosols is a cooling effect. For a pristine atmosphere, devoid of anthropogenic pollution, this has been shown to be likely to be true in the third part of this work. However, the first part has shown that, in the present day atmosphere, the cooling is all but removed due to a positive indirect anthropogenic forcing arising from interaction of SOA with pollution aerosols. Furthermore, taking the CO_2 inhibition of biogenic emissions into account, the sign of a climate feedback through biogenic SOA may in fact be positive, as was seen in part two of this work.

How do biogenic and anthropogenic aerosols interact?
There are many interactions between biogenic and anthropogenic aerosols, beginning with the condensation of biogenic SOA from the gas phase. Anthropogenic organic aerosols provide absorbing mass for such condensable gases. The interaction of SOA and anthropogenic aerosols has been shown in the first part of this work to lead to both increase and decrease in cloud condensation nuclei. Only increase of CCN due to SOA has previously been demonstrated. The decrease, which occurs in polluted regions, is the most important of the biogenic-anthropogenic interactions, since it leads to an indirect forcing that effectively cancels the direct cooling effect of SOA.

5.1.2 Summary of main findings

New findings of this work, that are of importance in themselves or for related research, include:

- First estimate of the radiative effect of biogenic aerosols
- Identification and quantification of anthropogenic forcing of climate due to interaction of anthropogenic aerosols, biogenic aerosols and clouds.
- Identification of SOA as the probable main source of observed upper troposphere organic aerosol worldwide
- That satellite-model hybrid estimates of anthropogenic direct radiative forcing may be overestimated due to the presence of large amounts of natural aerosol in the terrestrial fine mode
- That climate feedback due to biogenic aerosols is likely to be very weak in magnitude and possibly positive in sign in anthropogenically perturbed atmosphere
- First application of process-based a process-based dynamic global vegetation model to climate studies
- Model support for the idea that the traditional classification of clouds into continental and maritime reflects anthropogenic pollution rather than any inherent natural properties

5.2 Outlook

Secondary organic aerosols continue to present substantial challenges for understanding how atmospheric aerosols influence climate, but also for other areas on investigation, in particular for understanding and predicting air quality. Addressing these challenges requires continued efforts in laboratory measurements, in-situ observations, remote sensing, construction of emission inventories, and in modelling.

This work has shown that knowledge of SOA at low temperatures is indispensable in order to understand these aerosols in the mid- and upper troposphere. There are few facilities in the world that have the capability to investigate aerosols under controlled low-temperature conditions, a fact reflected in the very small number of publications related to such studies. Related to this is the very low level of knowledge about the interactions of organic aerosols with cloud ice.

The thermodynamic and optical properties of SOA also need further experimental investigation. For accurate representation of SOA in models, knowledge of the sink processes is equally important as knowledge of the production processes, which have received far more attention in recent years. This study calls attention to the importance of wet removal of condensable species from the gas phase. Accurate information about how the real spectrum of organic species produced by SOA precursor oxidation is taken up by cloud water should replace the *ad-hoc* choice of observed SOA compounds to use as surrogates for all products, as has been done in this and in all published global SOA modelling studies. A realistic estimate of the radiative forcing of aerosols requires knowledge of the optical properties of those aerosols over the whole spectrum in both solar and terrestrial thermal wavebands. Here again, there is less information available than is needed for accurate calculations of these effects.

Nucleation of new particles remains extremely challenging for theory, and for measurement, as characterisation of such nanoparticles pushes technology to its limits. This work should give further impetus to the investigation of the role of organics in nucleation, since it highlights the importance of organics in upper troposphere, where cold temperatures favour nucleation.

Several biogenic and anthropogenic species, for which global emission estimates have never been made, are known. The fact that the latest study of global anthropogenic VOC emission dates from 2000,

and the latest explicitly speciated study from1990, are also matters of concern, particularly given the rapid industrialisation that has taken place in Asia in the intervening years. Given their potential longevity in the atmosphere, and the rapid growth in traffic, aircraft emissions, which are not included in this study, warrant closer scrutiny. Emissions of biogenic precursors remain hugely uncertain, and much work is needed in order to better constrain this potentially very large source of atmospheric aerosols. Lastly as regards emissions, the daily and seasonal cycles of both primary aerosols and SOA precursor need to be characterised in different regions of the globe.

The investigation of the chemistry of SOA formation has made spectacular progress over the last 10-15 years. Many precursors have been identified, mechanisms of SOA formation involving particle and aqueous phase reactions have been elucidated, and dependencies such as those on NO_x and particle acidity explained, and such work continues apace. An important step towards a second generation of SOA models will be the parameterisation of each of these processes in a computationally-efficient way. Perhaps a larger obstacle is the task of describing the chemical evolution of SOA over longer time horizons, up to the several days' typical lifetime of atmospheric aerosols.

Full evaluation of an aerosol-climate model needs aerosol observations over wide areas, long time scales and in three dimensions. Composition-resolving field measurement campaigns have mainly focused on particular near-surface aerosol regimes, such as regions affected by dust or pollution outflow, and comparatively little information is available for the free and upper troposphere. This in exacerbated by the need (from the point of view of organic aerosols) to be able to deal with semi-volatile compounds by in-situ measurements. While not resolving composition questions, important new remote sensing capabilities have become available in recent years. The MODIS and MISR instruments on board the Terra and Aqua satellites have already proven invaluable in aerosol and cloud studies. New three-dimensional measurements are becoming available with the increasing deployment of ground-based LIDAR instruments, as well as the space-based instrument aboard the CALIPSO satellite.

Further model development need not wait for any of these anticipated developments. Integration of secondary organic aerosol model with a full chemistry model and with vegetation models can be done with advantage immediately. However, closing the gap that still remains between model and observation of organic aerosols will most likely require at least some key information that is yet to be elucidated.

A coordinated appoach encompassing observations, laboratory studies and modelling is therefore the best way to advance scientific understanding in this area.

The many scales of the SOA modelling challenge, from the nano-scale of SOA formation to the global scale of radiative effects, together with the large uncertainties and many unsolved issues in this research area, means that definitive answers to questions of the climate impact of the secondary organic aerosols are beyond the reach of the present state of scientific knowledge. This is why the word 'towards' is used in the title of this work. Yet in spite of these limits to our knowledge, this work has hopefully shown that informative, useful and sometimes surprising results are still possible with a global modelling approach. Future research will doubtless expand upon and refine these results greatly.

ACKNOWLEDGMENTS

I wish first and foremost to thank my supervisor Dr. Johann Feichter, for his guidance, insights, experience and not least, patience. Thanks are also due to Professor Hartmut Graßl and to Professor Heinke Schlünzen for their support and advice.

The Max Planck Institute for Meteorology, where this work was conducted is thanked for providing the means by which the work was carried out, as well as a stimulating research environment and many helpful colleagues, of whom Dr. Stefan Kinne, Dr. Sebastian Rast, Dr. Johannes Quaas and René Hommel provided much useful advice.

In the course of this work, the help of Dr. Kostas Tsigaridis (then of Laboratoire des Sciences du Climat et de l'Environenement, Gif-sur-Yvette, France), and of Professor John H. Seinfeld, Dr. Philip Stier, Dr. Daven Henze and Dr. Sally Ng at Caltech, Pasadena, California, USA has been of great value. The opportunity to visit the latter was made possible by a grant from the Zeit foundation, the former through EUCAARI.

The International Max Planck Research School of Earth System Modelling (IMPRS-ESM), and its organisers Dr. Antje Weitz and Cornelia Kampmann are greatly thanked for the many courses, seminars and retreats that they organised, and moreover for the invaluable opportunities for multi-disciplinary interaction that is a hallmark of the School.

BIBLIOGRAPHY

Ackerman, A. S., O. B. Toon, D. E. Stevens, A. J. Heymsfield, V. Ramanathan, E. J. Welton (2000), Reduction of Tropical Cloudiness by Soot, *Science,* **288**, 1042-1047

Albrecht, B. A (1989), Aerosols, cloud microphysics, and fractional cloudiness, *Science*, **245**, 1227-1230

Andreae, M. O., and P. Merlet (2001), Emissions of trace gases and aerosols from biomass burning, *Global Biogeochem. Cycles*, **15**, 955-966

Andreae, M. O. and P. J. Crutzen (1997), Atmospheric Aerosols: Biogeochemical Sources and Role in Atmospheric Chemistry,*Science,* **276**, 1052-1058

Arneth, A., Ü. Niinemets, S. Pressley, J. Bäck, P. Hari, T. Karl, S. Noe, I. C. Prentice, D. Serça, T. Hickler, A. Wolf and B. Smith (2007), Process-based estimates of terrestrial ecosystem isoprene emissions: incorporating the effects of a direct CO_2-isoprene interaction, *Atmos. Chem. Phys.* **7**, 31-53

Arneth, A., R. K. Monson, G. Schurgers, Ü. Niinemets and P. I. Palmer (2008), Whay are estimates of global terrestrial isoprene emissions so similar (and why is this not so for monoterpenes)? *Atmos. Chem.Phys.* **8**, 4605-4620

Artaxo, P., H. Storms, F. Bruynseels and R. Van Greiken (1988), Composition and Sources of Aerosols From the Amazon Basin, *J. Geophys. Res.* **93 (D2),** 1605-1615

Artaxo, P., J. V. Martins, M. A. Yamasoe, A. S. Procópio, T. M. Pauliquevis, M. O. Andreae, P. Guyon, L. V. Gatti, and A. M. Cordova Leal (2002), Physcical and chemical properties of aerosols in the wet and dry seasons in Rondônia, Amazonia, *J. Geophys. Res.,* **107 (D20)** 8081

Baltensperger, U., M. Kalberer, J. Dommen, D. Paulsen, M. R. Alfarra, H. Coe, R. Fisseha, A. Gascho, M. Gysel, S. Nyeki, M. Sax, M. Steinbacher, A. S. H. Prevot, S. Sjögren, E. Weingartner and R. Zenobi (2005), Secondary organic aerosols from anthropogenic and biogenic precursors, *Faraday Discuss.* **130**, 265-278

Baraldi, R., F. Rapparini, W. C. Oechel, S. J. Hastings, P. Bryant, Y. Cheng and F. Miglietta (2004), Monoterpene emission responses to elevated CO_2 in a Mediterranean-type ecosystem, *New Phytol.* **161**, 17-21

Bates, T., B. Huebert, J. Gras, F. Griffiths and P. Durkee (1998), International Global Atmospheric Chemistry (IGAC) Porject's First Aerosol Characterization Experiment (ACE-1): Overview, *J. Geophys. Res.* **103(D13)**, 16297-16318

Bellouin, N., O. Boucher, J. Haywood and M. Shekar Reddy (2005), Global estimate of aerosol direct radiative forcing from satellite measurements, *Nature* **438**, 1138-1141

Bond, T. C., D. G. Streets, K. F. Yarber, S. M. Nelson, J.-H. Woo and Z. Klimont (2004), A technology-based global inventory of black and organic combustion, *J. Geophys. Res.* **109**, D14203

Bonn, B., and G. K. Moortgat (2003), Sesquiterpene ozonolysis: Origin of atmospheric new particle formation from biogenic hydrocarbons, *Geophys. Res. Lett.*, **30(11)**, 1585

Bonn, B., M. Kulmala, I. Riipinen, S.-L. Sihto, and T. M. Ruuskanen (2008), How biogenic terpenes govern the correlation between sulfuric acid concentrations and new particle formation, *J. Geophys. Res.*, **113**, D12209

Capes, G.,J.G. Murphy, C. G. Reeves, J.B. McQuaid, J. F. Hamilton, J. R. Hopkins, J. Crosier, P. I. Williands and H. Coe (2009), Secondary organic aerosol from biogenic VOCs over West Africa during AMMA, *Atmos. Chem. Phys.* **9**, 3841-3850

Carlton, A. G., C. Wiedinmyer and J. H. Kroll, (2009) A review of Secondary Organic Aerosol (SOA) formation from isoprene, *Atmos. Chem. Phys.* **9**, 4987-5005

Christopher, S. A., J. Zhang, Y. J. Kaufman and L. Remer (2006), Satellite-based assessment of the top of the atmosphere anthropogenic aerosol radiative forcing over cloud-free ocean, *Geophys. Res. Lett.* **111**, L15816

Chung, S. H. and J. H. Seinfeld (2002), Global distribution and climate forcing of carbonaceous aerosols, *J.Geophys. Res.***107**(D19), 4407

Claeys, M., B. Graham, G. Vas, W. Wang, R. Vermeylen, V. Pashynska, J. Cafmeyer, P. Guyon, M. O. Andreae, P. Artaxo and W. Maenhaut (2004), Formation of Secondary Organic Aerosols Through Photooxidation of Isoprene, *Science* **303**, 1173-1176

Clegg, S. L., J. H. Seinfeld and P. Brimblecombe (2001), Thermoodynamic modelling of aqueous aerosols containing electrolytes and dissolved organic compounds, *J.Aerosol Sci.* **32**, 713-738

Clegg, S. L. and J. H. Seinfeld (2004), Improvement of the Zdanovskii-Stokes-Robinson model for mixtures containing solutes of different charge types, *J. Phys. Chem. A*, **108**, 1008-1017

Coakley, J. A., R. L. Bernstein and P. A. Durkee (1987), Effect of Ship-Stack Effluent on Cloud Reflectivity, *Science* **237**, 1020-1022

Cooke, W. F., C. Liousse, H. Cachier and J. Feichter (1999), A global black carbon aerosol model, *J. Geophys. Res.* **101**, 19395-19409

Cziczo, D. J., P. J. DeMott, S. D. Brooks, A. J. Prenni, D. S. Thomson,D. Baumgardner, J. C. Wilson, S. M. Kreidenweis, and D. M. Murphy (2004), Observations of organic species and atmospheric ice formation, *Geophys. Res. Lett*., **31**, L12116

Decesari, S. M. C. Facchini, M. Mircea, F. Cavalli and S. Suzzi (2003), Solubility properties of surfactants in atmospheric aerosol and cloud/for water samples, *J. Geophys. Res.*, **108(D21)**, 4865

Dentener, F., S. Kinne, T. Bond, O. Boucher, J. Cofala, S. Generoso, P. Ginoux, S. Gong, J. J. Hoelzemann, A. Ito, L. Marelli, J. E. Penner, J.-P. Putaud, C. Textor, M. Schulz, G. R. van der Werf, and J. Wilson (2006), Emissions of primary aerosol and precursor gases in the years 2000 and 1750 prescribed data-sets for AeroCom, *Atmos Chem. Phys.* **6**, 4321-4344

Dinar, E., A. Abo Riziq, C. Spindler, C. Erlick, G. Kiss, and Y. Rudich (2008), The complex refractive index of atmospheric and model humic-like substances (HULIS) retrieved by a cavity ring down aerosol spectrometer (CRD-AS), *Faraday Discuss.* **137,** 279-295

Duhl, T. R., D. Helmig and A. Guenther (2008), Sesquiterpene emissions from vegetation: a review, *Biogeosci.* **5**, 761-777

Duplissy, M. Gysel, M. R. Alfarra, J. Dommen, A. Metzger, A. S. H. Prevot, E. Weingartner, A. Laaksonen, T. Raatikainen, N. Good, S. F. Turner, G. McFiggans, and U. Baltensperger (2008), Cloud forming potential of secondary organic aerosol under near atmospheric conditions, *Geophys. Res. Lett*., **35**, L03818

Erdakos, G. B., I. E. Chang, J. F. Pankow and J. H. Seinfeld and (2006), Prediction of activity coefficients in liquid aerosol particles containing organic compounds, dissolved inorganic salts, and water – Part 3: Organic compounds, water and ionic constituents by consideration of short-, mid-, and long-range effects using X-UNIFAC3, *Atmos. Environ.* **40**, 6437-6452

Feingold, G., W. L. Eberhard, D. E. Veron and M. Previdi (2003), First measurements of the Twomey indirect efect using ground-based remote sensors, *Geophys. Res. Lett.* **30(6)**, 1287-1290

Forster, P., V. Ramaswamy, P. Artaxo, T. Berntsen, R. Betts, D. W. Fahey, J. Haywood, J. Lean, D. C. Lowe, G. Myhre, J. Nganga, R. Prinn, G. Raga, M. Schulz and R. van Dorland, (2007), Changes in Atmosperic Constituents and Radiative Forcing. *In: Climate Change 2007:The Physical Science Basis. Contribution of Working Group I to the Intergovernmental Panel on Climate Change* [Solomon, S. D.Qin, M. Manning, D. Chen,. M. Marquis, K.B. Averyt, M. Tignor and H.L. Miller (eds.)] Cambridge University Press, Cambridge, United Kingdom and New York, NY, USA

Forstner, H. J. L., J. J. Seinfeld and R. C. Flagan (1997a), Secondary organic aerosol formation from the photooxidation of aromatic hydrocarbons. Molecular composition *Environ. Sci. Technol.* **31** 1345-1358

Forstner, H. J. L., J. H. Seinfeld and R. C. Flagan, (1997b), Molecular speciation of secondary organic aerosol from the higher alkenes: 1-Octene and 1-decene, *Atmos. Environ.* **31** 1953-1964

Froyd, K. D., D. M. Murphy, T. J. Sanford, D. S. Thomson, J. C. Wilson, L. Pfister and L. Lait (2009), Aerosol composition of the tropical upper troposphere, *Atmos. Chem. Phys.,* **9**, 4363-4385

Galloway, M. M. P. S. Chabra, A. W. H. Chan, J.D. Surratt, R. C. Flagan, J. H Seinfeld and F. N. Keutch, (2009), Glyoxal uptake on ammonium sulphate seed aerosol: reaction products and reversibility of uptake under dark and irradiated conditions, *Atmos. Chem. Phys.* **9**, 3331-3345

Gao, S., M. Keywood, N. L. Ng, J. D. Surratt, V. Varutbangkul, R. Bahreini, R. C. Flagan and J. H. Seinfeld (2004a), Low-molecular-weight and oligomeric components in secondary organic aerosol from the ozonolysis of cycloalkenes and alpha-pinene, *J. Phys. Chem. A*, **108**, 10147-10164

Gao, S., N. L. Ng, M. Keywood, V. Varutbangkul, R. Bahreini, A. Nenes, J. He, K. Y. Yoo, J. L. Beauchamp, R. P. Hodyss, R. C. Flagan and J. H. Seinfeld (2004b), Particle phase acidity and oligomer formation in secondary organic aerosol, *Environ. Sci. Technol.* **38**, 6582-6589

Griffin, R. J., D. R. Cocker III, R. C. Flagan and J. H. Seinfeld (1999), Organic aerosol formation from the oxidation of biogenic hydrocarbons, *J. Geophys. Res.* **104(D3)**, 3555-3567

Grosjean, D. (1984), Particulate carbon in Los Angeles air, *Sci. Total Environ.*, **32**, 435-473

Guenther, A., P. Zimmermann, P. Harley, R. Monson, and R. Fall (1993), Isoprene and monoterpene emission rate variability: model evaluations and sensitivity analyses, *J. Geophys. Res.* **98**, 12609-12617

Guenther, A., C. Hewitt, D. Erickson, R. Fall, C. Geron, T. Graedel, P. Harley, L. Klinger, M. Lerdau, W. McKay, T. Pierce, B. Scholes, R. Steinbrecher, R. Tallamraju, J. Taylor and L. Torres (1995), A global model of natural volatile organic compound emissions, *J. Geophys. Res.,* **100**, 8873-8892

Guenther, A., T. Karl, P. Harley, C. Wiedinmyer, P. Palmer and C. Geron (2006), Estimates of global terrestrial isoprene emissions using MEGAN (Model of emissions of gases and aerosols from nature), *Atmos. Chem. Phys.* **6**, 3181-3210

Guenther, A. (2007), Corrigendum to "Estimates of global terrestrial isoprene emissions using MEGAN (Model of Emissions of Gases and Aerosols from Nature)" published in Atmos. Chem. Phys. 6, 3181-3210, 2006, *Atmos. Chem. Phys.* **7**, 4327-4327

Guyon, P., B. Graham, J. Beck, O. Boucher, E. Gerasopoulos, O. L. Mayol-Bracero, G. C. Roberts, P. Artaxo and M. O. Andreae (2003), Physical properties and concentration of aerosol particles over the Amazon tropical forest during background and biomass burning conditions, *Atmos. Chem. Phys.* **3**, 951-967

Gysel, M., E. Weingartner, S. Nyeki, D. Paulsen, U. Baltensperger, I. Galambos and G. Kiss (2004), Hygroscopic properties of water-soluble matter and humic-like organics in atmospheric fine aerosol, *Atmos. Chem. Phys.* **4**, 35-50

Hallquist, M., J. C. Wenger, U. Baltensperger, Y. Rudich, D. Simpson, M. Claeys, J. Dommen, N.M. Donahue, C. George, A. H. Goldstein, J. F. Hamilton, H. Herrmann, T. Hoffmann, Y. Iinuma, M. Jang, M. E. Jenkin, J. L. Jimenez, A. Kiendler-Scharr, W. Maenhaut, G. McFiggans, T. F. Mentel, A. Monod, A. S. H. Prévot, J. H. Seinfeld, J. D. Surratt, R. Szmigielski and J. Wildt (2009), The formation, properties and impact of secondary organic aerosol: current and emerging issues, *Atmos. Chem. Phys.* **9**, 5155-5236

Heald, C. L., D. J. Jacob, R. J. Park, L. M. Russell, B. J. Huebert, J. H. Seinfeld, H. Liao, R. J. Weber (2005), A large organic aerosol source in the free troposphere missing from current models, *Geophys. Res. Lett.* **32**, L18809

Heald, C. L., D. K. Henze, L. W. Horowitz, J. Feddema., J.-F. Lamarque, A. Geunther, P. G. Hess, F. Vitt, J. H. Seinfeld, A. H. Goldstein and I. Fung (2008), Predicted change in global secondary organic aerosol concentration in response to future climate, emissions and land use change, *J. Geophys. Res.* **113**, D05211

Heald, C. L., M. J. Wilkinson, R. K. Monson, C. A. Alo, G. L. Wang and A. Guenther (2009), Response of isoprene emission to ambient CO_2 changes and implications for global budgets, *Global Change Biol.* **15**, 1127-1140

Hegg, D. A., J. Livingston, P. V. Hobbs, T. Novakov and P. Russell (1997),Chemical apportionment of aerosol column optical depths off the mid-Atlantic coast of the United States, *J. Geophys. Res.* **102**, 25293-25303

Heintzenberg, J., W. Birmili, D. Theiss and Y. Kisilyakhov (2008), The atmospheric aerosol over Siberia, as seen from the 300m ZOTTO tower, *Tellus*, **60B,** 276-285

Henze, D. K. and J. H. Seinfeld (2006), Global secondary organic aerosol from isoprene oxidation, *Geophys. Res. Lett.* **33**, L09812

Henze, D. K., J. H. Seinfeld, J. H. Kroll, N. L. Ng, T.-M. Fu, D. J. Jacob and C. L. Heald, (2008), Global modelling of secondary organic aerosol formation from aromatic hydrocarbons: high- vs. low-yield pathways *Atmos. Chem. Phys.* **8**, 2405-2421

Heymsfield, A. J. and G. M. McFarquhar (2001), Microphysics of INDOEX clean and polluted trade cumulus clouds, *J. Geophys. Res.* **106** (D22), 28,653-28,673

Holben, B. N., T. F. Eck, I. Slutsker, D. Tanré, J. P. Buis, A. Setzer, E. Vermote, J. A. Reagan, Y. J. Kaufman, T. Nakajima, F. Lavenu, I. Jankowiak and A. Smirnov (1998), AERONET – A Federated Instrument Network and Data Archive for Aerosol Characterization, *Remote Sens. Environ.* **66**, 1-16

Hoffmann, T., J. R. Odum, F. Bowman, D. Collins, D. Klockow, R. C. Flagan and J. H. Seinfeld (1997), Formation of organic aerosols from the oxidation of biogenic hydrocarbons, *J. Atmos. Chem.* **26**, 189-222

Huebert, B. J., T. Bates, P. B. Russell, G. Shi, Y. J. Kim, K. Kawamura, G. Carmichael and T. Nakajima (2003), An overview of ACE-Asia: Strategies for quantifying the relationships between Asian aerosols and their climatic impact, *J. Geophys. Res.* **108(D23)**, 8663

Hoyle, C. R., T. Berntsen, G. Myhre and I. S. A. Isaksen (2007), Secondary organic aerosol in the global aerosol – chemical transport model Oslo CTM2, *Atmos. Chem. Phys.* **7**, 5675-5694

Hoyle, C. R., G. Myhre, T. K. Berntsen and I. S. A. Isaksen (2009), Anthropogenic influence on SOA and the resulting radiative forcing, *Atmos Chem. Phys.* **9**, 2715-2728

Huebert, B., T. Bertram, J. Kline, S. Howell, D. Eatough, B. Blomquist (2004), Measurements of organic and elemental carbon in Asian outflow during ACE-Asia from the NSF/NCAR C-130, *J. Geophys. Res.* **109**, D19S11

Iinuma, Y., O. Böge, T. Gnauk, and H. Herrmann (2004), Aerosol-chamber study of the α-pinene/O_3 reaction: Influence of particle acidity on aerosol yields and products, *Atmos. Env.* **38**, 761-773

Jacobson, M. C., H.-C. Hansson, K. J. Noone and R. J. Charlson (2000), Organic atmospheric aerosols : review and state of the science, *Rev. Geophys.* **38(2)**, 267-294

Jacobson, M. Z. (2001), Global direct radiative forcing due to multicomponent anthropogenic andnatural aerosols, *J. Geophys. Res.* **106(D2)**, 1551-1568

Jacobson, M. Z., A. Tabadazeh and R. P. Turco (1996), Simulating equilibrium within aerosols and nonequilibrium between gases and aerosols, *J. Geophys. Res.* **101(D4),** 9079-9091

Jang, M., N. M. Czoschke, S. Lee and R. M. Kamens (2002), Heterogenous atmospheric aerosol production by acid-catalyzed particle-phase reactions, *Science* **298**, 814-817, 2002

Jayne, J. T., D. C. Leard, X. F. Zhang, P. Davidovits, K. A. Smith, C. E. Kolb and D. R. Worsnop (2000), Development of an aerosol mass spectrometer for size and composition analysis of submicron particles, *Aerosol Sci, Tech.* **33**, 49-70

Jenkin, M. E. (2004), Modelling the formation and composition of secondary organic aerosol of α-pinene and β-pinene ozonolysis using MCMv3, *Atmos. Chem. Phys.* **4**, 1741-1757

Kalberer, M., J. Yu, D. R. Cocker III, R. C. Flagan and J. H. Seinfeld (2000), Aerosol formation in the cyclohexene-ozone system, *Environ. Sci. Technol.* **34** 4894-4901

Kalberer, M., D. Paulsen, M. Sax, M. Steinbacher, J. Dommen, A. S. H. Prévot, R. Fisseha, E. Weingartner, V. Frankevich, R. Zenobi and U. Baltensperger (2004), Identification of polymers as major components of atmospheric organic aerosols, *Science*, **303**, 1659-1662

Kanakidou, M., K. Tsigaridis (2000), F. J. Dentener and P. J. Crutzen, Human-activity-enhanced formation of organic aerosols by biogenic hydrocarbon oxidation, *J. Geophys. Res.* **105(D7)**, 9243-9254

Kanakidou, M., J. H. Seinfeld, S. N. Pandis, I. Barnes, F. J. Deneter, M. C. Facchini, R. Van Dingenen, B. Ervens, A. Nenes, C. J. Nielsen, E. Swietlicki, J. P. Putaud, Y. Balkanski, S. Fuzzi, J. Horth, G .K. Moortgat, R.

Winterhalter, C. E. L. Myhre, K. Tsigaridis, E. Vignati, E. G. Stephanou and J. Wilson (2005), Organic aerosol and global climate modelling: a review, *Atmos. Chem. Phys.* **5**, 1053-1123

Kaufman, Y.J., O. Boucher, D. Tanré, M. Chin, L. A. Remer and T. Takemura (2005), Aerosol anthropogenic component estimate from satellite data, *Geophys. Res. Lett.* **32**, L17804

Kesselmeier, J. and M. Staudt (1999), Biogenic Volatile Organic Compounds (VOC): An Overview on Emission, Physiology and Ecology, *J. Atmos. Chem.* **33,** 23-88

Khain, A. and A. Pokrovsky (2004), Simulation of effects of atmospheric aerosols on deep turbulent convective clouds using a spectral microphysics mixed-phase cumulus cloud model. Part II: Sensitivity study, *J. Atmos. Sci.* **61** 2963-2982

Khain, A. D. Rosenfeld and A. Podrovsky (2005), Aerosol impact on the dynamics and microphysics of deep convective clouds, *Q. J. R. Meteorol. Soc.*, **131**, 1-25

Kleindienst, T. E., D. F. Smith, W. Li, E. O. Edney, D. J. Driscoll, R. E. Speer and W. S. Weathers (1999), Secondary organic aerosol formation from the oxidation of aromatic hydrocarbons in the presence of dry submicron ammonium sulphate, *Atmos. Environ.* **33**, 3669-3681

Kleindienst, T. E., T. S. Conver, C. D. McIver and E. O. Edney (2004), Determination of secondary organic aerosol products from photooxidation of toluene and their implication in ambient $PM_{2.5}$, *J. Atmos. Chem.* **47**, 79-100

Koch, D. (2001), The transport and direct radiative forcing of carbonaceous and sulfate aerosols in the GISS GCM, *J.Geophys. Res.* **106**, 20311-20332

Kroll, J. H., N. L. Ng, S. M. Murphy, R. C. Flagan and J. H. Seinfeld (2006), Secondary Organic Aerosol Formation from Isoprene Photooxidation, *Environ. Sci. Technol.* **40**, 1869-1877

Kroll, J. H. and J. H. Seinfeld (2008) Chemistry of secondary organic aerosol: Formation and evolution of low-volatility organics in the atmosphere, *Atmos. Env.* **42**, 3593-3624

Kulmala, M., H. Vehkamäki, T. Petäjä, M. Dal Maso, A. Lauri, V.-M. Kerminen, W. Birmili and P. H. McMurry (2004a), Formation and growth rates of ultrafine atmospheric particles: a review of observations, *J. Aerosol Sci.* **35(2)**, 143-176

Kulmala, M., T. Suni, K. E. J. Lehtinen, M. Dal Maso, M. Boy, A. Reissell, Ü. Rannik, P. Aalto, P. Keronen, H. Hakola, J. Bäck, T. Hoffmann, T. Vesala and P. Hari (2004b), A new feedback mechanism linking forests, aerosols, and climate, *Atmos. Chem. Phys.* **4**, 557-562

Kulmala, M., K. E. J. Lehtinen, A. Laaksonen (2006a), Cluster activation theory as an explanation of the linear dependence between formation rate of 3nm particles and sulphuric acid concentration, *Atmos. Chem. Phys.* **6**, 878-793

Kulmala, M., A. Reissell, M. Sipila, B. Bonn, T. M. Ruuskanen, K. E. J. Lehtinenen, V.-M. Kerminen and J. Strom (2006b), Deep convective clouds as aerosol production engines: Role of insoluble organics, *J. Geophys. Res.,* **111(D17)**, D17202

Lathière, J., D.A. Hauglustaine, N. de Noblet-Ducoudre, G. Krinner and G.A. Folberth (2005), Past and future changes in biogenic volatile organic compound emissions simulated with a global dynamic vegetation model, *Geophys. Res. Lett.* **32**, L20218

Lee, L., A. H. Goldstein, J. H. Kroll, Ng, N. L., Varutbangkul, V, R. C. Flagan and J. H. Seinfeld (2006), Gas-phase products and secondary aerosol yields from the photooxidation of 16 different terpenes *J. Geophys. Res.* **111,** D17305

Liao, H., W. T. Chen and J. H. Seinfeld (2006), Role of climate change in global predictions of future tropospheric ozone and aerosols, *J. Geophys. Res.* **111(D12)**, D12304

Liggio, J. and S.-M. Li (2006), Organosulfate formation during the uptake of pinonaldehyde in acidic sulphate aerosols, *Geophys. Res. Lett.* **33,** L13808

Lim, Y. B. and P. J. Ziemann (2005), Products and Mechanism of Secondary Organic Aerosol Formation from Reactions of *n*-Alkanes with OH Radicals in the Presence of NO_x, *Environ. Sci. Technol.* **39**, 9229-9236

Liousse, C., J. E. Penner, C. Chuang, J. J. Walton, H. Eddleman, and H. Cachier (1996), A global three-dimensional study of carbonaceous aerosols, *J.Geophys. Res.*, **101**, 19411-19432

Lohmann, U. and J. Feicher (2005), Aerosol indirect effects: a review, *Atmos. Chem. Phys.* **5**, 715-737

Lohmann, U., P. Stier, C. Hoose, S. Ferrachat, S. Kloster, E. Roeckner and J. Zhang (2007), Cloud microphysics and aerosol indirect effects in the global climate model ECHAM5-HAM, *Atmos. Chem. Phys.* **7**, 3425-3446

Lohmann, U. (2008), Global anthropogenic aerosol effects on convective clouds in ECHAM5-HAM, *Atmos. Chem. Phys.* **8**, 2115-2131

Loreto, F., R. J. Fischbach, J. P. Schnitzler, P. Ciccioli, E. Brancaleoni, C. Calfapietra, G. Seufert (2001), Monoterpene emission and monoterpene synthase activities in the Mediterranean evergreen oak *Quercus ilex* L. grown at elevated CO_2 concentrations, *Global Change Biology* **7**, 709-717

Mäkelä, J. M., I. K. Koponen, P. Aalto and M. Kulmala (2000), One-year data of submicron size modes of tropospheric background aerosol in southern Finland, *J. Aerosol Sci.* **31(5)**, 595-611

Maria, S. F., L. M. Russell, B. J. Turpin, R. J. Porcja, T. L. Campos, R. J. Weber and B. J. Huebert (2003), Source signatures of carbon monoxide and organic functional groups in Asian Pacific Regional Characterization Experiment (ACE-Asia) submicron aerosol types, *J. Geophys. Res.* **108(D23)**, 8637

Matthias, V., D. Balis, J. Bösenberg, R. Eixmann, M. Iarlori, L. Komguem, I. Mattis, A. Papayannis, G. Pappalardo, M. R. Perrone and X. Wang (2004), Vertical aerosol distribution over Europe: Statistical analysis and Raman lidar data from 10 European Aerosol Research Lidar Network (EARLINET) stations, *J. Geophys. Res.* **109**, D18201

Meyer, N. K., Duplissy, M. Gysel, A. Metzger, J. Dommen, E. Weingartner, M. R. Alfarra, A. S. H. Prevot, C. Fletcher, N. Good, G. McFiggans, Å. M. Jonsson, M. Hallquist, U. Baltensperger, and Z. D. Ristovski (2009), Analysis of the hygroscopic and volatile properties of ammonium sulphate seeded and unseeded SOA particles, *Atmos. Chem. Phys.*, **9**, 721-732

Middlebrook, A. M., D M. Murphy, and D. S. Thomson (1998), Observations of organic material in individual marine particles at Cape Grim during the First Aerosol Characterization Experiment (ACE-1), *J. Geophys. Res.* **103 (D13)**, 16475-16483

Mie, G. (1908), Beiträge zur Optik trüber Medien, speziell kolloidaler Metallösungen, *Annalen der Physik* **330**, 377-445

Morgan, W. T., J. D. Allan, K. N. Bower, G. Capes, J. Crosier, P. J. Williams and H. Coe (2009), Vertical distribution of sub-micron aerosol chemical composition from North-Western Europe and the North-East Atlantic, *Atmos. Chem. Phys.* **9**, 5389-5401

Murphy, D. M., D. S. Thomson and M. J. Mahoney (1998), In Situ Measurements of Organics, Meteoritic Material, Mercury and Other Elements in Aerosols at 5 to 19 Kilometers, *Science*, **282**, 1664-1669

Myrhe, C. E. and C. J. Nielsen (2004), Optical properties in the UV and visible spectral region of organic acids relevant to tropospheric aerosols, *Atmos. Chem. Phys.* **4**, 1759-1769

Ng, N. L., J. H. Kroll, A. W. H. Chan, P. S. Chabra, R. C. Flagan and J. H. Seinfeld (2007a), Secondary organic aerosol formation from *m*-xylene, toluene and benzene, *Atmos. Chem. Phys.* **7**, 3909-3922

Ng, N. L., P. S. Chabra, A. W. H. Chan, J. D. Surratt, J. H. Kroll, A. J. Kwan. D. C. McCabe, P. O. Wennberg, A. Sorooshian, S. M. Murphy, N. F. Daleska, R. C. Flagan and J. H. Seinfeld (2007b), Effect of NO_x levels on the formation of secondary organic aerosols (SOA) from the photooxidation of terpenes, *Atmos. Chem. Phys.* **7**, 5159-5174

Novakov, T., D. A. Hegg and P. V. Hobbs (1997), Airborne measurements of carbonaceous aerosols on the east coast of the United States*J. Geophys. Res.* **102**, 30,023-30,030

O'Dowd, C. D., P. Aalto, K. Hameri, M. Kulmala and T. Hoffmann (2002), Aerosol formation – Atmospheric particles from organic vapours, *Nature* **416**, 497-498

O'Dowd, C.D., M.C. Facchini, F. Cavalli, D. Ceburnis, M. Mircea, S. Decesari, S. Fuzzi, Y.J. Yoon and J.-P. Putaud, (2004) Biogenically driven organic contribution to marine aerosol, *Nature* **431**, 676-680

Odum, J. R., T. Hoffman, F. Bowman, D. Collins, R. C. Flagan and J. H. Seinfeld (1996), Gas/Particle Partitioning and Secondary Organic Aerosol Yields, *Environ. Sci. Technol.* **30**, 2580-2585

Odum,, J. R., T. P. W. Jungkamp, R. J. Griffin, H. J. L. Forstner, R. C. Flagan and J. H. Seinfeld (1997a), Aromatics, Reformulated Gasoline, and Atmospheric Organic Aerosol Formation, *Environ. Sci. Technol.* **31**, 1890-1897

Odum, J. R., P. W. Jungkamp, R. J. Griffin, H. J. L. Forstner, R. C. Flagan and J. H. Seinfeld (1997b), The atmospheric aerosol-forming potential of whole gasoline vapour, *Science* **276** 96-99

Pankow, J. F. (1994a), An absorption model of gas/particle partitioning of organic compounds in the atmosphere, *Atmos.Env.* **28(2)**, 185-188

Pankow, J. F. (1994b), An absorption model of the gas/particle partitioning involved in the formation of secondary organic aerosol, *Atmos. Env.* **28(2)**, 189-193

Petters. M. D. and S. M. Kreidenweis (2007), A single parameter representation of hygroscopic growth and cloud condensation nucleus activity, *Atmos. Chem. Phys.* **7**, 1961-1971

Pincus, R. and M. A. Baker (1994), Effect of precipitation on the albedo susceptibility of clouds in the marine boundary layer, *Nature* **372**, 250-252

Presto, A. A., K. E. Huff Hartz and N. M. Donahue (2005), Secondary Organic Aerosol Production from Terpene Ozonolysis 2. Effect of NO_x Concentration, *Environ. Sci. Technol.* **39**, 7046-7054

Quaas, J., O. Boucher, N. Bellouin and S. Kinne (2008), Satellite-based estimate of the direct and indirect aerosol climate forcing, *J. Geophys. Res.* **113**, D05204

Raes, F., R. Van Dingenen, E. Vignati, J. Wilson, J. P. Putaud, J. H. Seinfeld and P. Adams (2000), Formation and cycling of aerosols in the global troposphere, *Atmos. Env.* **34**, 4215-4240

Ramanathan, V., P. J. Crutzen, J. Lelieveld, A. P. Mitra, D. Althausen, J. Anderson, M. O. Andreae, W. Cantrell, G. R. Cass, C. E. Chung, A. D. Clarke, J. A. Coakley, W. D. Collins, W. C. Conant, F. Dulac, J. Heintzenberg, A. J. Heymsfield, B. Holben, S. Powell, J. Hudson, A. Jayaraman, J. T. Kiehl, T. N. Krishnamurti, D. Lubin, G. McFarquhar, T. Novakov, J. A. Ogren, I. A. Podgorny, K. Prather, K. Priestley, J. M. Prospero, P. K. Quinn, K. Rajeev, P. Rasch, S. Rupert, R. Sadourny, S. K. Satheesh, G. E. Shaw, P. Sheridan and F. P. J. Valero (2001), Indian Ocean Experiment: An integrated analysis of the climate forcing and effects of the great Indo-Asian haze, *J. Geophys. Res.* **106 (D22)**, 28371-28398

Remer, L. A., R. G. Kleidman, R. C. Levy, Y. J. Kaufman, D. Tanré, S. Mattoo, J. Vanderlei Martins, C. Ichoku, I. Koren, H. Yu and B. N. Holben (2008), Global aerosol climatology from the MODIS satellite sensors, *J. Geophys. Res.* **113**, D14507

Rissler, J., Swietlicki, E., Zhou, J., Roberts, G., Andreae, M. O., Gatti, L. V., and Artaxo, P. (2004), Physical properties of the submicrometer aerosol over the Amazon rain forest during the wet to-dry season transition – comparison of modeled and measured CCN concentrations, *Atmos. Chem. Phys.*, **4**, 2119–2143,

Robinson, A. L., N. M. Donahue, M. K. Shrivastava, E. A. Weitkamp, A. M. Sage, A. P. Grieshop, T. E. Lane, J. R. Pierce and S. N. Pandis (2007), Rethinking organic aerosols: Semivolatile emissions and photochemical aging, *Science* **315**, 1259-1262

Rodrigo, S. A., R. G. E. Morales and M. A. Leiva (2009), Estimation of primary and secondary organic carbon formation in $PM_{2.5}$ aerosols of Santiago City, Chile *Atmos. Env.* **43(13)**, 2125-2131

Roeckner, E., P. Stier, J. Feichter, S. Kloster, M. Esch and I. Fischer-Bruns (2006), Impact of carbonaceous aerosol emissions on regional climate change, *Clim. Dyn.* **27(6)**, 553-571

Russell, P., P. Hobbs and L. Stowe (1999), Aerosol properties and radiative effects in the United States East Coast haze plume: An overview of the Tropospheric Aerosol Radiative Forcing Observational Experiment, *J. Geophys. Res.* **104(D2)**, 2213-2222

Sanadze, G. A. (1991) in: Trace Gas Emissions by Plants, T.D. Sharkey, E.A. Holland and H.A. Mooney (eds.), Academic Press, 1991.

Sanderson, M. G., C. D. Jones, W. J. Collins, C. E. Johnson and R. G. Derwent (2003), Effect of Climate Change on Isoprene Emissions and Surface Ozone Levels, *Geophys. Res. Lett.* **30(18)**, 1936

Sato, K., S. Hatakeyama and T. Imamura (2007), Secondary organic aerosol formation during the photooxidation of toluene: NO_x dependence of chemical composition, *J. Phys. Chem. A*, **111**, 9796-9808

Saxena, P. and L. M. Hildemann (1996), Water-soluble Organics in Atmospheric Particles: A Critical Review of the Literature amd Application of Thermodynamics to Identify Candidate Compounds, *J. Atmos. Chem.* **24**, 57-109

Schulz, M., C. Textor, S. Kinne, Y. Balkanski, S. Bauer, T. Berntsen, T. Berglen, O. Boucher, F. Dentener, S. Guibert, I. S. A. Isaksen, T. Iversen, D. Koch, A. Kirkevåg, X. Liu, V. Montanaro, G. Myhre, J. E. Penner,

G. Pitari, S. Reddy, Ø. Seland, P. Stier, and T. Takemura (2006), Radiative forcing by aerosols as derived from the AeroCom present-day and pre-industrial simulations, *Atmos. Chem. Phys.* **6**, 5525-5246

Schurgers, G., A. Arneth, R. Holzinger and A.H. Goldstein (2009) Process-based modelling of biogenic monoterpene emissions combining production and release from storage, *Atmos. Chem. Phys.* **9**, 3409-3423

Seinfeld, J. H. and J. F. Pankow (2003), Organic Atmospheric Particulate Material, *Annu. Rev. Phys. Chem.* **54**, 121-140

Seinfeld, J. H. and S. N. Pandis (2006), Atmospheric Chemistry and Physics,: from air pollution to climate change, 2nd Ed., Wiley Interscience, Hoboken, New Jersey

Sihto, S.-L., M. Kulmala, V.-M. Kerminen, M. Dal Maso, T. Petäjä, I. Riipinen, H. Korhonen, F. Arnold, R. Janson, M. Boy, A. Laaksonen, and K. E. J. Lehtinen, (2006), Atmospheric sulphuric acid and aerosol formation: implications from atmospheric measurements for nucleation and early growth mechanisms, *Atmos. Chem. Phys*. **6,** 4079-4091

Sitch, S., B. Smith, I. Prentice, A. Arneth, A. Bondeau, W. Cramer, J. Kaplan, S. Levis, W. Lucht, M. Sykes, K. Thonicke and S. Venevsky (2003), Evaluation of ecosystem dynamics, plant geography and terrestrial carbon cycling in the LPJ Dynamic Global Vegetation Model, *Glob. Change Biol.* **9**, 161-185

Smith, B., I. Prentice and M. Sykes (2001), Representation of vegetation dynamics in the modelling of terrestrial ecosystems: comparing two contrasting approaches within European climate space, *Glob. Ecol. Biogeogr.* **10**, 621-637

Smith J. N., M. J. Dunn, T. M. VanReken, K. Iida, M. R. Stolzenburg, P. H. McMurry, and L. G. Huey (2008), Chemical composition of atmospheric nanoparticles formed from nucleation in Tecamac, Mexico: Evidence for an important role for organic species in nanoparticle growth, *Geophys. Res. Lett*., **35**, L04808

Spanke, J., U. Rannik, R. Forkel, W. Nigge and T. Hoffmann (2001), Emission fluxes and atmospheric degradation of monoterpenes above a boreal forest: field measurements and modelling, *Tellus B*, **53**, 406-422

Staudt, M., R. Joffre, S. Rambal and J. Kesselmeier (2001), Effect of elevated CO_2 on monoterpene emission of young *Quercus ilex* trees and its relation to structural and ecophysiological parameters, *Tree Physiol.* **21**, 437-445

Stier, P., J. Feichter, S. Kinne, S. Kloster, E. Vignati, J. Wilson, L. Ganzeveld, I. Tegen, M. Werner, Y. Balkanski, M. Schulz, O. Boucher, A. Minikin and A. Petzold (2005), The aerosol-climate mode ECHAM5-HAM, *Atmos. Chem. Phys.* **5**, 1125-1156

Stier, P., J. Feichter, S. Kloster, E. Vignati and J. Wilson (2006), Emission-induced nonlinearities in the global aerosol system: Results from the ECHAM5-HAM aerosol-climate model, *J. Clim.* **19(16)**, 3845-3862

Stier, P., J. H. Seinfeld, S. Kinne and O. Boucher (2007), Aerosol absorption and radiative forcing, *Atmos. Chem. Phys.* **7**, 5237-5261

Surratt, J. D., S. M. Murphy, J. H. Kroll, N. L. Ng, L. Hildebrandt, A. Sorooshian, R. Szmiglievski, R. Vermeylen, W. Maenhaut, M. Claeys, R. C. Flagan and J. H. Seinfeld (2006), Chemical composition of secondary organic aerosol formed from the photooxidation of isoprene, *J. Phys. Chem. A*, **110**, 9665-9690

Surratt, J. D., J. H. Kroll, T. E. Kleindienst, E. O. Edney, M. Claeys, A. Sorooshian, N. L. Ng, J. H. Offenberg, M. Lewandowski, M. Jaoui, R. C. Flagan and J. H. Seinfeld (2007), Evidence for organosulfates in secondary organic aerosol, *Environ. Sci. Technol.* **41**, 5363-5369

Tao, W. K., X. Li,. A. Khain, T. Matsui, S. Lang and J. Simpson (2007), Role of atmospheric aerosol concentration on deep convective precipitation: Cloud-resolving model simulations, *J. Geophys. Res.* **112**, D24S18

Topping, D. O., G. B. McFiggans and H. Coe (2005), A curved multi-component aerosol hygroscopicity model framework: Part 2 – Including organic compounds, *Atmos. Chem. Phys.* **5**, 1223-1242

Tsigaridis, K., and M. Kanakidou (2003), Global modelling of secondary organic aerosol in the troposphere: a sensitivity analysis, *Atmos. Chem. Phys.* **3**, 1849-1869

Tsigaridis, K., M. Krol, F. J. Dentener, Y. Balkanski, J. Lathière, S. Metzger, D. A. Hauglustaine and M. Kanakidou (2006), Change in global aerosol composition since preindustrial times, *Atmos. Chem. Phys.* **6**, 5143-5162

Tsigaridis, K., and M. Kanakidou (2007) Secondary organic aerosol importance in the future atmosphere, *Atmos. Env.* **41**, 4682-4692

Tunved, P., H.-C. Hansson, V.-M. Kerminen, J. Ström, M. Dal Maso, H. Lihavainen, Y. Viisanen, P. P. Aalto, M. Komppula and M. Kulmala (2006), High Natural Aerosol Loading over Noreal Forests, *Science* **312**, 261-263

Turner, D. P., J. V. Baglio and A. G. Wones (1991), Climate change and isoprene emissions from vegetation, *Chemosphere* **1**, 37-56

Twomey, S. (1974) Pollution and the planetary albedo, *Atmos. Env.* **8**, 1251-1264, 1974

S. M. Uppala , P. W. Kållberg , A. J. Simmons, U. Andrae, V. Da Costa Bechtold, M. Fiorino, J. K. Gibson, J. Haseler, A. Hernandez, G. A. Kelly, X. Li, K. Onogi, S. Saarinen, N. Sokka, R. P. Allan, E. Andersson, K. Arpe, M. A. Balmaseda, A. C. M. Beljaars, L. Van De Berg, J. Bidlot, N. Bormann, S. Caires, F. Chevallier, A. Dethof, M. Dragosavac, M. Fisher, M. Fuentes, S. Hageman[6], E. Holm, B. J. Hoskins, L. Isaksen, P. A. E. M. Janssen, R. Jenne, A. P. McNally, J.-F. Mahfouf , J.-J. Morcrette, N. A. Rayner, R. W. Saunders, P. Simon, A. Sterl, K. E. Trenberth, A. Untch, D. Vasiljevic, P. Viterbo, and J. Woollen (2000), The ERA-40 re-analysis, *Q. J. R. Met. Soc.* **131**, 2961-3012

van Aardenne, J. A., F. J. Dentener, J. G. J. Oliver, J. A. H. W. Peters and L. N. Ganzeveld (2005), The EDGAR 3.2 Fast Track 2000 dataset, http://www.mnp.nl/edgar/Images/Description_of_EDGAR_32FT2000(v8)_tcm32-22222.pdf

van der Werf, G. R., J. T. Randerson, J. G. Collatz and L. Giglio (2003), Carbon emissions from fires in tropical and subtropical ecosystems, *Global Change Biol.* **9**, 547-562

Volkamer, R., J. L. Jimenez, F. San Martini, K. Dzepina, Q. Zhang, D. Salcedo, L. T. Molina, D. R. Worsnop and M. J. Molina (2006).: Secondary organic aerosol formation from anthropogenic air pollution: Rapid and higher than expected, *Geophys. Res. Lett.* **33**, L17811

Volkamer, R., P. J. Ziemann and M. J. Molina (2009), Secondary Organic Aerosol Formation from Acetylene (C_2H_2): seed effect on SOA yields due to organic photochemistry in the aerosol aqueous phase, *Atmos. Chem. Phys*., **9**, 1907-1928

Weber, R. J., D. Orsini, Y. Daun, Y. N. Lee, P. J. Klotz and F. Brechtel (2001), A particle-into-liquid collector for rapid measurement of aerosol bulk chemical composition, *Aerosol Sci. Tech.* **35**, 718-727

Went, F. W. (1960), Blue hazes in the atmosphere, *Nature*, **187**, 641-643

Yu, H., Y. J. Kaufman, M. Chin, G. Feingold, L. A. Remer, T. L. Anderson, Y. Balkanski, N. Bellouin, O. Boucher, S. Christopher, P. DeCola, R. Kahn, D. Koch, N. Loeb, M. Shakar Reddy, M. Schulz, T. Takemura and M. Zhou (2006), A review of measurement-based assessments of the aerosol direct effect and forcing, *Atmos. Chem. Phys.* **6**, 613-666

Zhou, J. C., E. Swietlicki, H. C. Hansson and P. Artaxo (2002), Submicrometer aerosol particle size distribution and hygroscopic growth measured in the Amazon rain forest during the wet season, *J. Geophys. Res*., **107,** 8055

Die gesamten Veröffentlichungen in der Publikationsreihe des MPI-M
„Berichte zur Erdsystemforschung“,
„Reports on Earth System Science“,
ISSN 1614-1199

sind über die Internetseiten des Max-Planck-Instituts für Meteorologie erhältlich:

http://www.mpimet.mpg.de/wissenschaft/publikationen.html



ISSN 1614-1199